

Copyright
by
Eugenio Felipe Unson Santillan
2014

**The Dissertation Committee for Eugenio Felipe Unson Santillan Certifies that this is
the approved version of the following dissertation:**

**Microbial Responses to CO₂ During Carbon Sequestration: Insights
into an Unexplored Extreme Environment**

Committee:

Philip C. Bennett, Supervisor

Meinhard Bayani Cardenas

Timothy M. Shanahan

Christopher R. Omelon

Susan J. Altman

**Microbial Responses to CO₂ During Carbon Sequestration: Insights
into an Unexplored Extreme Environment**

by

Eugenio Felipe Unson Santillan, B.S.

Dissertation

Presented to the Faculty of the Graduate School of
The University of Texas at Austin
in Partial Fulfillment
of the Requirements
for the Degree of

Doctor of Philosophy

The University of Texas at Austin

May 2014

Dedication

To my baby sister Patricia who reminds me of what it means to be a good person.

Acknowledgements

This work was very much a collaborative effort and I would not have gotten this done without the help of the numerous colleagues, friends, and family in my life. I would like to thank my advisor and my committee members for providing me insight and perspective during my graduate school experience, especially during times when my research outlooks looked bleak.

I would also like to thank my lab mates Megan, Aaron, Kim G., Kim M., John, Lindsey, Molly, Will, Evan, Tiffany, Gabe, and Heather for all the invaluable help in and out of the lab. Getting through the dissertation was not easy, but you all made it fun.

I also would like to extend a special thanks to everyone in the Shanahan lab, specifically Vera, Veronica, Curtis, Travis, and Kyra for all their help on the organic geochemistry aspect of my work. I appreciate the support from colleagues at Sandia National Laboratories, specifically Matt Kirk for his mentorship and Lucas McGrath for teaching me methods on biofilm characterization. Many thanks also go to Jonathan Major, Alex Urquhart, Mark Hesse, Rick Colwell, Melissa Masbruch, Stefan Kirby, and the employees of Moab Springs Ranch and Arches National Park for help with field site access. Additional thanks go to Scot Dowd, Daniel Zeigler, Dwight Romanovicz, Nate Miller, and Alex Sessions for help processing data or advising me with methodology.

Lastly, I would like to thank friends, family, Rain, and Ezri for the unconditional support and occasionally a shoulder to cry on when I needed them most.

This material is based upon work supported as part of the Centers for Frontiers in Subsurface Energy Security, an Energy Frontier Research Center funded by the U.S. Department of Energy, Office of Science, Office of Basic Energy Sciences under Award Number DE-SC0001114.

Microbial Responses to CO₂ During Carbon Sequestration: Insights into an Unexplored Extreme Environment

Eugenio Felipe Unson Santillan, Ph.D.

The University of Texas at Austin, 2014

Supervisor: Philip C. Bennett

When CO₂ is sequestered into deep saline aquifers, significant changes to the biogeochemistry of the system are inevitable and will affect native microbial populations both directly and indirectly. These communities are important as they catalyze many geochemical reactions in these reservoirs. We present evidence that the injection of CO₂ will cause a large scale disturbance to subsurface microbial populations which will ultimately affect the solution and mineral trapping of CO₂ as well as the movement of CO₂ charged water through the subsurface.

Representative subsurface microorganisms including a Gram negative bacterium (G⁻), two Gram positive bacteria (G⁺), and an archaeon were tested for CO₂ survival at pressures up to 50 bar and exposure times up to 24 hours. CO₂ tolerance varied but shows effects on microbes is more complex than just decreasing pH and is not significantly dependent on cell wall structure. Imaging reveals that CO₂ disrupts the cytoplasm possibly from changes to intracellular pH. The geochemical effect of CO₂ stress is a decrease in metabolic activity such as Fe reduction and methanogenesis.

Subsurface microbial populations interact with the surrounding reservoir minerals which likely influence their ability to survive under CO₂ stress. When the G⁻ organism was grown in the presence of a mineral substrate, survival depended on the mineral type. Quartz sandstone provided a good substrate for survival while kaolinite provided a poor substrate for survival. Biofilms on quartz sandstone were rich in extracellular polymeric substances (EPS) that likely act as a barrier to slow the penetration of CO₂ into the cell. The release of toxic metals from mineral dissolution at high PCO₂ enhanced cell death.

To understand the long term effects of CO₂ on microbial communities, water samples were taken from CO₂ springs in the western United States and compared to unaffected springs. Community 16S rRNA sequence data suggests that CO₂ exposed environments exhibit lower microbial diversity, suggesting environmentally stressed communities. However, differences among diversity in the springs surveyed also indicates other environmental factors that affect diversity beyond CO₂. Furthermore, the isolation of a novel fermentative *Lactobacillus* strain from a CO₂ spring, indicates viable microbial communities can exist at high PCO₂.

Table of Contents

List of Tables	x
List of Figures	xi
Chapter 1: Introduction	1
Geologic Carbon Sequestration	3
Deep Subsurface Microbes	5
CO ₂ Effects on Microbes	11
Microbial Geochemistry of CO ₂ Sequestration	16
Research Questions	17
Hypotheses and Research Approach.....	18
Chapter2: Microbial Physiological and Morphological Responses to CO ₂ Exposure	
.....	20
Abstract	20
Introduction.....	21
Materials and Methods.....	26
Model Organisms.....	27
Culture Conditions	27
CO ₂ Experiments	28
Lipid Extraction and Identification.....	29
Transmission Electron Microscopy	30
Results.....	31
Growth and Metabolism	31
Morphology.....	34
Membrane Response	35
Discussion	37
Chapter 3: Mineral influence on Microbial Survival During Carbon Sequestration	58
Abstract	58
Introduction.....	59

Materials and Methods.....	63
Culture conditions.....	63
CO ₂ Toxicity	65
Mineral Effects on CO ₂ toxicity	66
Sample characterization	67
Results.....	68
Discussion.....	72
Implications.....	83
Chapter 4: Microbial Communities in Terrestrial CO ₂ Springs.....	101
Abstract.....	101
Introduction.....	102
Site Descriptions	105
Little Grand Wash Fault.....	105
Moab Springs Ranch.....	106
Arches Headquarters.....	107
Bravo Dome	107
Klickitat.....	108
Methods.....	108
Field Sampling.....	108
Geochemical Analysis	110
Sequence Analysis	110
Results.....	112
Water Chemistry	112
Diversity.....	113
Discussion	116
Chapter 5: Isolation and Characterization of a Novel CO ₂ -Tolerant Lactobacillus Strain from Crystal Geyser, Utah, U.S.A.....	142
Abstract.....	142
Introduction.....	143
Materials and Methods.....	146

Field sampling.....	146
Culture Experiments	148
Lipid Analysis.....	150
Cloning, Sanger Sequencing.....	151
Transmission Electron Microscopy	152
Results.....	153
Discussion.....	157
Organism Description	166
Chapter 6: Conclusions	175
Bibliography	183

List of Tables

Table 2-1 <i>Bacillus subtilis</i> survival at varying PCO_2 and pH 4.5	47
Table 3-1 Minerals and their approximate chemical compositions used for this study	85
Table 3-2 CO_2 survival for SO, GS, and MT in unbuffered media with no mineral amendments.	86
Table 3-3 Select cation data for batch cultures containing various minerals at the start of cell culturing and after CO_2 incubation	87
Table 4-1 Composition of sites sampled.....	127
Table 4-2 Bacterial alpha diversity values.....	128
Table 4-3 Unweighted unifrac values for sites sampled	129
Table 5-1 CG-1 physiological parameters examined.....	167
Table 5-2 CG-1 fatty acid content at 1 and 10 bar CO_2	168

List of Figures

Figure 2-1 <i>Shewanella oneidensis</i> growth and iron reduction	48
Figure 2-2 SO growth with nitrate or thiosulfate as TEAs	49
Figure 2-3 <i>Geobacillus stearothermophilus</i> growth curves	50
Figure 2-4 <i>Methanothermobacter thermoautotrophicus</i> CH ₄ production with varying PCO ₂	51
Figure 2-5 TEM images of SO.....	52
Figure 2-6 TEM images of GS.....	53
Figure 2-7 TEM images of BS.....	54
Figure 2-8 TEM images of MT.....	55
Figure 2-9 Bacterial fatty acid ratios at 2 bar CO ₂ exposure	56
Figure 2-10 Bacterial fatty acid profiles at 25 or 50 bar PCO ₂	57
Figure 3-1 Schematic representation of how CO ₂ affects a bacterial cell.....	88
Figure 3-2 Schematic representation of biofilm colonization on the mineral surface	89
Figure 3-3 The effects of different depressurization rates on cell viability for SO and GS using rates of 10 bar N ₂ min ⁻¹ and 25 bar N ₂ min ⁻¹	90
Figure 3-4 SO survival at 25 bar CO ₂ in buffered and unbuffered media and in HCl acidified media simulating the pH drop at those pressures.....	91
Figure 3-5 SO CO ₂ survival with pH buffering minerals.	92
Figure 3-6 SO CO ₂ survival with silicate rocks and minerals.	93
Figure 3-7 SO CO ₂ survival with miscellaneous rocks and minerals.	94
Figure 3-8 SO CO ₂ survival with clays.....	95
Figure 3-9 SO 8 hour CO ₂ survival with various minerals.	96

Figure 3-10 SEM images of SO on various minerals before and after 25 bar CO ₂ exposure	97
Figure 3-11 Effects of sonication on SO CO ₂ survival.....	98
Figure 3-12 Effects of toxic metals on SO biofilm CO ₂ survival.....	99
Figure 3-13 M1 media pH changes due to increased PCO ₂ with and without dolomite.	100
Figure 4-1 Sample locations within the United States.....	130
Figure 4-2 Moab Springs Ranch.....	131
Figure 4-3 Arches Headquarters	132
Figure 4-4 Crystal Geyser.....	133
Figure 4-5 Airport Spring	134
Figure 4-6 Bravo Dome	135
Figure 4-7 Klickitat Mineral Spring	136
Figure 4-8 Piper diagram representing the water chemistry of the springs sampled	137
Figure 4-9 Bacterial community composition of the springs sampled	138
Figure 4-10 Archaeal community composition of the springs sampled	139
Figure 4-11 Bacterial rarefaction curves.....	140
Figure 4-12 Constrained correspondence analysis of the sites sampled.....	141
Figure 5-1 Location of Crystal Geyser	169
Figure 5-2 Lipid composition of the water at Crystal Geyser.	170
Figure 5-3 Phylogenetic tree showing CG-1 in relation to other organisms belonging to the genus <i>Lactobacillus</i>	171
Figure 5-4 CG-1 physiological data.....	172
Figure 5-5 CG-1 fatty acid composition at 1 bar and 10 bar CO ₂	173
Figure 5-6 TEM images of CG-1	174

Figure 6-1 Conceptual model of microbial redistribution	182
---	-----

Chapter 1: Introduction

Deep saline aquifers host microbial communities that can influence the permeability and geochemistry of the surrounding environment (Pedersen, Arlinger et al. 1996, Fredrickson, Zachara et al. 1998, Onstott, Phelps et al. 1998, Gorbushina 2007, Sahl, Schmidt et al. 2008, Baker, Comolli et al. 2010, Banks, Taylor et al. 2010, Davidson, Silver et al. 2011). These bacteria and archaea utilize the surrounding rocks and minerals for respiration, nutrients, and colonization surfaces, and these activities result in distinct biosignatures and byproducts. Iron, for example, is a metal ubiquitous in many saline aquifers (Kharaka, Cole et al. 2006, Kharaka, Thordsen et al. 2010, Kirk 2011) and this metal can be cycled through the activity of dissimilatory iron reducing bacteria (DIRB) (Lovley 1993, Fredrickson, Zachara et al. 1998, Nealson, Belz et al. 2002). During this process, DIRB respire iron oxides present in rocks by transferring an electron taken from an energy source such as H_2 or lactate and depositing it on ferric iron. The immobile ferric iron is then converted to the mobile ferrous iron. This process enhances rock dissolution and may also leave biogenic Fe precipitates such as siderite, magnetite, and vivianite (Lies, Hernandez et al. 2005).

Other organisms that can affect saline aquifers are methanogenic archaea, which utilize CO_2 and H_2 in the surrounding environment to create CH_4 , resulting in plumes found in the deep subsurface (Kotelnikova 2002). Additionally, fermenting bacteria release organic acids as metabolic byproducts enhancing mineral dissolution (Li, Xu et al. 2006). However, by enhancing mineral dissolution, microbes also free up nutrients from rocks (Bennett, Rogers et al. 2001).

Deep saline aquifers provide many different stresses to the native microorganisms present. Aquifers can be oligotrophic and anaerobic, as many of the nutrients and carbon sources have long been depleted from water that recharge the system (Griebler and Lueders 2009). The primary sources of carbon, terminal electron acceptors (TEAs), and nutrients typically come from the surrounding host rock as a result. Additionally, increases in the surrounding temperature due to the geothermal gradient as well as the high salinity of the groundwater may contribute additional stresses. Despite these conditions, microbial signatures and biomass have been confirmed in deep subsurface environments with counts ranging from 10^3 to 10^5 cells/g of rock (Colwell, Onstott et al. 1997, Fredrickson, Zachara et al. 1998).

When carbon dioxide is sequestered in saline aquifers, a tremendous stress is placed on the system, perturbing microbial populations. At supercritical CO_2 (scCO_2) pressures, CO_2 dissolves microbial membranes and sterilizes microbial communities (Dillow, Dehghani et al. 1999, White, Burns et al. 2006). At lower pressures where CO_2 dissolves in the aqueous phase, CO_2 is also toxic to microbes as CO_2 is liposoluble. As a result, CO_2 enters cells, acidifies the cytoplasm, and disrupts cellular functions (Ballestra, Dasilva et al. 1996). However, the details of the microbial responses to this stress are still vague, and many unanswered questions remain, such as, which microbes are most resistant to CO_2 stress, how resistant microbial membranes are to CO_2 dissolution, and how microbial communities change as a result of CO_2 perturbation.

In this study, I investigated the effects of CO_2 pressures below supercritical CO_2 on subsurface microbes at spatial scales from the cell to the microbial community. My

approach used laboratory model organisms, data from terrestrial sequestration analogues, and from environmental isolates from high CO₂ environments. This investigation will provide insight on how CO₂ sequestered in the deep subsurface will affect microbial communities, and how this affects the fate of CO₂ over short and long time scales.

Geologic Carbon Sequestration

Geologic carbon sequestration involves the capture, compression, and storage of anthropogenic CO₂ into a deep saline aquifer. Typically, saline aquifers are chosen as they are greater than 1 km below the subsurface, confined, and contain water unsuitable for human consumption. Reservoirs targeted for sequestration are diverse and can range anywhere from sandstone to basalt aquifers to carbonate (McGrail, Schaef et al. 2006, Kaszuba, P. et al. 2009).

CO₂ sequestered in these aquifers will enter the subsurface as a plume of phase-separated scCO₂. The CO₂ will slowly finger into the surrounding pore spaces and snap off into zones of scCO₂ and displace brine in a process known as residual trapping (Bachu 2008). Surrounding the fingers of scCO₂ will be areas where CO₂ dissolves into the surrounding pore water, so called solubility trapping. Over the course of geologic time, this dissolved CO₂ will eventually interact with the host rock and dissolve it to create HCO₃⁻. Eventually, this will lead to the precipitation of carbonate minerals, known as mineral trapping.

The composition of fluids in the target formations is derived from the originally emplaced fluids, the effects of evaporation, and subsequent rock-water interactions with the formation minerals (Dworkin and Land 1996, Hardie 1980). Depending on the

original composition and key element ratios, the resulting brine could be Na-Cl rich with scant calcium, or it could be Ca-Cl rich, or have other dominant ions (Bein and Dutton 1993). The Mesozoic aged gulf coast formations for example have very high Ca and Mg compared to the Cenozoic aged formations (Hyeong and Capuano 2001). Many of these formations have important ions for microbial metabolism including solid phase iron oxides, dissolved organic carbon and dissolved sulfate ion (SO_4^{2-}), and the signatures of microbial activity such as dissolved ferrous iron (Fe^{2+}), biogenic CO_2 and CH_4 , and H_2S . After burial, the source of additional dissolved ions can be from the dissolution of halite, or from diagenesis of the formation minerals over time and with increasing temperature. Reactions such as the smectite-illite transition, or albitization, will alter the composition of both the water and the surrounding rocks. Often these reactions are slow however, and the system will reach a pseudo steady state condition with little change over time.

High concentrations of dissolved CO_2 will create an aggressive fluid that will accelerate these mineral diagenetic reactions and elevate the concentration of dissolved ions while creating new secondary mineral phases (Kaszuba and Janecky 2009, Lu et al 2010). Sequestration field studies in Frio, Texas (Kharaka et al 2006) were conducted in a sandstone formation composed of reactive feldspars, clays, carbonates, iron oxides and resulted in elevated bicarbonate, dissolved Fe and Al, and other dissolved ions. Laboratory experiments with high $P\text{CO}_2$ fluids also show that silicate weathering is greatly accelerated at the low pH conditions that will be present, with increased mobility of Al and Fe in particular (Kaszuba and Janecky 2009, Lu et al 2010).

Deep Subsurface Microbes

Bacteria and Archaea are two types of microorganisms present in the subsurface that metabolize and affect the geochemistry in saline aquifers. A key difference between organisms in the Archaea and Bacteria is cell membrane structure. Archaea are composed of ether-linked phospholipids with saturated, branched isoprenoid units of fixed length. These membrane structures form a monolayer and provide Archaea with extremely rigid membranes that let them tolerate wide ranges of environments. They are stable at very high and low temperatures and also makes membranes more impermeable to acidification at low pH ranges (Gambacorta, Trincone et al. 1994, Arakawa, Kano et al. 1999).

In contrast, bacteria contain cell membranes composed of a bilayer of a phosphate head group ester-linked to a hydrocarbon tail (White 2007). The bacterial hydrocarbon tail can be of variable chain length, with C16 and C18 hydrocarbons generally being the most abundant. Bacteria modify these hydrocarbon tails in response to environmental stresses by varying unsaturation, branching, and cyclization, which in turn alter membrane permeability and fluidity. Many bacteria can also be distinguished by characteristic fatty acids. Organisms of the genus *Lactobacillus* produce a characteristic cyclopropyl C19 fatty acid while many *Bacilli* are distinguished by the production of branched-chained fatty acids (Veerkamp 1971, Kaneda 1977).

Within the Bacterial domain, bacteria also differ from each other based on cell wall composition. Most bacteria are surrounded by a cell wall that overlays the cell membrane. The cell wall contains many different functions, however one major function is to maintain a cell's turgor pressure (White 2007). These cell walls are composed of

peptidoglycan: a structure composed of the oligosaccharide glycan cross linked by peptides, a construction that provides the cell wall with strength and rigidity.

Gram positive (G^+) organisms vary from Gram negative (G^-) organisms based on the thickness of the cell wall. G^+ cells contain thick cell walls, approximately 15 to 30 nm in length. G^- cells have significantly thinner cell walls. However, these organisms also contain an outer layer of lipopolysaccharides (LPS), composed of oligosaccharides and lipids layered above the cell wall. Because of the presence of an outer membrane in G^- bacteria, a periplasmic space is formed between outer and inner membranes that sandwich the cell wall. This space is vital in G^- anaerobic respiration as this space contains components for respiration and other functions. Different cell wall structures result in different metabolic strategies between G^+ and G^- bacteria.

G^+ organisms differ from G^- and Archaea in that they create endospores, highly resistant structures that form in the presence of stress. Endospores are dormant cells, composed of dehydrated DNA and ribosomes, surrounded by several thick layers of specialized peptidoglycan (Nicholson, Munakata et al. 2000). These spores are made such that they do not perform metabolic functions and remain dormant until conditions favor their germination back into vegetative cells. Dormant spores exhibit incredible longevity and have been found in virtually every type of environment on Earth from thermophilic springs, to cold lake sediments (Madigan 2012). They have also been reported to be as old as 10^5 years old (Nicholson, Munakata et al. 2000). Endospores have been shown to survive under heat, osmotic, acid, and oxidative stress. They have also been shown to survive supercritical CO_2 (Wynne and Foster 1948, Dillow, Dehghani et al. 1999,

Spilimbergo and Bertuccio 2003, Watanabe, Furukawa et al. 2003, Furukawa, Watanabe et al. 2004, Damar and Balaban 2006, White, Burns et al. 2006).

In addition to morphology, deep subsurface microbes can also be characterized by their metabolic capabilities. Many different populations perform similar metabolic functions and these groups can be classified as metabolic guilds. Geochemically, microbial metabolic processes are important as they often catalyze redox reactions that would otherwise be kinetically inhibited. The conversion of Fe^{3+} to Fe^{2+} , for example, while thermodynamically favorable, is a reaction that does not occur very quickly abiotically due to the activation energy required to move the reaction forward. DIRB present in the environment catalyze this reaction as a means for respiration. Our study pays special attention to DIRB as the release of ferric iron was seen during the Frio pilot project (Kharaka, Cole et al. 2006, Kharaka, Thordsen et al. 2010). Additionally, we will examine methanogens, and fermenters as these metabolic functions utilize CO_2 in their pathways.

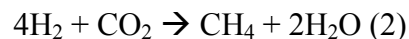
DIRB are bacteria capable of taking ferric iron and reducing it to ferrous iron as a form of respiration. Many of the known DIRB are G^- such as *Shewanella* and *Geobacter*. However, there have been reports of both G^+ and Archaea as DIRB, though their mechanisms for Fe reduction have not been elucidated (Lovley 1993, Nealson, Belz et al. 2002). Fe reduction in G^- DIRB follow a similar theme: oxidation of an energy source such as lactate yields an electron following the reaction:



These electrons are shuttled through an electron transport chain consisting of various flavoproteins and quinones. The oxidation of these proteins translocates protons to the outer membrane which eventually returns into the cell through a membrane-bound ATP synthase protein to create ATP for the cell. Excess electrons, depending on the organism, are then shuttled out of the cells through cytochromes, onto the solid phase ferric mineral.

DIRB may also leave traces of their activities in sedimentary environments due to the release of ferrous iron. Minerals such as magnetite, siderite, and vivianite may form depending on environmental conditions such as pe and pH (Fredrickson, Zachara et al. 1998). The potential to enhance DIRB during CO₂ sequestration may have several advantages. Consumption of proton during the DIRB process results in enhanced dissolution trapping, as described by (Kirk 2011). Furthermore, release of Fe²⁺ in addition to the increase in alkalinity will increase the saturation index for Fe-carbonate minerals like siderite, creating a favorable environment for the mineral trapping of CO₂ (Xu, Apps et al. 2005, Kirk 2011).

Methanogens are organisms that take an electron donor, such as H₂ or acetate, and reduce CO₂ to create CH₄ and energy following the reaction:



Their presence has been found in the subsurface in both terrestrial and marine environments (Colwell, Onstott et al. 1997, Kotelnikova 2002, Jones, Head et al. 2008, Lever 2013, Takano, Kaneko et al. 2013). All methanogens are anaerobic and their metabolism is the least energy-yielding of the anaerobic respiration reactions. As a result

of this, methanogens are often outcompeted by organisms that catalyze more energetically favorable redox reactions such as iron and sulfate reducers.

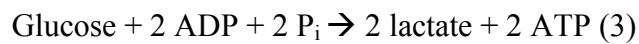
All methanogens belong to the Archaeal domain and pathways leading to methane production are complex and poorly understood. Methanogens produce energy from CO_2 reduction through a series of flavin-derived cofactors, sulfur containing coenzymes, and a unique Ni-containing cofactor. During this process, CO_2 is activated by being incorporated into a formyl group on a coenzyme. It is then rearranged where it is eventually converted to CH_4 . The rearrangement from CO_2 to CH_4 creates a proton gradient, fueling an ATPase and resulting in the production of energy (White 2007).

The methanogens' ability to utilize CO_2 in their metabolism may suggest a high tolerance to CO_2 , potentially allowing for their selection over other metabolic guilds. Sterilization of existing microbial populations within the subsurface will remove a lot of the competition and free up limiting nutrients such as phosphate, nitrate, and H_2 . An enrichment of methanogens in the subsurface can create plumes of CH_4 , a gas that is far less soluble than CO_2 . This would also result in a need to change how CO_2 will be monitored in the deep subsurface.

Fermenters are another metabolic guild in the subsurface that obtain energy through direct substrate-level phosphorylation and ATP production. This pathway results in metabolic byproducts such as acetate, lactate, alcohol, or various organic acids. Fermenters are metabolically diverse with different pathways to rearrange a carbon molecule to create byproducts. In anaerobic respiration, energy is gained by releasing an electron from either H_2 or a carbon source and depositing this electron to a TEA. During

fermentation, there are several steps to oxidizing organic carbon, and this carbon molecule also acts as the substrate to accept electrons. This study pays special attention to lactic acid fermentation.

During lactic acid fermentation, a carbon source such as glucose is broken down into 2 lactate molecules. In this process, ADP is also phosphorylated to create ATP in the following reaction:



In this process, the 6-carbon glucose molecule is rearranged and then cleaved into two 3-carbon phosphoglyceraldehyde molecules, then eventually pyruvate and lactate.

Rearrangements into phosphoglyceraldehyde and pyruvate yield 2 ATP molecules in the process.

Fermenters contribute to subsurface microbial communities as many fermentation pathways release H_2 (Konhauser 2006, White 2007), which can be used in syntrophy, an interspecies hydrogen transfer that provides an energy source for other microbial populations in the subsurface, such as with methanogenesis (2). Fermentation is also an important step in the degradation of hydrocarbons, creating byproducts that may feed other microbial populations (Konhauser 2006). Enrichment of fermenters during carbon sequestration could result in the buildup of fermentation byproducts in the subsurface, such as organic acids. Many of these products can aid in rock dissolution, creating a feedback mechanism for enhancing porosity and fracture formation (Li, Xu et al. 2006).

Many fermenting organisms are also capnophilic, i.e., these organisms thrive in CO_2 enriched environments due to their close association with organisms that produce

CO₂. However, while many capnophiles grow in CO₂ pressures ranging from 0.02 to 0.25 bar, CO₂ sequestration pressures will go well beyond that. These organisms utilize CO₂ metabolic pathways such as the carboxylation of phosphoenolpyruvate to eventually create oxaloacetate and then succinate. Other organisms take CO₂ and use this molecule as a means to carboxylate amino acids to create other amino acids.

CO₂ Effects on Microbes

Current research on CO₂ effects on microbes originate from the food and medical industries where CO₂ is used to sterilize food items and medical supplies because it is fast and inexpensive. Sterilization in these studies refers to the complete inactivation of cell cultures (>99%) containing at least at 10⁶ CFU/ml (Dillow, Dehghani et al. 1999, White, Burns et al. 2006). Multiple representative organisms spanning the domain Bacteria with different membrane morphologies have been studied. They have all been sterilized by scCO₂ including *Escherichia coli*, *Bacillus cereus*, *Staphylococcus aureus*, *Salmonella salford*, *Listeria innocua*, *Proteus vulgaris*, *Lactobacillus plantarium*, and *Pseudomonas aeruginosa* (Dillow et al 1999, Erkmén 1999, Hong and Pyun 1999, Spilimbergo et al 2002). Organisms examined varied in the amount of time it took for complete sterilization to occur.

The presence of water is also important in deactivating cells during CO₂ exposure, likely because CO₂ affects cells internally by acidifying the cytoplasm. By enhancing the dissolution of CO₂ in solution through the use of a microbubble system, Shimoda and others (1998) were able to demonstrate that inactivation of organisms under *PCO₂* is possible without having to increase CO₂ pressures to the supercritical phase and beyond.

This data suggests that while increasing the pressures of CO₂ does affect bacterial viability, the ultimate culprit in inactivating microbial cells is the dissolved CO₂ in the solution rather than the CO₂ pressure the cells are exposed to. Additionally, in comparison to dried cultures, *E. coli* cultures containing water were sterilized much faster (Dillow, Dehghani et al. 1999).

One hypothesis for why CO₂ sterilizes is the rapid depressurization of CO₂ after exposure. The fast escape of CO₂ from the solutions during the sampling process results in expanding bubbles that lyse cells (Nakamura, Enomoto et al. 1994). Evidence supporting this hypothesis comes from SEM observations on yeast (Nakamura et al 1994). However, microorganisms vary in size and complexity and when cultures of *E. coli* and *L. plantarum* were treated to flash depressurization there was no evidence of lysis, indicating that microbial inactivation is a much more complex process (Hong and Pyun 1999).

In all experiments, sterilization time varied based on differences in bacterial morphology including the thickness of the cell wall as well as the cell shape. Rods and cocci, as well as G⁺ and G⁻ cells differ in the surface to volume ratio of scCO₂ contact with the cell, which in turn changes the kinetics of their inactivation, possibly allowing slightly longer survival times for cocci and G⁺ cells (Spilimbergo and Bertucco 2003). Experiments on *Lactobacillus* show that the major factor in killing cells is the transfer rate of CO₂ into cells. By increasing pressure and temperature, this transfer rate could increase and allow for cells to die faster (Shimoda, Yamamoto et al. 1998).

Experiments on the inactivation of bacteria have been performed using different incubation temperatures. Data on this is conflicting with some studies indicating that an increase in temperature results in a faster inactivation of cell cultures and vice versa (Nakamura, Enomoto et al. 1994, Isenschmid, Marison et al. 1995, Ballestra, Dasilva et al. 1996, Erkmen 2000, Spilimbergo and Bertucco 2003, Damar and Balaban 2006). This demonstrates that microbes have different thermal tolerances depending on species. At a constant CO₂ pressure of 68 bar with cultures of *L. plantarium*, for example, Hong and Pyun (1999) demonstrate that inactivation occurs much faster at 30° C rather than at 40°C. This however, could be explained by a decrease in CO₂ solubility at higher temperatures. For cultures of the G⁻ *Listeria monocytogenes*, Erkmen (1999) demonstrates that increases in temperature with equivalent gas pressures results in a faster inactivation of cells. This may be due to the increase in cell membrane fluidity as well as the diffusivity of CO₂ at higher temperature, which may facilitate the penetration of CO₂ into the cell itself.

The growth media used for CO₂ sterilization in laboratory investigations is complex but highlights the importance of pH as an additional factor in killing microbial cells (Erkmen 2000). For experiments using *L. monocytogenes*, growth media containing some ability to buffer pH, including whole milk and buffered physiological saline gave cultures the best ability to survive in comparison to cultures grown in unbuffered media. For microbes in carbon sequestration settings, growth media is the surrounding brine. These saline waters have a great degree of alkalinity, suggesting these media may act as a pH buffer during CO₂ dissolution. Further interactions with carbonate minerals present

may keep the pH from dropping. In Frio, for example, the sequestration of CO₂ resulted in an increase in alkalinity (Kharaka, Thordsen et al. 2010).

Growth phase is also important for survival during CO₂ exposure. Experiments on *L. plantarium* show that cultures in the stationary phase are much more capable of surviving CO₂ exposure than cells in the late log phase (Hong and Pyun 1999). While the reasons for this are poorly understood, bacteria in the stationary phase live in much more stressful environmental conditions than cells in the log phase and synthesize proteins and express phenotypes that favor survival (Hong and Pyun 1999, Finkel 2006). Cells living in the deep subsurface live in very stressful, nutrient limited environments and may live in conditions similar to cells in stationary phase. The expression of proteins to handle the various stresses associated with starvation and other stresses could prolong survival length of cells during CO₂ sequestration.

While hypotheses exist for the mechanism of CO₂ inactivation on cell cultures, even less is understood on how CO₂ inactivates spores. In general, bacterial spores are extremely resistant to the antimicrobial effects of CO₂ (Ballestra, Dasilva et al. 1996, Watanabe, Furukawa et al. 2003). As with vegetative cells, different spores have variable amounts of resistance to CO₂. In comparison to various *Bacillus* species, Watanabe et al (2003) found that *Geobacillus stearothermophilus* was the most resistant to CO₂. Spore inactivation happened at CO₂ pressures up to 300 bar and temperatures at 95° C.

In all experiments on spores, temperature was seen as a bigger contributor to spore inactivation than CO₂. The method for spore inactivation using high pressures of CO₂ may in fact be twofold. Increased amounts of CO₂ present in the environment results

in the germination of spores (Wynne and Foster 1948, Furukawa, Watanabe et al. 2004). Germinated spores may then be more susceptible to temperature treatment, resulting in faster inactivation. In general, however, the resilience of spores to environmental stresses suggests that while vegetative cells may be sterilized during sequestration, spores will remain. However, the addition of CO₂ into the subsurface may also germinate other microbes, resulting in sterilization of some spore-forming organisms.

Experiments on CO₂ toxicity have largely originated in the food science area and are focused primarily on planktonic cell cultures, yet these represent only a minor fraction of the subsurface microbial community (Ballestra, Dasilva et al. 1996, Hong and Pyun 1999, Oule, Tano et al. 2006). Microbes also live as sessile communities composed of biofilms of bacterial cells and extracellular polymeric substances (EPS) attached to the mineral surface (Wanger, Southam et al. 2006, Gorbushina 2007). Microbes attach to minerals for many reasons. DIRB colonize iron oxide surfaces to give them a TEA in the absence of oxygen (Lovley 1993, Nealson, Belz et al. 2002, Lies, Hernandez et al. 2005). Microbes can also colonize silicate surfaces and dissolve minerals in order to obtain trace nutrients such as phosphate (Bennett, Rogers et al. 2001, Roberts 2004). Because microbes attach onto the mineral surface, the mineral itself acts as the local microbial habitat, providing a means of protecting or selecting against various bacteria during different stressful conditions.

The effect CO₂ will have on subsurface microbes will vary based on which organisms are present and how they interact with the aquifer mineralogy. Previous work has shown that biofilms are more resistant to CO₂ than planktonic cultures. Biofilms

grown on sandstones, for example, showed greater resilience to scCO₂ treatments than planktonic cultures (Mitchell, Phillips et al. 2008, Mitchell, Phillips et al. 2009, Santillan, Kirk et al. 2013). This may be due to the presence of EPS in the biofilms which act as a barrier to slow the diffusion of CO₂ into cells.

Microbial Geochemistry of CO₂ Sequestration

Microbes in saline aquifers will likely be affected by CO₂ in several ways. The aggressive fluid created by dissolved CO₂ will further accelerate mineral dissolution and free up other limiting nutrients such as carbon, phosphate, trace metals, and TEAs that potentially stimulate microbial growth (Kharaka, Cole et al. 2006, Kharaka, Thordsen et al. 2010, Kirk 2011). Stimulation of growth however, will also depend on microbial tolerances to CO₂, acidity, and the metal release caused during mineral dissolution. Those organisms capable of handling high amounts of CO₂ will be able to take advantage of the influx of nutrients added to the deep subsurface. This will result in their selection and potential dominance in the ecosystem. If Fe reducers are selected for in this new environment, the release of Fe²⁺ in the environment as well as the increase in alkalinity from Fe reduction could enhance both solubility trapping as well as mineral trapping with the creation of Fe-carbonates like siderite (Kirk 2011). However, if methanogens have the highest tolerance to high *PCO*₂ and the other environmental conditions, their selection will result in a buildup of CH₄, a molecule far less soluble than CO₂ but far more potent as a greenhouse gas. Leakage of CH₄ from saline aquifers could have the potential to counter the original intent of CO₂ sequestration, which is to decrease greenhouse gas emissions.

The mere physical presence of microbes in the deep subsurface will alter the immediate trapping of CO₂ on the pore scale. Biofilms colonizing pore spaces alter permeability, affecting the movement of CO₂ through groundwater (Mitchell, Phillips et al. 2009). Sterilization of microbes will cause a mobilization and alteration of subsurface permeability that will be difficult to quantify (Kirk, Santillan et al. 2012). Biofilms colonizing the mineral surface may potentially alter wettability, as charged surfaces on EPS may change the ability for CO₂ droplets to adhere onto mineral surfaces. This in turn can then change how liquid and supercritical CO₂ droplets adhere on surfaces during residual trapping (Chaudhary, Cardenas et al. 2013).

Research Questions

1. *What are the effects of CO₂ on growth and metabolism in microbial populations?* How do subsurface microbial populations respond to high pressures of CO₂? Is survival possible at high PCO₂? Are certain microbial metabolisms favored over others? Does microbial membrane and cell wall structure influence survival at high PCO₂?
2. *How does environment influence microbial CO₂ survival?* How does the mineralogy of a saline aquifer enhance or decrease survival under high PCO₂?
3. *How diverse are CO₂ rich environments?* Do microbial communities exist in high PCO₂ environments? How are these communities alike and how are they different? What environmental factors control diversity?
4. *Can microbes adapt to high pressures of CO₂?* Are microbes in high PCO₂ environments viable? What metabolisms are present at high PCO₂?

Hypotheses and Research Approach

Chapter 2: Previous work on microbes at high CO₂ pressures indicate that bacteria are generally sterilized. Because of this, I hypothesized that growth and metabolism will decrease in DIRBs. Additionally, because previous literature has shown G⁺ organisms to survive CO₂ exposure better than G⁻ organisms, I hypothesized that CO₂ sequestration will select for G⁺ bacteria. Lastly, methanogens utilize CO₂ as their TEA. The addition of this potential limiting nutrient will select for these organisms resulting in the enhancement of methanogenesis.

To approach this study, I studied 4 model organisms representing 2 different metabolisms and 3 different microbial membrane structures. These organisms were grown in batch cultures and exposed to CO₂ pressures ranging from 0.2 to 50 bar. Growth and metabolism was monitored and cellular responses were assessed through imaging and lipid analysis.

Chapter 3: I hypothesize that carbonate minerals including calcite, dolomite, and siderite would provide the best survival for microbes due to their ability to buffer the environment from large pH changes associated with CO₂ dissolution. Additionally, I postulated that minerals containing metals such as clays and feldspars would enhance microbial sterilization at high PCO₂ due to the release of toxic metals such as Al and As when these metals dissolve. To approach this, the model DIRB was grown in batch cultures to stationary phase and with minerals. Cultures were then exposed to lethal CO₂ pressures and tested for viability through plate counting and imaging.

Chapter 4: Because CO₂ is a stress on microbes, CO₂ springs represent an extreme environment that I hypothesized would host microbial communities.

Additionally, I hypothesized that organisms residing in these environments would represent capnophilic organisms including fermenters and methanogens. To approach this study, I sampled 3 different CO₂ springs and utilized 454 sequencing of the 16S rRNA gene. Alpha and beta diversity between samples was then compared through the use of the program QIIME (Caporaso, Kuczynski et al. 2010).

Chapter 5: Capnophilic organisms have been shown to grow in environments with atmospheres containing increased CO₂, generally with pressures ranging from 0.05 to 0.2 bar. In this chapter, I hypothesize that there are viable capnophilic organisms that can survive in CO₂ pressures of 10 bar or greater. Moreover, I postulated that these organisms require CO₂ as a metabolic requirement for growth. To approach this, I took field samples, cultured them in selective media, and grew them under pressure in the field. Enrichments were eventually tested for growth, metabolic capabilities, morphology, and lipid content.

Chapter2: Microbial Physiological and Morphological Responses to CO₂ Exposure

ABSTRACT

Microbial populations catalyze many important geochemical reactions in the subsurface. When CO₂ is sequestered in saline aquifers, these subsurface populations will be affected, potentially altering the geochemistry. To understand the effects CO₂ will have on these populations and the resultant geochemical effects, 4 model organisms were tested for their growth, metabolisms, membrane responses, and morphologies to high and low pressures of CO₂. The organisms were a Gram-negative (G⁻) dissimilatory iron reducing bacterium (DIRB) *Shewanella oneidensis* MR-1 (SO), a G⁺ sporulating bacterium *Geobacillus stearothermophilus* (GS), a G⁺ non-sporulating mutant *Bacillus subtilis* (BS), and a methanogenic archaeon *Methanothermobacter thermoautotrophicus* (MT). Growth and metabolism for SO and MT were assessed at CO₂ pressures ranging between 0 to 10 bar. Survival was determined for all four organisms by exposing stationary phase cultures to 0-50 bar PCO₂ and evaluating morphological and membrane changes. Results indicate that growth and metabolism decrease with increasing PCO₂, though the MT CH₄ production appears unaffected until 10 bar. Fe reduction is enhanced at the expense of growth, likely as a stress response to CO₂. Survival is poor at >10 bar PCO₂ for all organisms regardless of membrane structure due to intracellular disruption. At low PCO₂, both G⁻ and G⁺ express fatty acids suggestive of a decrease in cell size, typical as a stress response. In contrast, all organisms showed the ability to survive at low pH. Results indicate that while increased PCO₂ will result in a decrease in growth, metabolisms can still continue and may potentially be enhanced as a result of the increase

in stress. Furthermore, at PCO_2 below 10 bar, different organisms will have varied tolerance to CO_2 leading to the selection of organisms based on their tolerance to CO_2 . As a result, microbial populations will be redistributed based on tolerances to CO_2 changing the distribution of geochemical reactions occurring in saline aquifers.

INTRODUCTION

When CO_2 is sequestered in the deep subsurface, many changes to the environment will occur, including the introduction of a new stress to the native microbial populations. These microbes, which live in pore spaces and fractures within the host rock, perform many important geochemical transformations such as Fe reduction, H_2S generation, and methanogenesis. In order to understand the full effects of CO_2 on the subsurface environment, it is important to determine how these different microbial populations interact with CO_2 . The CO_2 effect on subsurface microorganisms is poorly characterized and needs to be determined in order to get a full understanding of the biogeochemical effects of CO_2 sequestration.

The deep subsurface sustains a microbial habitat that has largely been unexplored. While microbial counts in these environments can be low (Colwell, Onstott et al. 1997, Onstott, Phelps et al. 1998, Onstott 2003, Wanger, Southam et al. 2006), the deep subsurface comprises a large amount of the Earth's crust and stores a vast amount of Earth's biomass (Griebler and Lueders 2009, Reith 2011). Microbes have dwelled in these environments possibly since burial or from infiltration from groundwater, which could span time scales up to millions of years (Lee, James et al. 1997, Liu, Zhou et al. 1997, Onstott, Phelps et al. 1998, Gihring, Moser et al. 2006, Wanger, Southam et al.

2006, Wang, Lin et al. 2007, Sahl, Schmidt et al. 2008, Davidson, Silver et al. 2011).

While their titers are low, their long residence times in these reservoirs means that their metabolic byproducts have had the chance to accumulate, such as reduced Fe, CH₄ and associated minerals.

The deep subsurface is an extreme environment: microbes often reside in fairly saline, oligotrophic waters and it is likely they have very little input of nutrients from the surface. Nonetheless, microbes in the deep subsurface survive, partly because they utilize rocks and minerals in the environment for energy and nutrients. Iron minerals, for example, are utilized as terminal electron acceptors (TEA) for dissimilatory iron reducing bacteria (DIRB) (Lovley 1993, Liu, Zhou et al. 1997, Andrews, Robinson et al. 2003, Gorbushina 2007, Gadd 2010). Methanogens utilize CO₂ to produce methane (Pedersen 1993, Kotelnikova 2002, Whitman, Bowen et al. 2006). Microbes also actively dissolve minerals to get nutrients such as phosphate present in the rock (Bennett, Hiebert et al. 1996, Bennett, Rogers et al. 2001, Roberts 2004). When CO₂ is sequestered in the deep subsurface, the effects of CO₂ will likely alter the composition of the native microbial populations.

CO₂ at high pressures has a toxic effect on microbes. Previous work has shown that supercritical CO₂ can be used as a means to sterilize surfaces from biofilms (Nakamura, Enomoto et al. 1994, Isenschmid, Marison et al. 1995, Dillow, Dehghani et al. 1999, Oule, Tano et al. 2006). The supercritical fluid, which can extract organic molecules, readily diffuses into cells resulting in the removal of intracellular substances, the perforation of the cytoplasmic membrane, and the ejection of the intracellular

material (Oule, Tano et al. 2006, Oule, Dickman et al. 2010). In addition, CO₂ penetrating the cell likely acidifies the cytoplasm, further resulting in the inactivation of vital cellular functions (Dillow, Dehghani et al. 1999).

While CO₂ appears to have a bactericidal effect at high pressures, lower pressures of CO₂ can have bacteriostatic effects, i.e., the accumulation of the toxic substance is not enough to kill microbial cells but enough to inactivate them (Oule, Tano et al. 2006). In addition to acidifying the surrounding environment, CO₂ itself is neutral and liposoluble, easily diffusing across cell membranes and into the cytoplasm. This decreases cytoplasmic pH, denatures intracellular proteins, and disrupts membrane fluidity (Ballestra, Dasilva et al. 1996, Hong and Pyun 1999, Erkmen 2000, Damar and Balaban 2006, Oule, Tano et al. 2006). Most studies on the effects of CO₂ on microbes have been in the context of food and medical sciences, and very little has been done to characterize how CO₂ can affect organisms in an environmental context.

The threshold at which CO₂ causes bacteriostatic effects on cells may depend on the organism and its ability to detoxify against CO₂. Methanogens, for example, use CO₂ in their metabolic processes and may have ways to utilize increased CO₂ pressures to their advantage, allowing them to survive higher pressures than Fe reducers. This has immense implications on subsurface geochemistry as microbial populations may be redistributed based on their tolerance to high aqueous CO₂ resulting in different geochemical zones surrounding the supercritical CO₂ plume altering the dominant geochemical transformations occurring in the subsurface.

When CO₂ dissolves in groundwater, pH drops as carbonic acid is created. Ferric iron, which is abundant in saline aquifers, is more soluble at low pH values, freeing up a potential TEA for DIRB. This Fe mobilization was observed in sequestration pilot studies (Kharaka, Cole et al. 2006). An increase in available iron may enrich for DIRB who, in order to get energy from the oxidation of organic carbon, transfer electrons obtained from organic carbon and shuttle it to ferric iron. Additionally, CO₂ can act as a TEA for methanogenic archaea. With the addition of CO₂ into the environment comes an abundance of a resource that could initially have been limiting. Rock and mineral dissolution due to a pH drop may also free up trace metals such as Ni which are important cofactors in CH₄ metabolism (Kotelnikova 2002, White 2007).

In addition to examining subsurface microbial populations by their metabolic capabilities such as DIRB and methanogens, cells can also be examined by their morphology, and the differences in microbial morphologies may have implications on the types of organisms that will be selected for during CO₂ sequestration. Microbes in the deep subsurface are comprised of prokaryotes from the Archaeal and Bacterial domains as well as protists that graze on bacteria and viruses that infect the organisms. Of the microbes, the two prokaryotic domains have many differences, but one key difference is cell membrane structure: bacteria have cell membranes composed of ester-linked phospholipids while Archaea have membranes composed of ether-linked phospholipids (White 2007). This difference gives Archaea more membrane rigidity but also confers a tolerance to extreme environments such as very hot or very saline conditions (Chong

2010). Previous work has shown that both Gram-negative organisms and Archaea are sensitive to CO₂ regardless of their membrane structure (Santillan et al 2013).

Even within the Bacterial domain, organisms differ from each other in cell wall structure. Bacterial cell walls are composed in part of peptidoglycan and a key difference between Gram-positive (G⁺) and Gram-negative (G⁻) organisms is the thickness of this component. Gram-positive organisms have thick cell walls composed primarily of peptidoglycan while Gram-negative organisms have thin layers of peptidoglycan coated with a layer of lipopolysaccharides (LPS). In many cases, the thick cell wall present in G⁺ organisms confers advantages to environmental stresses that G⁻ bacteria do not have due to the thick reactive barrier of the wall (Cervantes, Ji et al. 1994). During CO₂ exposure, it has been hypothesized that the differences in cell wall and cell membrane thickness and rigidity may help organisms differ in their survival (Dillow, Dehghani et al. 1999). Previous work on CO₂ and G⁺ organisms however, have been inconclusive, as it could not be determined whether cell survival under high *PCO*₂ was due to the presence of a thick cell wall or from endospore formation (Santillan, Kirk et al. 2013).

There are many ways to determine CO₂ stress responses in bacteria, such as through the observation of metabolic rate by measuring substrate uptake, or the production of metabolic byproducts. Another, more specific method is to assess the nature of the membrane fatty acids and examine them for stress responses. Bacterial lipids are composed of a phosphate headgroup attached to a hydrocarbon tail. The hydrocarbon tail is a variety of fatty acids: saturated fatty acids (SFA), monounsaturated fatty acids (MUFA), polyunsaturated fatty acids (PUFA), branched fatty acids (BFA),

and cyclopropyl fatty acids (CFA) and can vary in relative abundances based on the organism. These fatty acids have different physical properties resulting in changes to microbial membrane fluidity and cell size.

During times of stress, bacteria alter the proportions of these various fatty acids to affect membrane fluidity, permeability, or cell size. In colder conditions, for example, bacteria often increase the relative abundances of MUFAs as these fatty acids have lower melting points and would keep a membrane more viscous in colder environments (Hazel and Eugene Williams 1990, Zhang and Rock 2008). At stationary phase, there is a prevalence of CFAs (Brown, Ross et al. 1997, Chang and Cronan 1999). In cases with the accumulation of a toxic substance, organisms that are unable to replicate may change their MUFA configurations to favor *trans* fatty acids over *cis* fatty acids in order to increase membrane packing and to decrease cell size (Keweloh and Heipieper 1996).

Our previous studies have shown that laboratory model organisms are killed off at PCO_2 of 10 bar and greater (Santillan, Kirk et al. 2013). Because of this, the aim of this study was to determine how microbes respond to CO_2 pressures when it induces bacteriostatic effects and at what pressures cultures may stop being metabolically active.

MATERIALS AND METHODS

The approach of this study was to culture organisms representative of both the types of membrane structures and metabolisms potentially present in saline aquifers. Growth and survival was assessed for PCO_2 below 10 bar, PCO_2 above 10 bar, and low pH conditions. Cellular responses were then determined by observing changes in metabolism, cell structure, and lipid content.

Model Organisms

Shewanella oneidensis (SO) strain MR-1 (ATCC BA-1096) is a G^- , facultative aerobe. This organism is capable of utilizing multiple TEAs, including NO_3^- , Mn, $S_2O_3^{2-}$, U, and Fe. The organism is found in many environments, especially sedimentary and deep sea. This organism was used to represent G^- bacteria as well as DIRB.

Geobacillus stearothermophilus (GS, ATCC 7953) is an aerobic, thermophilic, G^+ , spore forming bacterium. This organism has been isolated from multiple environments including hot springs and oil fields. For these experiments, GS was used to represent G^+ bacteria as well as sporulating microbes.

Bacillus subtilis (BS) Δ sp01 mutant was obtained through the Bacillus Genetic Stock Center (BGSC 1S53, Columbus, OH). BS is a mesophilic, aerobic G^+ bacterium found commonly in soils and vegetation. It is normally capable of forming endospores but due to a deletion in the sp01 gene, this particular strain cannot. This organism was used in our experiments to determine G^+ CO_2 survival in the absence of endospores.

Methanothermobacter thermoautotrophicus (MT, ATCC 29096) is an obligately anaerobic, thermophilic archaeon. MT produces methane by utilizing H_2 and CO_2 and is found largely in subsurface and hot spring environments. MT was chosen to represent methanogenic as well as archaeal membrane responses to CO_2 .

Culture Conditions

Shewanella oneidensis strain MR-1, *Geobacillus stearothermophilus*, and *Methanothermobacter thermoautotrophicus* were cultured under conditions previously described (Santillan, Kirk et al. 2013). *Bacillus subtilis* Δ sp01 mutant (BS) was initially

grown in tryptic soy broth (TSB) to stationary phase. For experiments, BS was grown aerobically in a minimal medium composed of (per L of distilled water): 0.2 g nitrilotriacetic acid, 0.15 g $\text{MgSO}_4 \cdot 7\text{H}_2\text{O}$, 0.1 mg $\text{CaCl}_2 \cdot 2\text{H}_2\text{O}$, 0.11 mg $\text{FeSO}_4 \cdot 7\text{H}_2\text{O}$, 0.5 g K_2HPO_4 , 0.2 g KH_2PO_4 , 0.3 g NH_4Cl , and 0.5 g NaNO_3 . Cultures were given 2 mM glucose as the electron donor. Media was brought to pH 7 with the addition of 10% KOH and autoclaved.

CO₂ Experiments

Both growth and survival were both assessed in the presence of CO₂. Growth experiments were performed at relatively lower PCO_2 to determine if organisms could metabolize and potentially respond to increased CO₂ present in the environment. Survival experiments were performed at higher PCO_2 than growth experiments to determine how long healthy cultures could survive at lethal CO₂ pressures.

Growth and metabolism experiments for cultures exposed to CO₂ pressures below 10 bar were grown in 10 mL of sterile media in 15 mL borsilicate hungate tubes with butyl stoppers, pressurized with CO₂. Headspace gas for GS cultures was evacuated twice daily and repressurized using a gas mix containing approximately 80% N₂ and 20% O₂, followed by the addition of CO₂. MT cultures were kept in 30 ml serum bottles capped with butyl stoppers to ensure cultures remained anaerobic. For experiments looking at the effects of acidic pH, media was acidified with 1 N HCl to a set pH prior to autoclaving. Growth was monitored using optical density (OD₇₀₀) and Fe reduction was monitored through the ferrozine method (To, Nordstrom et al. 1999). CH₄ production was monitored

through gas chromatography. Growth of MT cultures was not assessed as serum bottles were not conducive to optical density measurements.

For survival experiments, stationary phase cultures grown in hungate tubes were then pressurized in 2 bar CO₂ for 2 to 24 hours. SO cultures were also kept at 2 bar for 66 days to determine any long-term cell changes associated with CO₂. For experiments above 10 bar, cultures were grown in 10 ml borosilicate test tubes with plastic caps containing media as described above. Cultures were then exposed to varying CO₂ pressures by placing test tubes in modified Parr reactors as described previously (Santillan, Kirk et al. 2013).

Lipid Extraction and Identification

Prior to lipid extraction, bacterial cultures were centrifuged and then freeze dried. Lyophilized samples were then microwave extracted (CEM MARS 100°C, 10 minutes) using 20 mL of a 9:1 methylene chloride:methanol mixture to provide a total lipid extract. The lipid extract was evaporated under N₂ and saponified at 70°C for 1 hour using a 0.5 M NaOH solution. The solution was cooled, acidified, and then extracted 3 times using methyl tert-butyl ether (MTBE). Samples were then evaporated and resuspended in methylene chloride for column purification.

Solid phase extraction of fatty acids was performed using an amino-propyl stationary phase (0.5 g of Supelclean-NH₂⁺, Supelco, Bellefonte, PA). Fatty acids were eluted with 50:1 DCM/formic acid. The fraction was then evaporated under N₂ and resuspended in hexane.

Fatty acids were converted into fatty acid methyl esters (FAMES) using previously described methods (Rodriguez-Ruiz, Belarbi et al. 1998). Samples were methylated using a 20:1 methylation mixture of methanol/acetyl chloride. Samples were then heated at 100°C for 10 minutes and cooled to room temperature. After cooling, distilled water was added to create two phases. The upper hexane phase was extracted, and concentrated prior to analysis.

Samples were characterized and quantitated by gas-chromatography mass-spectrometry (GC-MS). One microliter of the sample in hexane was injected into an Agilent 7890A GC with a split/splitless injector operated in splitless mode at 300 °C, a DB-5 column (0.25mm i.d., 0.25 µm film thickness, 30m length), 2.0 cm³ min⁻¹ He flow and programmed heating of the oven from 40 to 170°C at 4°C/min then to 240°C at 30°C/min. An Agilent 5973 quadrupole mass spectrometer was used for detection. Compounds were identified by elution time and comparison with published mass-spectra.

Transmission Electron Microscopy

Samples were prepared for transmission electron microscopy (TEM) following methods outlined by (Romanovicz 2011). Pelleted samples were fixed overnight in a 2.5% glutaraldehyde solution. After 2 washes and centrifugations with a 0.1 N Na-cacodylic buffer, cultures were stained using a 1 mL mixture of 1% OsO₄ solution and 2% K-ferrocyanide for 1 hour. Stained pellets were washed with cacodylic buffer and suspended in thin (approximately 0.5 cm) 3% agarose “worms.” Agarose-suspended samples were incubated in 50% ethanol for 15 minutes and transferred to a solution

containing 2% uranyl acetate in 70% ethanol for 2 hours. After incubation in uranyl acetate, samples were sequentially dehydrated in ethanol solutions starting with 90% to 100% for 15 minutes each. Samples were twice rinsed in LR White resin and embedded in the same resin.

Embedded samples were then sliced into 70 nm thin sections with a diamond knife (DiATOME, Hatfield, PA) using a Leica Ultracut UTC Ultramicrotome at the University of Texas ICMB Core Facility (Austin, TX). Images were viewed using a FEI Tecnai Transmission Electron Microscope at the same facility.

RESULTS

Growth and Metabolism

From 0.2 to 2 bar, SO growth and metabolism decreases with increasing PCO_2 , with almost no measurable growth and Fe reduction above 1.4 bar (Figures 2-1A and C). The highest cell density is from cultures grown with no CO_2 supplied. Decrease in cell counts occurs in steps: there is a 10^8 cells/ml decline in stationary cell count with the addition of 0.2 bar PCO_2 and another with 0.4 bar. By 0.8 bar CO_2 , stationary phase cell counts are only $\frac{1}{4}$ of cell counts with no CO_2 added and very little growth measured by 2.0 bar.

From 0 to 1 bar, Fe reduction is still observed. There is an 89% reduction in the amount of Fe^{2+} produced at 1.4 bar compared to the maximum amount of Fe^{2+} produced. At 2 bar, there is a 96% reduction (Figure 2-1C). However, after 3 days of incubation under elevated CO_2 conditions, cells still survive as depressurization of tubes produced turbidity in culture tubes after 1 day. When expressed as a ratio of the amount of Fe^{2+}

produced/cell, results indicate that more Fe^{2+} is produced/cell at 1.0 bar PCO_2 and decreases with both increasing and decreasing PCO_2 . At 1.4 and 2.0 bar, there is very little Fe^{2+} produced/cell (Figure 2-1E).

Growth with nitrate and thiosulfate as the electron acceptors also diminishes with increasing CO_2 pressures following curves similar to that of Fe (Figure 2-2A and B). However, the decrease in growth with thiosulfate was initially more gradual but with a large decline in stationary phase cell counts between 1.4 to 2 bar (Figure 2-2B). A similar response is seen for NO_3^- reduction: there is a gradual decrease in growth until 0.8 bar when there is a large drop in stationary phase cell counts (Figure 2-2A).

To assess the whether CO_2 toxicity is principally due to media acidification, SO cultures were grown with Fe as the TEA in HCl acidified media corresponding to pH changes associated with increased PCO_2 . Cultures were pressurized with N_2 gas at corresponding CO_2 pressures to ensure changes in survival were not associated with pressure effects. After 70 hours of incubation, SO exhibits optimal growth at pH values of 6.61 and greater. Slight decreases in growth and Fe reduction occur as pH decreases (Figures 2-1B and D) though there was also a slight benefit to Fe reduction at a few pH values lower than 7.

At increasing pH, there is a lot of variability between replicates of Fe reduced/cell during the lag phase. However, results indicate that the most Fe^{2+} released per cell is highest at pH 6.32 followed by pH 6.43, then pH 6.19. Fe^{2+} released per cell is moderate at neutral pH and lowest at pH values of 6.80 and 6.67 although the titer is higher at these pH values. After 80 hours of growth, the amount of Fe^{2+} released per cell reaches similar

values for all cultures (Figure 2-1F) but is much lower than values of Fe^{2+} released per cell for cultures exposed to CO_2 .

Growth with thiosulfate varies slightly with different pH values with the most growth found at a pH of 6.74 and the least growth found at 6.29, though there was no trend towards decreased growth with decreasing pH (Figure 2-2D). Growth with NO_3^- exhibits pH sensitivity with optimal growth seen at pH 6.5 and the least growth seen at pH values less than 6.36 (Figure 2-2C).

Previous work has shown stationary phase GS to survive all pressures of CO_2 . To determine if survival was due to endospore formation or due to the thick cell wall of a G^+ bacterium, BS was exposed to a similar suite of PCO_2 to GS, as described in Santillan et al. (2013). BS exhibits poor survival at high PCO_2 with cultures surviving at 10 bar up to 8 hours. Survival lasted less than 2 hours at 25 bar and at 50 bar (Table 2-1).

To determine whether CO_2 toxicity for BS is principally due to the acidification of the media, stationary phase cultures were exposed to pH 4.5 for 2 to 24 hours using HCl. Results are similar to SO, GS, and MT cultures with cells showing viability beyond 24 hours of exposure (Table 2-1). BS cultures exposed to pH 4 retain the same morphology as unstressed BS cells.

GS cultures exposed to CO_2 as low as 0.2 bar showed no growth in comparison to unexposed cultures. In contrast, acidified cultures grown in acidified media showed enhanced growth in comparison to cultures grown at pH 7. Growth was best at pH values of 5.79 and 6.11 (Figure 2-3 A and B).

MT methane production is slightly decreased at increasing PCO_2 from 0.2 to 4 bar. In these cultures, headspace CH_4 values level off between 80 to 110 hours, indicating cultures have reached stationary phase. At 10 bar, methane production still occurs, however, the amount of headspace methane present is an order of magnitude less than cultures grown with 4 bar CO_2 . At 10 bar, some methane is still produced although cells begin to lose viability after 8 h of exposure (Santillan et al 2013) (Figure 2-4). Methane production was also observed when cultures were acidified.

Morphology

SO cells in control cultures are rod-shaped. Cells contain a periplasmic space clearly visible between the cell wall and the cell membrane. The inner cell shows an even distribution of intracellular material. Under CO_2 stress, SO's rod shape begins to lose its rounded appearance and cell shape becomes more irregular. CO_2 stressed cells exhibit an intracellular disruption in the form of the clumping of cytoplasmic material. When exposed to pH 4.5, SO retains a similar appearance to healthy SO cells. However, surrounding the SO cell wall is a wavy sheath (Figure 2-5A to C).

GS cultures, while also rods, also contain cells that are more rectangular in shape. As with SO cultures, GS cells have a visible cell wall and cell membrane. Additionally, endospores are visible in GS cultures. Cells containing endospores also exhibit similar morphologies to non-endospore containing cells including a rod-shape and an evenly distributed intracellular material (Figure 2-6A and C).

After 2 hours of 50 bar CO_2 exposure, GS cells maintain the same rod shape though this shape begins to exhibit irregularities along the cell wall. Like SO cultures, the

intracellular material of stressed GS cultures shows clumping. However, endospores present in CO₂ exposed cultures look similar to endospores present in healthy GS cultures. Cells containing endospores exhibit intracellular clumping and increased waviness to the cell walls (Figure 2-6B and D).

Unstressed BS cells are rods with a slight rectangular appearance. They contain a visible cell wall as well as an evenly distributed cytoplasm. Within cells is a dark aggregate of material, presumably a malformed endospore as this organism contains a deletion in a sporulating gene. After 24 hours of exposure to 50 bar of CO₂, a similar intracellular clumping can be observed in BS cells. Stressed cells also exhibit irregularities in shape (Figure 2-7A to C).

MT cells display differing morphologies at varying CO₂ pressures. Unexposed MT cells are rod-shaped, and contain an even distribution of cytoplasmic contents within the cell. Additionally, small black dots, possibly precipitates are present unevenly within the cell. MT cells exposed to 25 bar CO₂ for 24 hours display a less even intracellular distribution, especially within the cell center and contain more intracellular precipitates. Acid-exposed MT cells showed the largest amount of intracellular unevenness. Acid-stressed cells have a wavy, clumped appearance within the cell, with cells appearing to lose cohesion (Figure 2-8A to C).

Membrane Response

Changes in lipid composition were examined for bacterial cells at lethal CO₂ pressures, determined from Santillan et al. (2013) to verify loss in cell viability and not culturability. Figure 2-10A shows changes in SO lipid composition over time. At higher

(25 bar) PCO_2 , there is little change between the relative abundances of fatty acids after 2 hours of incubation. After 8 h exposure, there is 20% increase in the relative abundance of SFA. There is also a slight increase in the relative abundance of PUFA and a decrease in the relative abundance of MUFAs.

Relatively few fatty acids comprise the GS cell membrane. Approximately 80% of GS cell membrane is composed of SFA shown in Figure 2-10B. There are also some MUFA and PUFAs present as well. There is little change between control cultures and CO_2 exposed cells at 50 bar.

BS fatty acid composition favors SFA and BFA (Figure 2-10C). At 25 bar CO_2 exposure, BS experiences an initial increase in saturated fatty acid relative abundance at 2 hours followed by a drop at 8 hours. The relative abundance of branched fatty acids also decreases initially but increases after 8 hours. There is also a steady increase in MUFA and PUFA relative abundance over the course of the 8 hour incubations.

Lipid responses to sublethal CO_2 pressures was also examined for both SO and BS as these two organisms showed the most sensitivity to CO_2 . Figure 2-9 show fatty acid ratios for stationary phase cultures exposed to 2 bar PCO_2 . For the first 8 hours of exposure to PCO_2 , there is slight increase in MUFA and BFA relative to SFA which begins to decrease by 24 hours. There is a steady decrease in CFAs relative to SFAs over the course of incubation. There is also an increase in trans fatty acids relative to cis fatty acids for the first 24 hours of exposure. By 66 days of exposure, this ratio changes to show an increase in cis fatty acids. Over the course of 24 hours CO_2 exposure at 2 bar, BS increases in MUFA and PUFA content relative to SFA. There is also an initial

increase in BFA relative to SFA in the first 2 hours of exposure. By 8 hours and 24 hours, the amount of BFA decreases. (Figure 2-9A and B).

DISCUSSION

At lower pressures, CO₂ demonstrates its bacteriostatic effects where microbes retain some limited functionality despite the increased CO₂. However these effects can be reversible. After 1 month of incubation at high *PCO*₂ followed by a depressurization, cultures rebounded and reached stationary phase. Additionally, GS spores remained viable even after 1 month of incubation at 2 bar. In deep subsurface conditions, this could be important because inactive cells may lay dormant until conditions change.

In SO, both growth and metabolism can still occur, albeit in a limited capacity for all TEAs tested. With slight (0.2 bar) increases in *PCO*₂, SO growth declines, with an order of magnitude difference in stationary phase cell density from control cultures to 2.0 bar *PCO*₂ (Figures 2-1A, 2-2A, and 2-2B). Fe reduction continues up to 1.0 bar *PCO*₂ suggesting cells are still metabolizing at these CO₂ stresses despite decreased cell counts (Figure 2-1B). This limited metabolism suggests cells under CO₂ stress during sequestration still have the capability of altering geochemistry, such as through iron reduction or methanogenesis. Similar metal reduction results were observed for manganese respiration (Wu, Shao et al. 2010).

One potential explanation for the decrease in Fe reduction during CO₂ exposure could be thermodynamic, where the increase of products in the system may cause the reaction to go in reverse, such as in the oxidation of lactate with the reduction of goethite:



In this case, the buildup of CO_2 in the products means iron will not be reduced and the reaction will not proceed forward. The fact that an enhancement in Fe reduction per cell at higher $P\text{CO}_2$ is observed suggests that the decreases in growth and Fe reduction at high $P\text{CO}_2$ may also involve cellular mechanisms in addition to thermodynamic reasons. Furthermore, an increase in acidity in the medium should result in an enhancement in Fe reduction. However, in most cases where the media is acidified, there is less Fe reduced per cell in comparison to CO_2 exposed cultures, further showing that CO_2 effects on DIRB are more complex than simply the thermodynamic favorability of the reaction and must involve interactions with the cell as well (Figure 2-1 E and F).

Figure 2-2A and B demonstrate that CO_2 affects multiple cell functions in SO beyond cell division and Fe respiration. However, the differences in sensitivity to CO_2 when supplied with different TEAs suggests respiration for these different TEAs may be located within different parts of the cell that may be more sensitive to CO_2 . Nitrate and Fe respiration, for example, take place in the periplasm where CO_2 may diffuse into the cells first and affect the cell's ability to utilize these TEAs (Heidelberg, Paulsen et al. 2002). Thiosulfate respiration may take place further inside the cell where intracellular buffering may allow for respiration to continue happening at slightly higher $P\text{CO}_2$. Once this intracellular buffering is affected, all growth and metabolism then stops. This suggests that metabolic functions that occur inside the cell are better preserved than those that occur on the cell membrane and that cells that have intracellular respiration capabilities may survive the best under CO_2 stress.

Similarly, growth is inhibited in GS when exposed to CO₂ and this inhibition is not due to the acidification of the surrounding environment. Its tolerance to CO₂ appears far lower than that of SO, with bacteriostatic pressures beginning as low as 0.2 bar. Its low tolerance for CO₂ further shows that cell wall thickness is not a factor in CO₂ survival. Furthermore, respiration for this aerobic organism is a membrane-bound function, further adding to the hypothesis that CO₂ likely inhibits membrane functions (Figure 2-3A and B).

If CO₂ affects cells internally, multiple functions are likely disrupted as a result including DNA replication, glycolysis, and respiration. Under stress, cells may be expending energy to survive at the expense of multiple functions, such as growth, as evidenced in Figure 2-1E, where more Fe is reduced *per cell* under increased *PCO₂* despite decreases in titer with increasing *PCO₂*. This carries important implications to DIRB affected by carbon sequestration. CO₂ may cause a decrease in cell growth but the *PCO₂* within the environment may actually enhance Fe reduction, and this creates the potential to significantly remove acidity in the environment, aiding in the solubility trapping of CO₂. The increase in bicarbonate concentrations will also raise alkalinity, enhancing the favorability of carbonate precipitation and mineral trapping (Kirk 2011) following the equation:



Methanogens also exhibit CO₂ sensitivity although methanogenesis appears more tolerant to higher CO₂ pressures than Fe reduction. MT continues to produce methane at

PCO_2 ranging from 0.2 to 4 bar. At 10 bar, some CH_4 is produced, however cells lose viability after 8 hours of exposure and CH_4 production plateaus (Santillan, Kirk et al. 2013) (Figure 2-4). Similar to thiosulfate reduction, methanogenesis is a process that happens intracellularly, and the organism's heightened ability to tolerate PCO_2 may stem from the amount of buffering present within the cell as methanogens tend to contain enzymes like carbonic anhydrase to fix CO_2 into bicarbonate to increase the efficiency of methanogenesis (Ferry 1999). At some point, the amount of CO_2 present is too much for the enzyme to actively detoxify and MT is inactivated.

Though methanogenesis is inactivated at 10 bar, this metabolism is not completely inhibited at lower PCO_2 and methanogenic archaea may still be important when figuring out the fate of solubility-trapped CO_2 over long time scales. Because CH_4 is far less soluble than CO_2 ($K_{HCH_4}=10^{-2.83}$, $K_{HCO_2}=10^{-1.47}$), the long term activities of methanogens can result in the creation of CH_4 plumes that will reside at the caprock rather than dissolve into the surrounding groundwater. Leakage of methane from the aquifer would then be counter to CO_2 sequestration as CH_4 is a much more potent greenhouse gas.

The pH effect on microbes at corresponding CO_2 pressures, is at most, bacteriostatic. There is a slight pH effect on microbes, although this effect is not as severe as the effect seen with increased PCO_2 and growth and survival does not decrease significantly with increased acidity. When SO was grown in pH values that matched their corresponding PCO_2 , there was even a slight benefit to growth and Fe reduction at a lower pH.

Growth and Fe reduction were optimum at pH values of 6.48 and 6.60 though the highest amount of Fe reduced per cell was between pH values of 6.19 to 6.32 suggesting an increase in Fe reduction due to acid stress, though differences between treatments were slight. Growth with thiosulfate was not significantly affected by decreased pH further supporting the hypothesis that CO₂ effects on cells are different than pH effects.

Unlike Fe and thiosulfate, SO growth with NO₃⁻ decreases with lower pH. While growth with NO₃⁻ occurred between pH values of 6.5 to 7.0, there is a sharp drop in growth at pH 6.26 suggesting NO₃⁻ reduction occurs at a narrow pH range for SO. Environmental NO₃⁻ reduction can occur at pH ranges from 5.5 to 8.0 indicating SO is more sensitive to pH during NO₃⁻ reduction than other denitrifying organisms possibly due to a difference in its nitrate reductase activity (Rivett, Buss et al. 2008). Denitrifiers exhibit variations in nitrogen byproducts with pH. At higher pH values, NO₃⁻ is reduced to N₂. At lower pH values, NO₂⁻ dominates as the byproduct, which can be toxic to organisms (Simek, Jisova et al. 2002, Rivett, Buss et al. 2008). The accumulation of NO₂⁻ may alternatively explain the decrease in growth at decreased pH.

MT exhibits a resilience to low pH, though the organism does display signs of stress. When stationary phase cultures are exposed to pH values of approximately 4.5, CH₄ production is still observed. Cultures taken from these low pH conditions and recultured also regrow, indicating cells remain viable under these conditions (Santillan et al 2013).

At 10 bar and greater, CO₂ is bactericidal among cells of different membrane morphology. Previous work characterizing differences in CO₂ survival among different

membrane morphologies suggested G^+ cells were best at surviving very high pressures of CO_2 (Santillan, Kirk et al. 2013). The G^+ GS showed survival beyond 50 bar PCO_2 , though it was never determined whether its ability to survive these pressures was due to its membrane structure or its ability to form endospores, which are dormant, non-metabolizing cells. Experiments with BS indicate that the ability for GS to survive CO_2 was indeed, due to its ability to form endospores, as the strain of BS utilized in these studies was incapable of forming these structures. This suggests that during CO_2 sequestration, bacteria can survive within areas of very high CO_2 though the structures residing in these conditions will be nonviable. At 10 bar or greater, CO_2 is bactericidal and differences in membrane structure across domains and within bacteria do not appear to confer any increase in survival (Table 2-1) (Santillan, Kirk et al. 2013).

TEM images present evidence of an intracellular disruption occurring for cells exposed to lethal CO_2 pressures, possibly explaining the bactericidal effects of CO_2 (Figures 2-5B, 2-6B, 2-7B, and 2-8B). All unexposed cells exhibit uniformly distributed cytoplasmic contents. However, the exposure to high pressures of CO_2 changes cell morphology to show clumping and coagulation within the cytoplasm, changing the distribution of the intracellular contents to make them uneven. This change in cell morphology suggests CO_2 has a disruptive effect on the inner cell, translating to a loss in cell function and viability. Previous work has shown that the result of CO_2 toxicity on cells is the acidification of the cell's cytoplasm, resulting in the denaturation of intracellular proteins, metabolites, and DNA (Ballestra, Dasilva et al. 1996, Hong and

Pyun 1999, Erkmen 2000, Oule, Tano et al. 2006). TEM images of this clumping morphology may be evidence of this happening.

In comparison, TEM images of bacteria under pH stress do not exhibit the intracellular disruption found during CO₂ stress, and in some cases, cells show a morphological response to pH. Instead, cells appear to generally have a similar morphology to healthy cells. In addition, TEM images of acid stressed SO cells show the presence of a wavy sheath surrounding the cells which may be an extracellular method to actively slow down the diffusion of proton into the cell (Kidd 2011). MT cells, unlike the bacteria, showed evidence of stress during pH exposure with a loss of evenness of the cytoplasmic distribution of the organism. While this particular methanogen exhibits stress under low pH conditions, there are methanogens that can produce CH₄ at low pH (Kotsyurbenko, Friedrich et al. 2007) and this methanogen is still able to produce CH₄ at decreased pH.

Previous work has shown that at 25 bar CO₂ exposure causes a total loss in cell viability after 2 hours of exposure in SO (Santillan, Kirk et al. 2013). The similarity in SO fatty acid composition between control and 2 hour-exposed cells suggests cells were quickly inactivated and killed without any ability to respond to the CO₂ stress. The lipid composition after 24 hours may simply reflect cell degradation with MUFA and CFAs degrading first and increasing the relative abundances of SFAs. Similarly, GS does not respond to high pressures of CO₂ as lipid profiles follow similar patterns to SO (Figure 2-10A and B) further showing evidence that G⁺ organisms are not necessarily better at CO₂ survival than G⁻ organisms.

At 25 bar of exposure, BS exhibits a sharp decrease in BFA relative abundance followed by a sharp increase after 8 hours of exposure. This is also concomitant with a sharp increase in SFA followed by a sharp decrease. Our data shows that BS is extremely sensitive to 25 bar CO₂ and loses viability by 2 hours of exposure. This sharp decrease in BFA may also be an initial, response to high PCO₂ between 0 to 2 hours of exposure. Because BFAs increase membrane fluidity, BS may be rapidly removing this from its membrane to decrease fluidity as a final survival attempt. After 8 hours, cells are no longer viable and lipid profiles may be reflecting degradation (Figure 2-10C).

Membrane data at low PCO₂ indicates cells are attempting a response to CO₂ stress. At low PCO₂, the ratio of *cis* to *trans* MUFA for SO decreases with length of exposure. This ratio increases over the course of a 66 day incubation however. Previous work has shown that the isomerization of fatty acids aids in bacterial membrane structure can happen as a stress response where cells are unable to replicate due to the accumulation of a toxic, bacteriostatic substance (Keweloh and Heipieper 1996). The change from *cis* to *trans* configuration increases membrane packing to make cells smaller and more stable (Figure 2-9A).

Both SO BFA and MUFA abundances initially increase then decrease relative to SFA over a 24 hour exposure. An eventual increase in SFA over time is indication of tighter membrane packing, useful for decreasing cell size. CFA abundance decreases over the course of CO₂ exposure and is another stress response reported in bacteria linked to membrane rigidity (Veerkamp 1971, Brown, Ross et al. 1997, Chang and Cronan 1999). CFAs are energetically costly to make and its decrease in abundance suggests SO is

diverting energy costs from membrane modification to other stress responses. After 66 days of CO₂ exposure, MUFA, BFA, and CFA all decrease relative to SFA suggesting over a long-term exposure, SFAs are produced to help cells shrink (Figure 2-9A).

G⁺ organisms, though sensitive to CO₂ appear to have a different membrane CO₂ response than SO. BS fatty acids are largely composed of BFAs and SFAs consistent with findings from Kaneda (1977). During stress at 2 bar *PCO*₂ BS increases its BFA content followed by a sharp decrease after 8 hours, a reaction opposite to that found at 25 bar. The eventual decrease in BFAs is also concomitant with an increase in both MUFA and PUFA suggesting a response to increased CO₂ pressures is to increase cell packing through a SFA increase (Zhang and Rock 2008). There is also a slight increase in MUFAs and PUFAs, suggesting BS still attempts to maintain some membrane fluidity as cell sizes shrink (Kaneda 1991) (Figure 2-9B).

Our data shows that while CO₂ is toxic to cells at high pressures, cells are still capable of response, growth, and metabolism to lower pressures. Moreover, while growth decreases as a function of increasing *PCO*₂, metabolism can actually increase per cell, likely as a means to spend energy on detoxification. This has important geochemical ramifications: CO₂ sequestration may actually enhance the activities of organisms such as Fe reducers and methanogens. The fact that these metabolic guilds may still function at increased efficiencies in the subsurface suggests an added complication to the fate and movement of CO₂ dissolving into the groundwater that should be characterized and considered when tracking the CO₂ plume.

Additionally, the differences in survival among varying cell morphologies suggests CO₂ sequestration may redistribute subsurface microbial populations. This may effectively create geochemical “zones” surrounding the supercritical CO₂ where different microbial processes will be occurring based on the organism’s CO₂ tolerance. Methanogens, for example, may be selected in locations of higher *PCO₂* while Fe reducers may be on the outer fringes of the solubility-trapped CO₂.

Of the organisms surveyed, organisms that were able to metabolize under the highest *PCO₂* were the organisms with metabolic processes occurring internally, namely MT, where methanogenesis occurs within the cell unlike Fe or NO₃⁻ reduction that happens in the cell’s periplasm. Other organisms with internal metabolic processes, such as fermenters, are also capable of survival and metabolism under high CO₂ pressures (Santillan et al, in prep). This suggests that cells containing internal mechanisms to utilize and detoxify CO₂ will be the best at surviving the added disturbance to the subsurface system and that membrane-dependent metabolisms will be most susceptible to CO₂ toxicity. At lower *PCO₂*, cells are stressed and decrease in size, however they still maintain some limited viability or exhibit dormancy. Dormant cells will not be metabolizing and would pave the way for other opportunistic organisms that can tolerate high *PCO₂* to dominate the subsurface community. However, given the large amount of horizontal gene transfer among organisms, it may be possible that even dormant organisms would eventually adapt to a high CO₂ environment.

	2 bar	10 bar	25 bar	50 bar	pH 4.5
2 hours	+	+	-	-	+
8 hours	+	+	-	-	+
24 hours	+	-	-	-	+

Table 2-1 *Bacillus subtilis* survival at varying PCO_2 and pH 4.5.

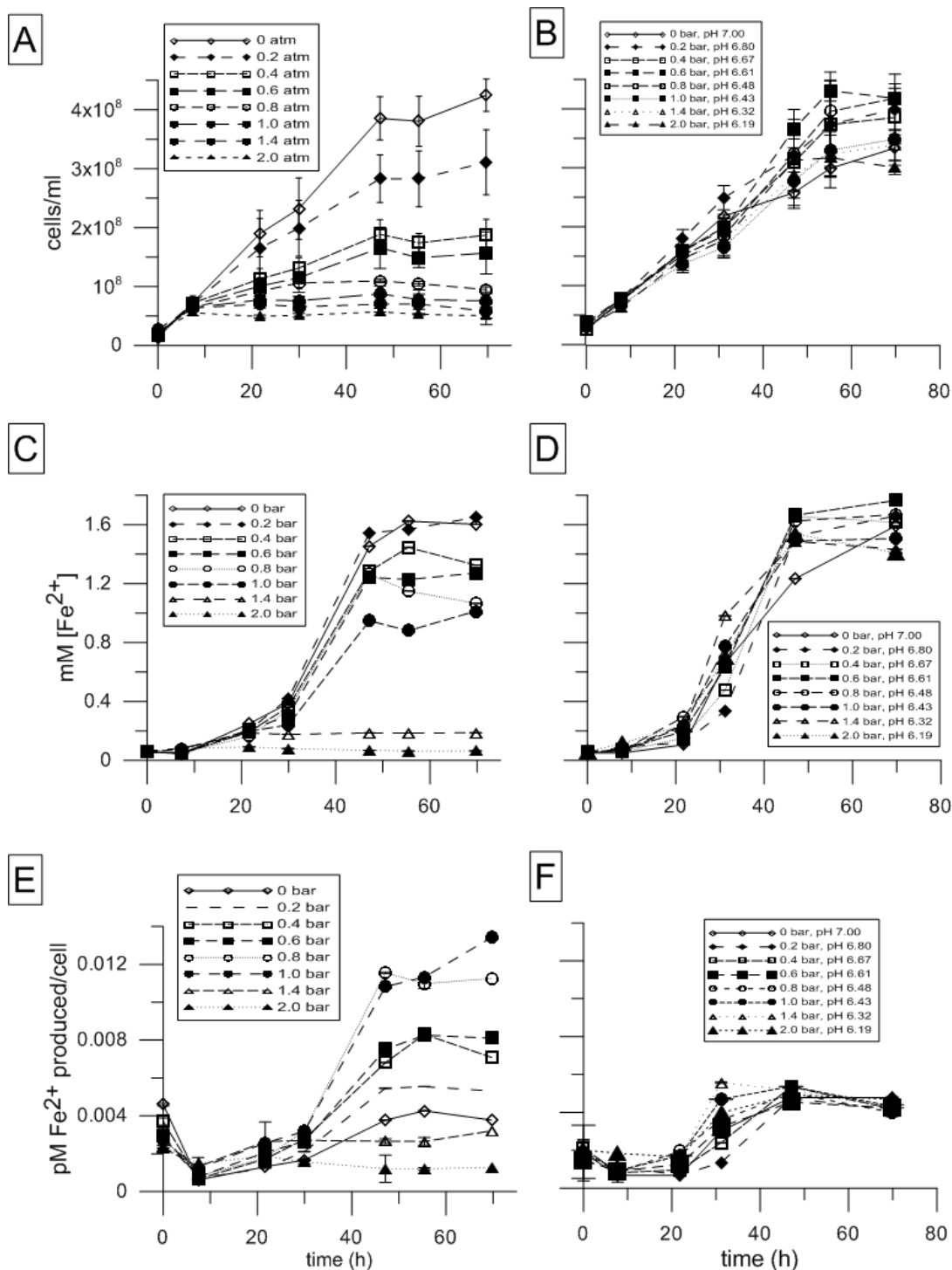


Figure 2-1 *Shewanella oneidensis* growth and iron reduction. (A) Growth with increasing PCO_2 ; (B) growth with decreasing pH and increasing PN_2 ; (C) Fe reduction at increasing PCO_2 ; (D) Fe reduction at decreasing pH and increasing PN_2 ; (E) Fe reduction per cell with increasing PCO_2 ; (F) Fe reduction per cell with decreasing pH and increasing PN_2 .

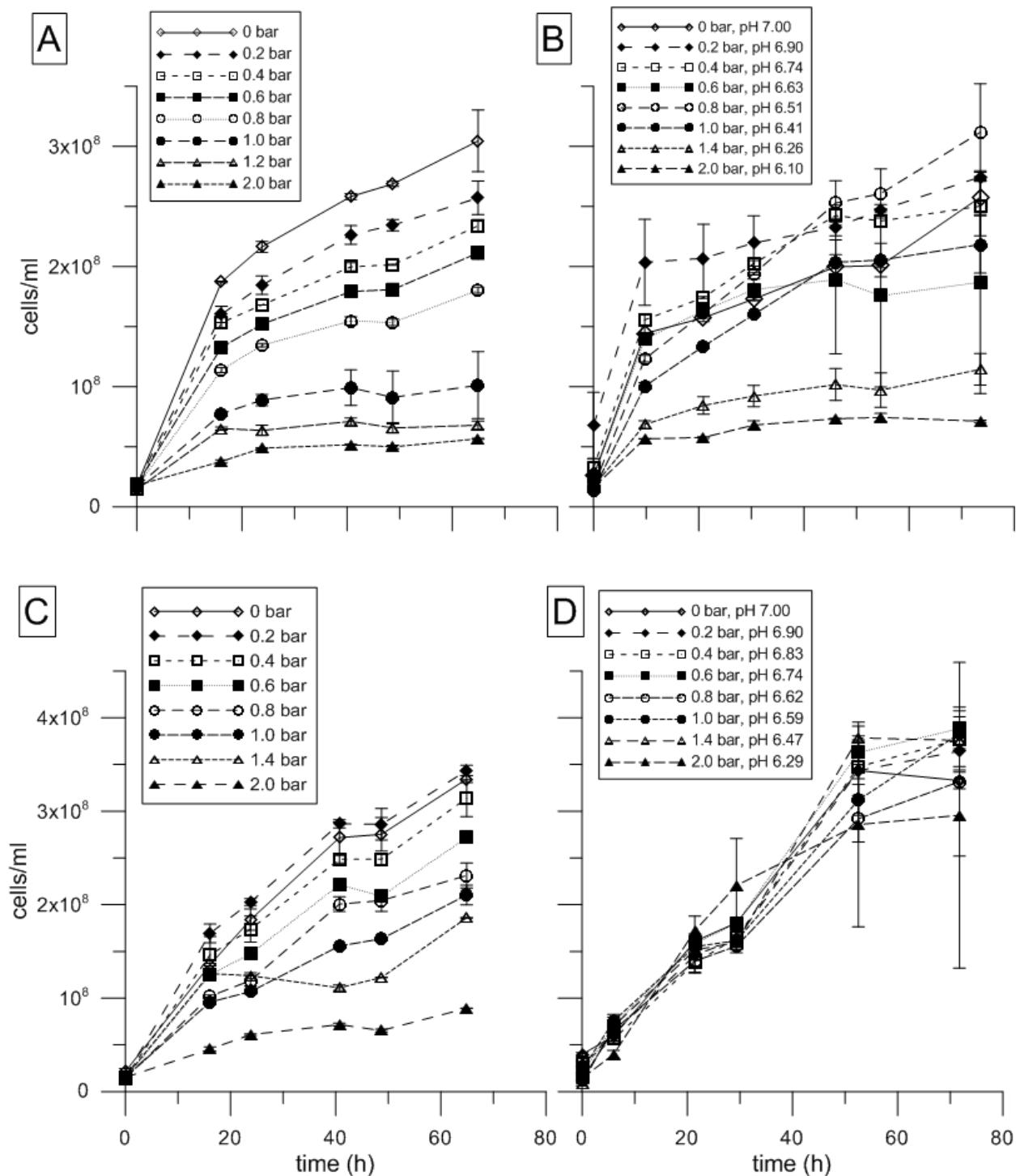


Figure 2-2 SO growth with nitrate or thiosulfate as TEAs. (A) Growth with nitrate and increasing PCO_2 , (B) growth with thiosulfate and increasing PCO_2 ; (C) growth with nitrate and decreasing pH and increasing PN_2 ; (D) growth with thiosulfate with decreasing pH and increasing PN_2 .

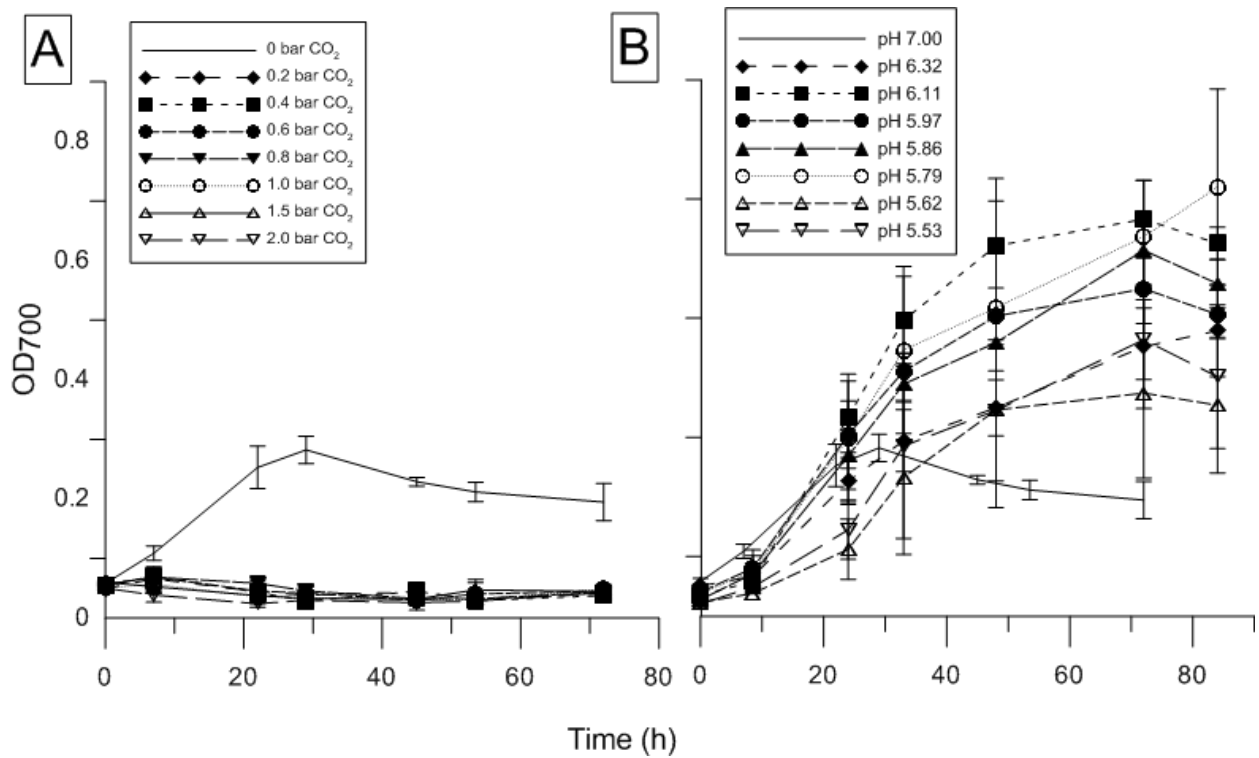


Figure 2-3 *Geobacillus stearothermophilus* growth curves (A) at high PCO_2 and (B) decreased pH.

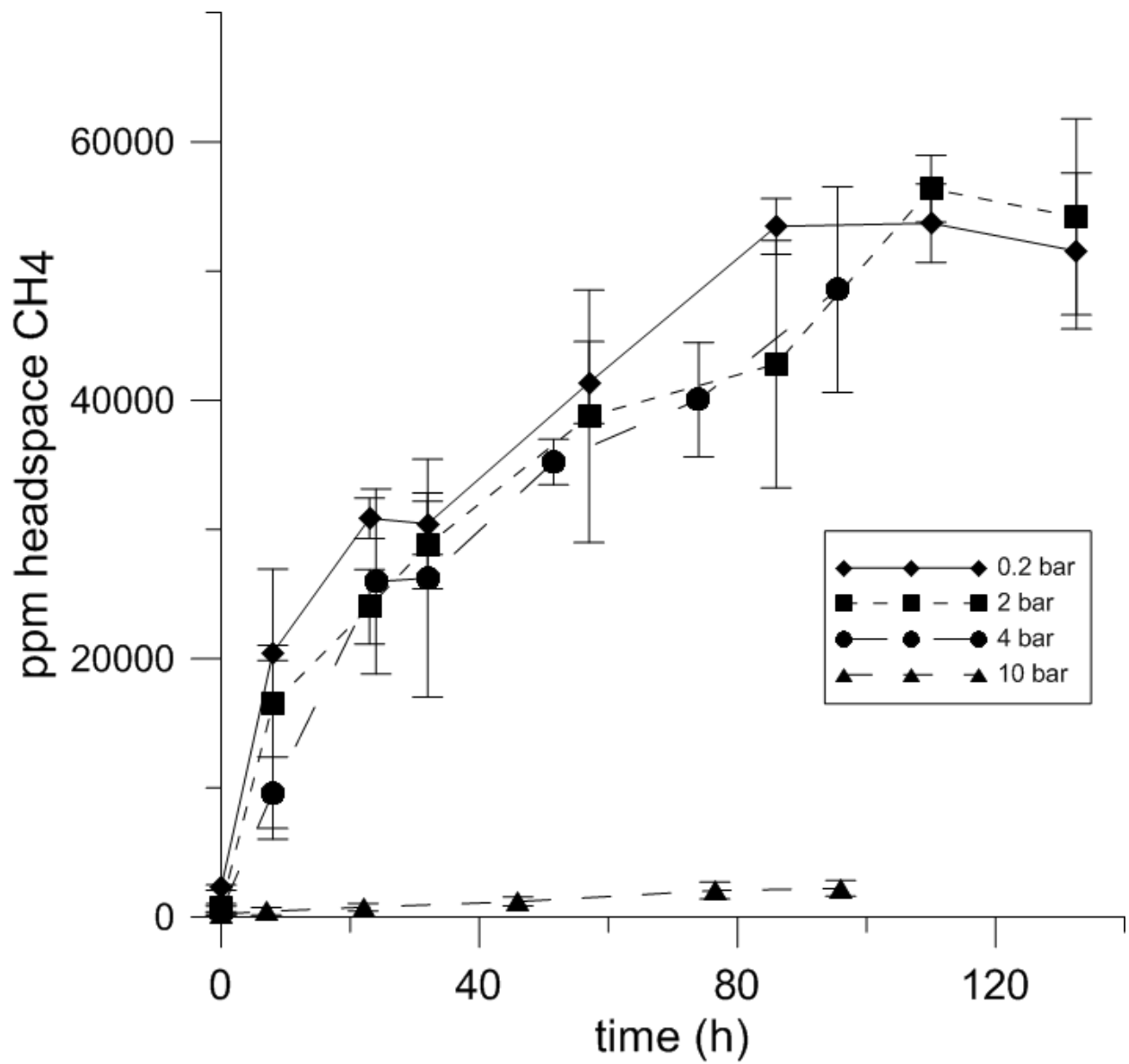


Figure 2-4 *Methanothermobacter thermoautotrophicus* CH₄ production with varying PCO₂.

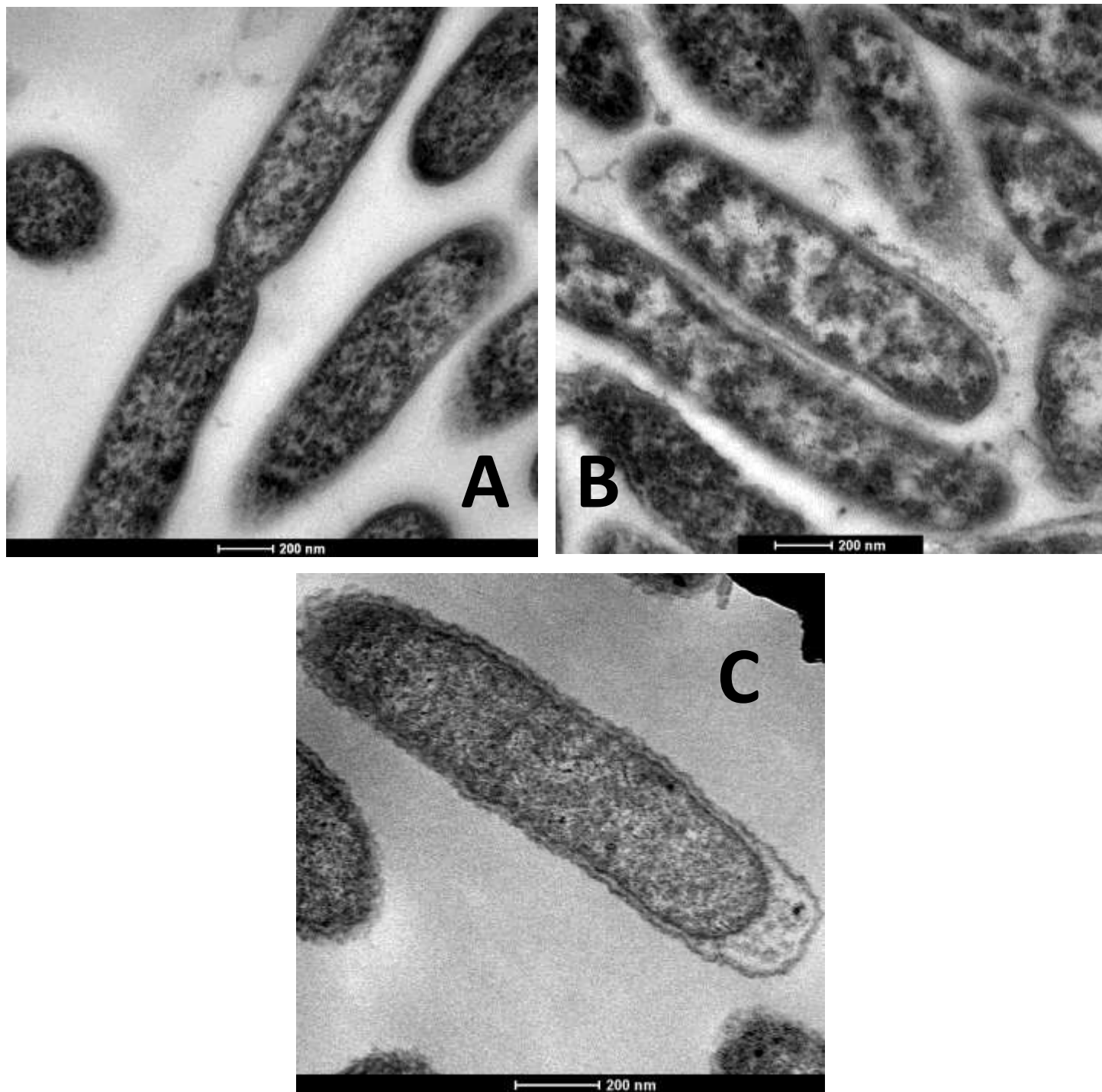


Figure 2-5 TEM images of SO with (A) no CO₂; (B) 2 hours at 25 bar CO₂; and (C) pH 4.5 for 24 hours.

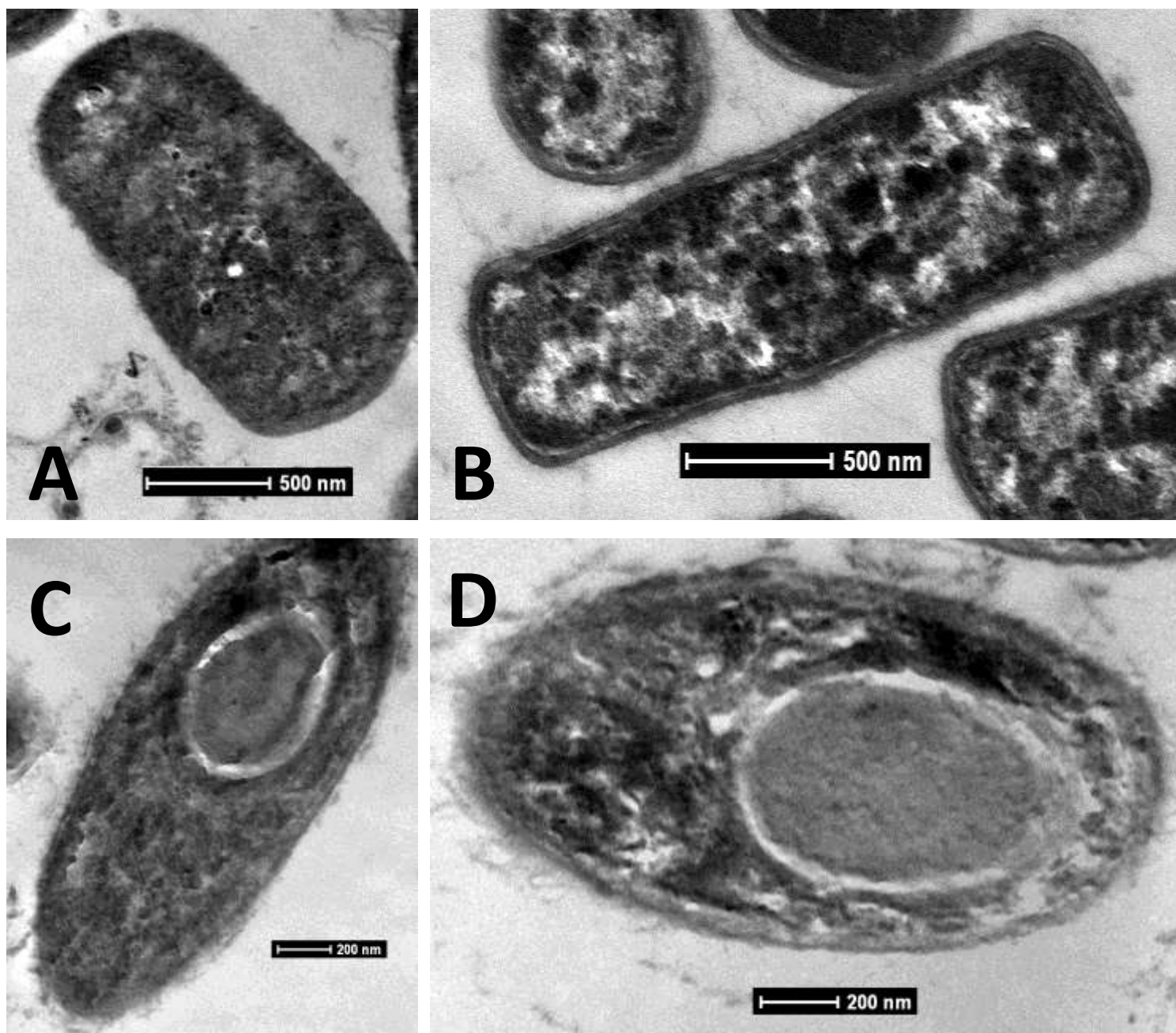


Figure 2-6 TEM images of GS with no CO₂ (A,C) and exposed to 50 bar CO₂ for 2 hours (B,D). Endospores are also pictured in (C) and (D).

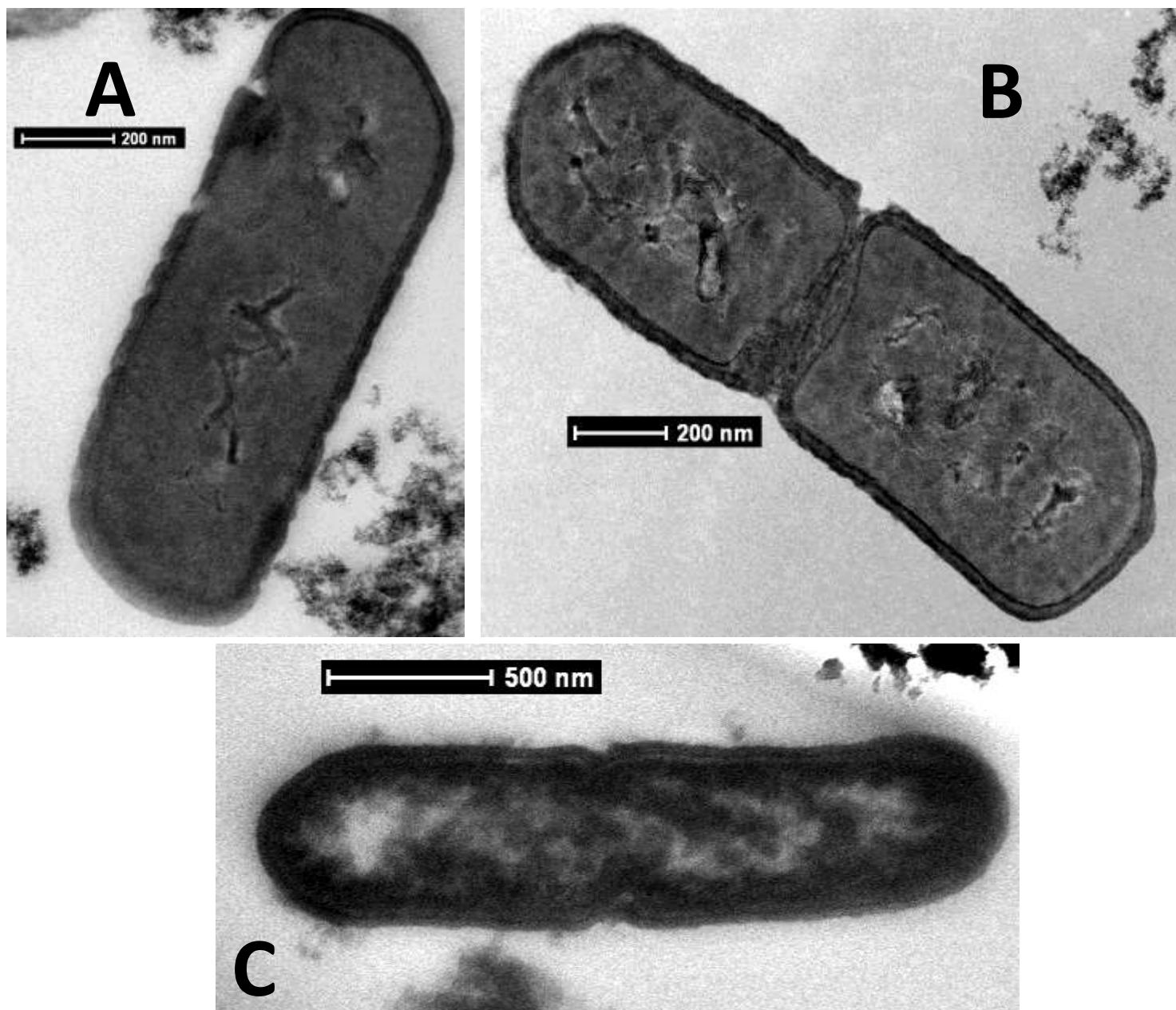


Figure 2-7 TEM images of BS with (A) no CO₂ present; (B) pH 4.5 for 24 hours; and (C) 50 bar for 8 hours.

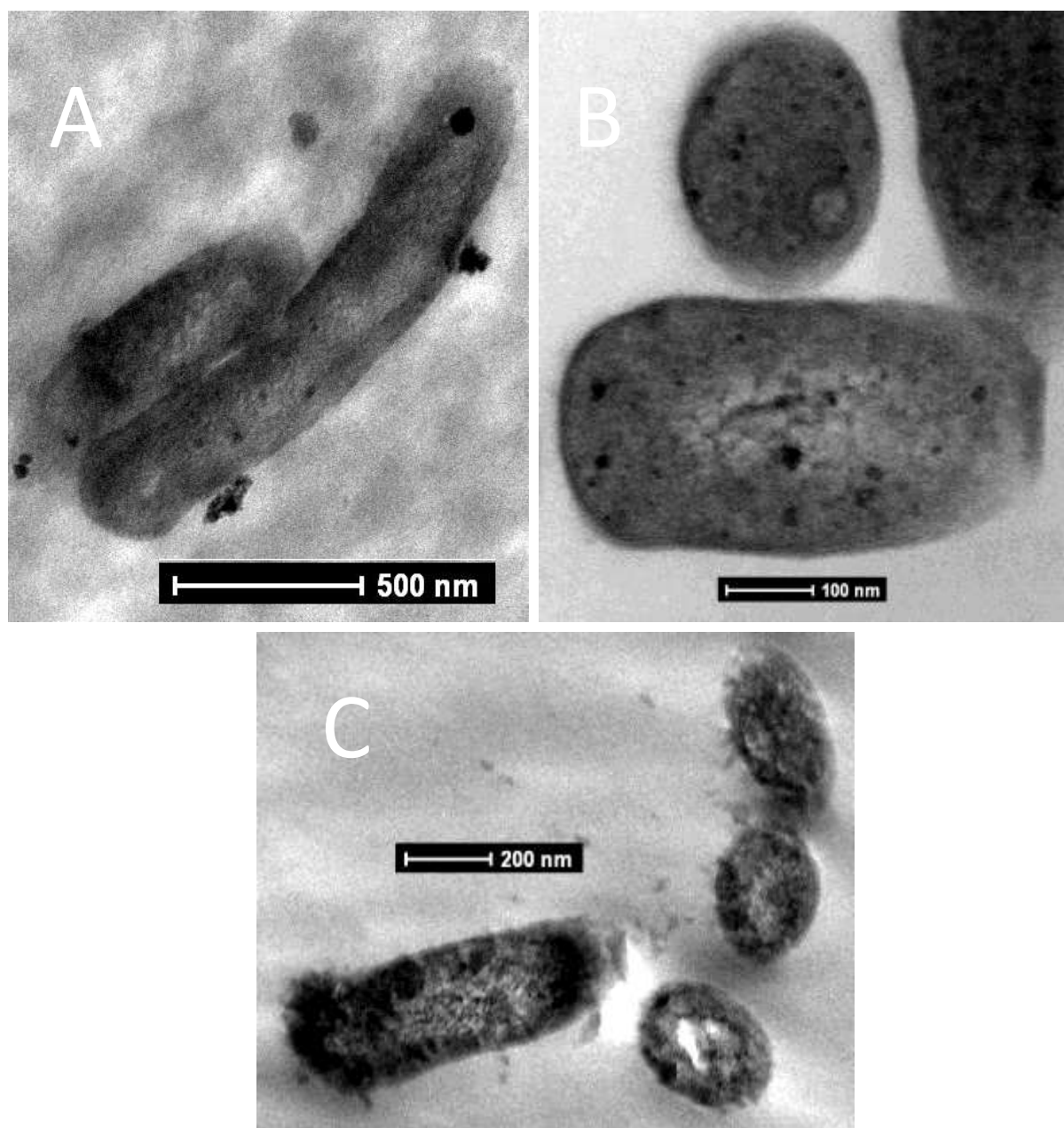


Figure 2-8 TEM images of MT with (A) no CO₂; (B) 2 hours at 25 bar; and (C) 24 hours at pH 4.5.

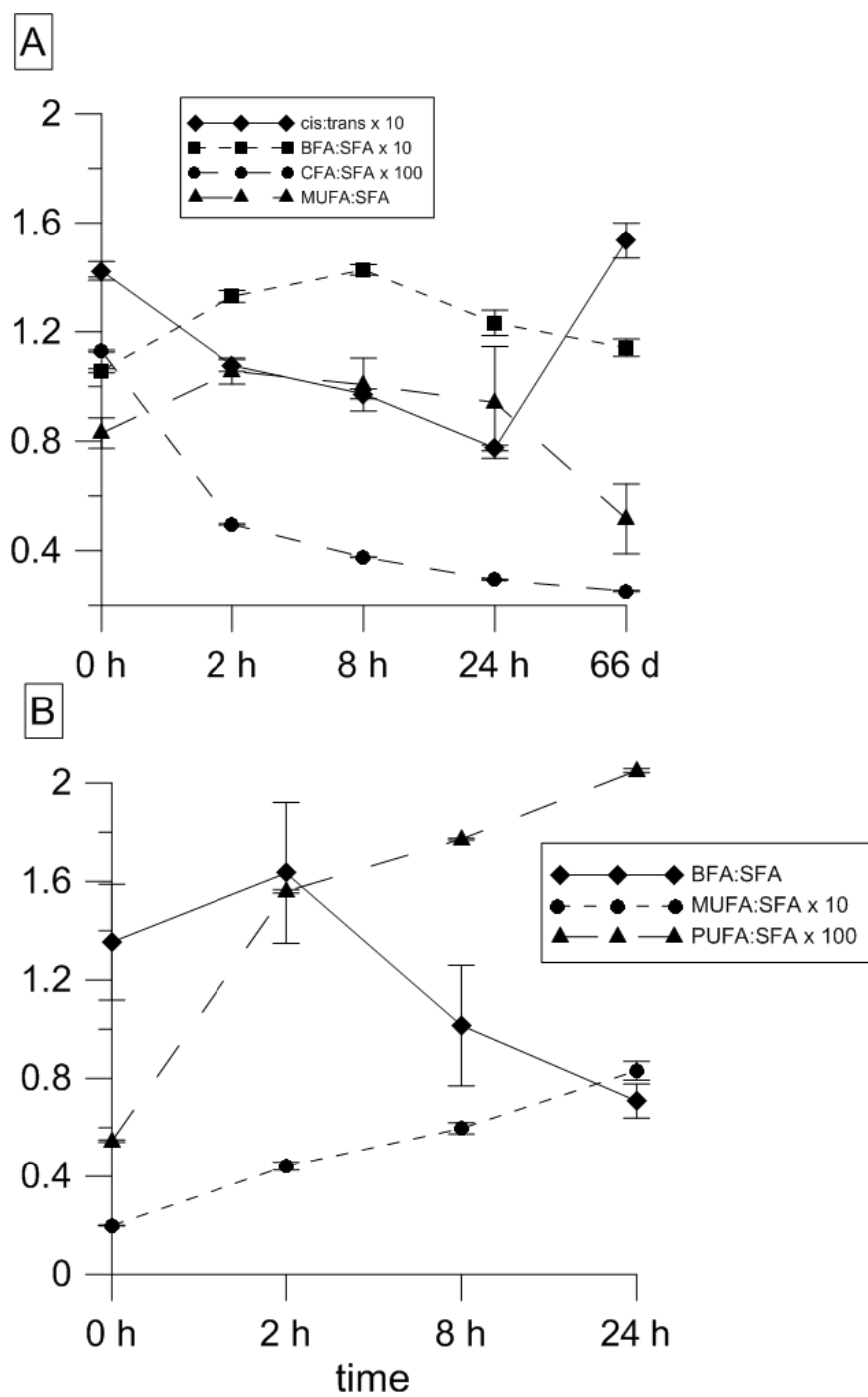


Figure 2-9 Bacterial fatty acid ratios at 2 bar CO₂ exposure: (A) SO; (B) BS.

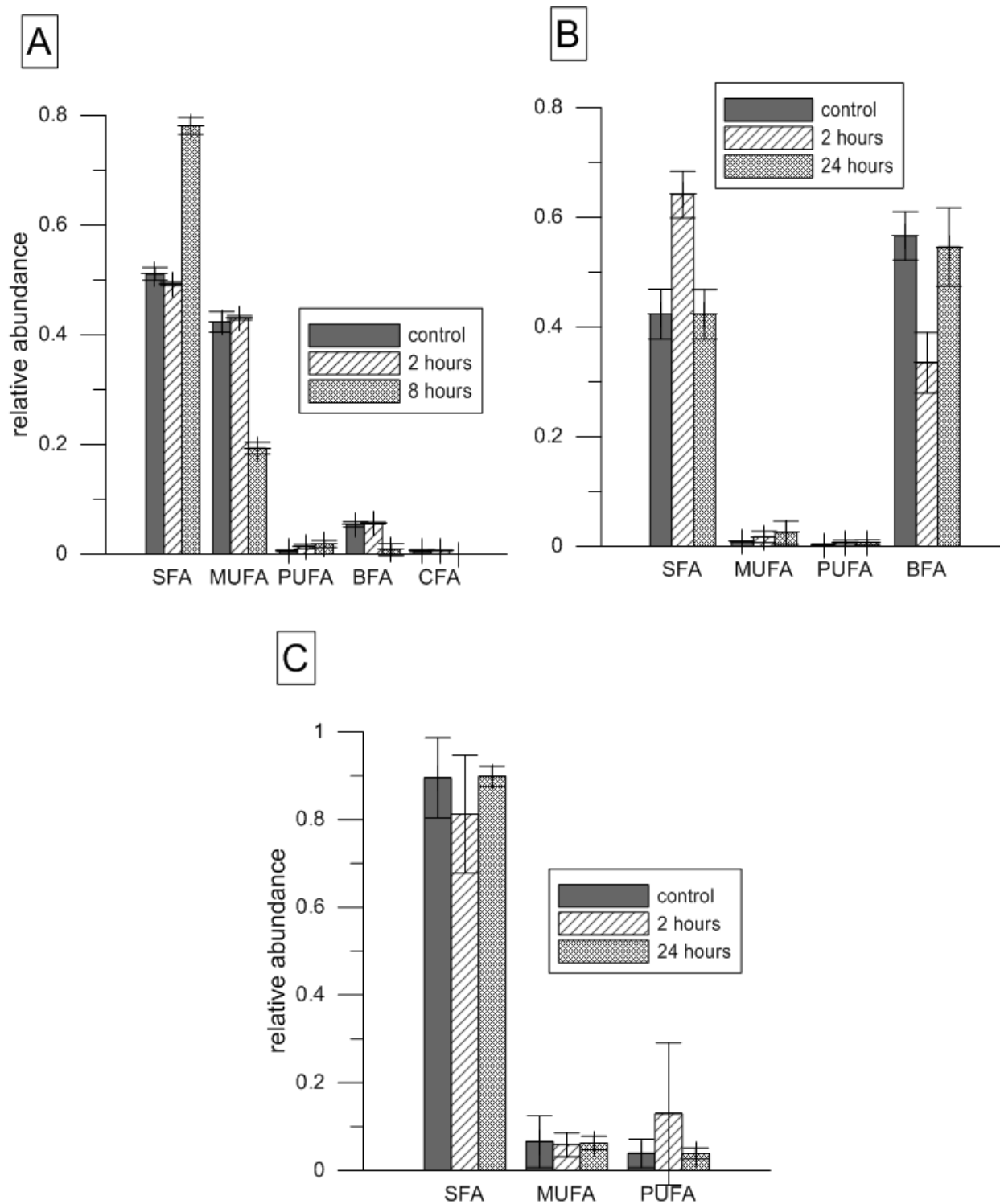


Figure 2-10 Bacterial fatty acid profiles at 25 or 50 bar PCO_2 . (A) SO at 25 bar; (B) GS at 50 bar; (C) BS at 25 bar.

Chapter 3: Mineral influence on Microbial Survival During Carbon Sequestration

ABSTRACT

Geologic carbon sequestration involves the injection of supercritical carbon dioxide into deep saline aquifers. Some of the CO₂ dissolves into the brines, perturbing water chemistry and water rock interactions, and impacting microbial habitat and survival. In this study, a model dissimilatory iron reducing bacterium (DIRB) *Shewanella oneidensis* strain MR-1 was grown in batch cultures containing various minerals and rocks representative of deep saline aquifers. Cultures were exposed to 25 bar of CO₂ for 2 to 8 hours and were plated for viable cell counts. Results show that biofilm formation on the mineral surface is important in protecting *Shewanella* from the harmful effects of CO₂ with quartz sandstones providing the best protection. Results also show that the release of toxic metals like Al or As from minerals such as clays and feldspars may enhance microbial death under CO₂ stress.

INTRODUCTION

Geological carbon sequestration has been proposed for long-term subsurface storage of carbon dioxide (CO_2) that would otherwise be released to the atmosphere. CO_2 emissions from coal-fired power plants are captured, compressed to a supercritical (sc) fluid, and then pumped into deep (>2km), confined saline aquifers. The increase in CO_2 partial pressure ($P\text{CO}_2$), and the associated acidity, perturbs the subsurface ecosystem and dramatically alters rock-water equilibria and reaction dynamics. While the physics and chemistry of this process have received increasing attention, neither the short nor long-term microbiological ramifications have been investigated, even though there are many biogeochemical processes that will be impacted.

The sequestered CO_2 pumped into the subsurface displaces pore water and is trapped as a hydrophobic supercritical fluid at the ambient temperatures and pressures encountered in target reservoirs (Bachu 2008). The aqueous phase is expected to be brackish to extremely saline. The target formation will be a permeable sandstone unit confined by low permeability shale or mudrock. The snapped off droplets of scCO_2 will slowly dissolve into the surrounding aqueous phase up to its equilibrium solubility, a process also known as solubility trapping (Suekane, Nobuso et al. 2008). Acidic CO_2 rich water will be found within the injection zone around individual scCO_2 bubbles, and around the injection pool. The types of biogeochemical reactions that result will be affected by the partial pressure of carbon dioxide, the aquifer mineralogy, the microbial community, and the composition of the saline waters.

In these formations, both the solid and aqueous phases contain elements necessary for microbial metabolism including nutrients, carbon substrate, and electron acceptors such as solid phase iron oxides and dissolved sulfate (SO_4^{2-}). The deep subsurface supports complex, viable microbial communities to temperatures in excess of 120°C. These communities originate both from burial or transport from the surface (Ehrlich 1971, Colwell, Onstott et al. 1997, Onstott, Phelps et al. 1998), and exist under typically oligotrophic conditions with very slow growth rates and limited nutrient and carbon supply. Microbial metabolism consumes these constituents leaving behind signatures of activity such as dissolved ferrous iron (Fe^{2+}) and biogenic H_2S . Microbial metabolic processes also influence rock-water reactions by dissolving and precipitating minerals such as reduced iron precipitates (Nealson, Belz et al. 2002). Often these reactions are slow however, and the system will reach a pseudo steady state condition with little change over time.

High concentrations of dissolved CO_2 will disrupt this steady state scenario and create an aggressive fluid that will accelerate abiotic mineral diagenesis reactions and increase the concentration of dissolved ions while creating new secondary mineral phases (Kharaka, Cole et al. 2006, Kaszuba, P. et al. 2009, Lu, Fu et al. 2011). One result of these reactions is the mobilization of Al, and the dissolution of Fe oxides with adsorbed toxic elements such as As. The perturbed subsurface system and mobilized metals will have a dramatic effect on the native microbial populations. The injected scCO_2 will both directly impact these microbial populations and change the water chemistry that will also affect the microorganisms.

The hydrophobic and liposoluble CO₂ molecule itself can directly affect microbial cells. CO₂ readily transits cell membranes, alters membrane properties, and affects a variety of intracellular functions (Ballestra, Dasilva et al. 1996, Oule, Tano et al. 2006, Wu, Shao et al. 2010). CO₂ accumulates in the cytoplasm decreasing pH while increasing the disorder of lipid chains in the membrane bilayer. This reduces membrane viscosity resulting in cytoplasm leakage as well as a change in intracellular salt concentrations (Figure 3-1), (Damar and Balaban 2006, Oule, Tano et al. 2006). Cytoplasm acidification changes the conformation of critical proteins essential for metabolic and regulating functions including active transport of ions, amino acid and peptides. It will also affect glycolysis and proton translocation (Oule, Tano et al. 2006). While many of these alterations are reversible, cells will eventually be inactivated from acid stress that disrupts the pH gradient essential for the proton motive force (Figure 3-1) (Ballestra, Dasilva et al. 1996).

Studies on microbial CO₂ toxicity however largely focus on planktonic cell cultures, yet these represent only a small fraction of the subsurface microbial community (Ballestra, Dasilva et al. 1996, Hong and Pyun 1999, Oule, Tano et al. 2006). Microbes also live as sessile communities composed of biofilms of bacterial cells and extracellular polymeric substances (EPS) attached to mineral surfaces (Wanger, Southam et al. 2006, Gorbushina 2007). Microbes attach to minerals for many reasons. Dissimilatory iron reducing bacteria (DIRB), for example, colonize iron oxide surfaces that act as a terminal electron acceptor (TEA) in the absence of oxygen (Lovley 1993, Nealson, Belz et al. 2002, Lies, Hernandez et al. 2005). Microbes can also colonize silicate surfaces and

dissolve minerals in order to obtain trace nutrients such as phosphate (Bennett, Rogers et al. 2001, Roberts 2004). Because microbes attach onto the mineral surface, the mineral itself acts as the local microbial habitat, providing a means of protecting or selecting against various bacteria during different stressful conditions (Jones and Bennett 2012 submitted). The effect CO₂ will have on subsurface microbes will vary based on which organisms are present and how they interact with the aquifer mineralogy.

The EPS component of a biofilm may provide a barrier to protect cells against the harmful effects of CO₂. Biofilms of *Bacillus mojavensis* and *Shewanella frigidimarina* showed increased resilience to supercritical CO₂ challenges in comparison to planktonic cells (Mitchell, Phillips et al. 2008, Mitchell, Phillips et al. 2009). Cells deep within the biofilm were thought to be protected due to concentration gradients and the slow or incomplete penetration of CO₂ through the biofilm (Figure 3-2), (Mitchell, Phillips et al. 2008).

Here we examine the toxicity of CO₂ on representative subsurface microorganisms but in a geological context, i.e. with minerals present. Because of the intimate connection between aquifer mineralogy and microbes, we also examined how minerals present in saline aquifers may enhance, or decrease survival during CO₂ stress. Our results illustrate the importance of mineralogy as a consideration to the effects on microbial life in the deep subsurface and the subsequent community and geochemical changes.

MATERIALS AND METHODS

The experimental approach was to examine microbial survival during exposure to CO₂ and the effects of different minerals on surviving CO₂ toxicity. Three different organisms, representative of populations found in deep subsurface environments were chosen; one Gram positive (G+), one Gram negative (G-) and one Archaeon. The cultures were exposed to 2-50 bar of CO₂ for time periods of 1 to 24 hours. The most sensitive organism to CO₂ was then evaluated for resistance to CO₂ toxicity during the presence of different minerals or rocks.

CULTURE CONDITIONS

Shewanella oneidensis (SO) strain MR-1 (ATCC BA-1096) was grown aerobically in LB broth. After approximately 72 hours incubation at 30°C, cultures were centrifuged and washed with sterile phosphate buffered saline (PBS) 3 times. After the third centrifugation, cells were resuspended in PBS. These cells were then grown in a modified M1 growth medium (Kostka and Nealson 1998). This medium contains per liter of distilled water: 2.4 g (NH₄)₂SO₄, 0.23 g KH₂PO₄, 0.45 g K₂HPO₄, 0.2 g MgSO₄*7H₂O, 0.29 g CaCl₂*2H₂O, 0.02 g EDTA disodium salt, 0.01g FeSO₄*7H₂O, 1.4 mg CoSO₄*7H₂O, 2.0 mg Ni(NH₄)₂(SO₄)₂*6H₂O, 0.058 g NaCl, 2.2 mg Na₂SeO₄, and 1 mL of Wolfe's trace metal solution. Media was adjusted to pH 7 using 1 N NaOH and autoclaved at 121°C for 30 minutes. After sterilization, 10 mL of a filter sterilized solution of mixed amino acids containing 0.2 mg/L of L-arginine, L-serine, and L-glutamic acid as well as 10 mL of 0.2 M NaHCO₃ solution were added per liter of medium. Prior to inoculation, growth media was supplemented with 10 mM sodium

lactate as an electron donor and 2 mM Fe-citrate as an electron acceptor. In cultures containing hematite and magnetite, Fe-citrate was not added as these minerals provided ferric iron as a TEA.

Geobacillus stearothermophilus (GS, ATCC 7953) was grown aerobically in nutrient broth at 30°C for 72 hours, and then washed and prepared as described above. The cells were transferred to a minimal salts media (Welker and Campbell 1963) without supplements for 72 hours and grown to stationary phase. This media contains per liter of distilled water: 105 mg L-arginine, 60 mg DL-methionine, 144 mg DL-valine, 500 mg K-acetate, 1.0 g KH_2PO_4 , 2.5 g KH_2PO_4 , 1.0 g NH_4Cl , 1 g NaCl, 5.0 mg $\text{FeCl}_3 \cdot 6\text{H}_2\text{O}$, 5.0 mg $\text{MgCl}_2 \cdot 6\text{H}_2\text{O}$, 5.0 mg $\text{CaCl}_2 \cdot 6\text{H}_2\text{O}$, 0.15 mg thiamine-HCl, 15 mg nicotinic acid, and 0.09 mg D-biotin. Media was adjusted to pH 7 using 1 N HCl and then autoclaved at 121°C for 30 minutes. Cultures were grown aerobically with 2 mM glycerin as the electron donor.

Methanothermobacter thermoautotrophicus (MT, ATCC 29096) was grown anaerobically in pre-reduced anaerobically sterilized (PRAS) media for 1 week to stationary phase. MT was grown in a medium adapted from (Zeikus and Wolfe 1972) containing per liter of distilled water: 0.3 g KH_2PO_4 , 0.3 g $(\text{NH}_4)_2\text{SO}_4$, 0.6 g NaCl, 0.12 g $\text{MgSO}_4 \cdot 7\text{H}_2\text{O}$, 0.08 g $\text{CaCl}_2 \cdot 2\text{H}_2\text{O}$, 1.5 g K_2HPO_4 , and 4 g Na_2CO_3 . This media was boiled for approximately 4 hours then immediately gassed with N_2 for 15 minutes followed by CO_2 for 15, both on ice. Media was titrated to pH 7 using 1 N HCl or NaOH then placed in an anaerobic chamber containing 5% CO_2/H_2 in an N_2 atmosphere overnight (Coy Laboratory Products Inc, Grass Lake, MI). Resazurin was added to

indicate anaerobic conditions. 0.3 g of both L-cysteine-HCl-H₂O and Na₂S*9H₂O were added as reducing agents to ensure removal of trace oxygen. 10 ml of media was dispensed into hungate tubes, capped, and autoclaved at 121°C for 30 minutes. Prior to inoculation, 0.1 ml of a sterile, anaerobic Wolfe's vitamin solution was added. MT cultures were incubated at 60°C, shaken at 150 rpm and gassed daily using a 70%/30% H₂/CO₂ headspace.

CO₂ Toxicity

Cell cultures grown to stationary phase were incubated at 2-50 bar of CO₂ for time periods ranging from 1-24 hours at 30°C. These experiments were designed to evaluate standard practice in food science studies for the inactivation of bacteria under high CO₂ pressures e.g., (Damar and Balaban 2006), and to find the critical pressure for survival of each of the three organisms.

To investigate the possibility that the experimental protocol would result in an artificially low survival rate due to rapid depressurization, the methodology was first evaluated using high pressure nitrogen which was pressurized and depressurized at the same rate as with the CO₂ procedure. Cell cultures of GS and SO grown to stationary phase were incubated at 50 bar of pure nitrogen for 2 hours, and then depressurized over a period of 2 minutes and 5 minutes (25 bar min⁻¹, 10 bar min⁻¹), and the triplicate cultures were evaluated for survival using the pour plate method with LB agar (Koch 2007).

To investigate CO₂ toxicity, cultures grown in glass test tubes were placed in pressure reactors (Parr instruments, Moline, IL) and the pressure slowly increased (10 bar

min⁻¹) to the final experimental conditions. The reactors were maintained at the final pressure and at constant temperature for the duration of the experiment. Samples were then slowly outgassed over approximately 2 minutes. After depressurization, cultures were sonicated for 10 minutes to remove biofilms from the culture tube and separate attached cells. Samples were diluted with PBS and evaluated for survival by plating cells for viability using the pour plate method with LB agar for SO and GS. All experiments were performed in triplicate. For MT cultures, 1 ml of CO₂ exposed cultures were recultured and checked for growth at OD₆₈₀.

Mineral Effects on CO₂ toxicity

The initial experiments showed that the G- organism (SO) was the most susceptible to CO₂, so this organism was chosen to examine in depth the effects of mineral solid phases on CO₂ toxicity.

Minerals and rocks (Table 3-1) were obtained from Ward's Natural Science (Rochester, NY). Samples were crushed to coarse sand size using an iron mortar and pestle and cleaned of residual iron with a hand magnet, then sterilized at 121°C for 30 minutes. One gram of each mineral was used for every experiment, although the surface area varied with mineral and grain size. 10 mL of growth medium was dispensed into sterile 15 mL test tubes containing 1 g of autoclaved mineral. Media containing minerals was inoculated with SO using an initial titer of 10⁶ cells/ml determined as OD₇₀₀ by spectrophotometry. Cultures were incubated at 30°C anaerobically in a GasPak anaerobic jar from BD Diagnostic Systems (Sparks, MD) for 3 days prior to experimentation. SO cultures were exposed to 25 bar CO₂ for up to 8 hours, and the media plated for viability.

Prior to plating, cultures were sonicated to remove any biofilms attached to the mineral surface.

To determine whether biofilm formation provided protection against CO₂ toxicity, selected mineral culture experiments of quartz sandstone (QS) and albite were repeated. Starting cultures were sonicated prior to CO₂ exposure to biofilms on the minerals following the methods of (Trampuz, Piper et al. 2007) to remove biofilms growing on surfaces. After sonication, cultures were then exposed to high CO₂ pressures as described previously.

To evaluate the effects of toxic metal release from minerals, biofilm cultures with QS were amended with 0.1 mM total Al or 0.1 mM total As. Growth media was amended with 0.1 mM as determined from the core batch mineral-microbe cultures. Cultures at stationary phase were then exposed to 25 bar of CO₂ for 2 hours and plated for viability.

Sample characterization

Solution chemistry was characterized for cultures prepared with kaolinite, gibbsite, illite, albite, hematite, and dolomite. Cultures were sampled before inoculation, after growth to stationary phase, and then after exposure to 2 hours of CO₂. Before CO₂ exposure, 5 ml of each culture was extracted, filtered to 0.2 µm, and then acidified with 10 µl of concentrated ultrapure HNO₃. For samples exposed to CO₂, 5 ml of water was collected directly into test tubes containing 10 µl of concentrated HNO₃ as filtration under 25 bar of CO₂ was not practical. These samples were then immediately filtered. Samples were analyzed for dissolved metals using an Agilent 7500ce ICP-MS.

Representative samples of QS, hematite, albite, and dolomite, and associated biofilms were imaged using a Zeiss Supra 40 VP Scanning Electron Microscope at the UT Microscope and Imaging Facility. Prior to imaging, cells were fixed by chemical critical point drying as outlined by (Bennett, Engel et al. 2007), Pt/Pd sputter coated and imaged under high vacuum.

RESULTS

Rapid depressurization of reactors charged with 50 bar N₂ does not result in measurable loss of cell viability. SO and GS survived depressurization rates of both 10 bar min⁻¹ and 25 bar min⁻¹ (Figure 3-3) The solubility of N₂ however is lower than CO₂, 10^{-3.21} compared to 10^{-1.48} at 25°C (Sander 1999).

Cell survival in unbuffered media without mineral amendments is summarized in Table 3-2 as a function of pressure and incubation time. In general microorganisms tolerate exposure to low *PCO*₂ well, with all organisms surviving more than 24 hours at 2 bar CO₂. The model organisms also tolerate short exposures to higher *PCO*₂, with all organisms surviving 1 hour exposure to 25 bar CO₂. Survival time decreases with increasing *PCO*₂ however; SO cultures in particular being very sensitive (Table 3-2). While SO viability is still found after 24 hours at 2 bar of CO₂, viable cells are not observed longer than 1 hour at partial pressures of 10 bar or greater. SO also tolerates 50 bar of CO₂ for less than 1 hour. MT survives longer at high *PCO*₂ than SO, with viable cells surviving for at least 8 hours at 10 bar CO₂, while at 25 and 50 bar, MT survives 2 hours of exposure. GS shows the longest survival with the largest range of *PCO*₂ with viable cells observed at all exposure times and *PCO*₂. However, GS produces endospores

which can be highly resistant to environmental stresses including CO₂ (Watanabe, Furukawa et al. 2003).

SO survival in buffered and unbuffered media at 25 bar of CO₂, and in acidic media without added CO₂, is summarized in Figure 3-4. Viability is not significantly affected by acidification to pH 4.5, approximately the pH expected in the unbuffered SO media equilibrated to 25 bar PCO₂. When cultures exposed at 25 bar CO₂ are buffered with 70 mM HEPES however, survival time doubles in comparison to unbuffered cultures. After 2 hours of exposure, viable cell count is only reduced by 2 log units (Figure 3-5) while unbuffered cultures have no viable cells. After incubation times of 4 hours and longer however even buffered cultures have complete loss of cell viability (Figure 3-5).

In mineral-amended cultures, cell viability varies widely at 25 bar PCO₂, but in general, the presence of a mineral increases the fraction of cells that survive CO₂ exposure, except with kaolinite (Figures 3-5 to 3-8). Reduction in viable cell numbers range from 1 to 8 log units after 2 hours compared to a total loss of viability in unbuffered liquid media. Cultures containing pH-buffering minerals including calcite, dolomite, and siderite show only a 2 - 3 log reduction from the starting titer after 2 hours. The largest decrease in viable cells is with calcite and dolomite amended cultures, while siderite has the least reduction, and has results similar with HEPES buffered medium (Figure 3-5).

Cultures containing Fe rich minerals also show improved survival after 2 hours of 25 bar CO₂ exposure. Media containing hematite, pyrite, and basalt all exhibit only ~2

log reduction in counts. Pyrite-amended cultures show the best survival with less than 2 log unit reduction. Magnetite-amended cultures show the least improvement in survival with a 5 log unit reduction. Additionally, magnetite-amended cultures display significant variability in survival with some replicates showing a near total loss in viable cells (Figure 3-7).

Cultures containing silicate rocks and minerals have highly variable survival at 2 hours of 25 bar CO₂. Albite, K-feldspar, biotite, and arkose sandstone containing media have between a 2 and 3 log unit reduction in viable cell numbers. Both albite and arkose sandstone also show a large experimental variability in survival ranges with some replicates experiencing a 5 log reduction while others only experiencing a 2 log reduction. Cells grown with quartz sand have an approximate 5 log reduction, with replicates showing a near-total loss in viable cell numbers. Cultures grown with QS have the smallest loss of viability, with less than a 1 log reduction in viable cell counts after CO₂ exposure for 2 hours (Figure 3-6).

Variable cell survival to 2 hours of 25 bar CO₂ is also found in samples grown with clays. Illite and Na-montmorillonite have similar reduction in cell counts of an approximately 1 log reduction, while media containing shale have an approximate 3 log reduction, with some replicates indicating a 4 log removal from the original titer. Cultures containing gibbsite have nearly a 5 log reduction in viable cell count though replicate cultures also show a total loss in cell viability. Kaolinite-amended media have no surviving cells after 2 hours of CO₂ exposure.

Shewanella was also grown with QS, illite, albite, hematite, and dolomite and exposed to 25 bar CO₂ for up to 8 hours (Figure 3-9). Cultures grown with the QS indicate the longest survival, with viable cells observed beyond the 8 hour test limit. Survival is also enhanced with cultures grown with albite, hematite, and dolomite, with cells lasting longer than 6 hours. Cultures containing illite however have relatively poor outcomes with no viable cells found beyond 2 hours.

SEM imaging of QS reveals biofilm adhesion on the grain surface (Figure 3-10a). Cells are distributed throughout the QS grains with EPS that appears to be thick and smooth. The EPS covers the cells and connects cells to the grain surface. After 8 hours of CO₂ exposure, biofilm is still present appears unchanged (Figure 3-10b). QS exhibits a large amount of roughness and biofilm was found in crevices present in the substratum.

The uncolonized albite mineral surface is smoother than that of QS. However, bacterial cells are found all over the mineral surfaces as well with large amounts of EPS attached to cells and the mineral (Figure 3-10c). As with QS, biofilm morphology is thick and smooth. No change in cell or biofilm morphology is observed after CO₂ exposure (Figure 3-10d).

SO colonized on dolomite mineral surfaces also exhibit biofilm (Figure 3-10e). However, the biofilm appearance on these mineral surfaces is different from that found on albite and QS. EPS on dolomite mineral grains have a cotton-like appearance and is more porous than the smooth, thick biofilms found on the QS and on albite (Figure 3-10a to 3-10d). However, even after CO₂ exposure, EPS is still present on the mineral surface and appear unchanged (Figure 3-10f). While SO cells are found colonized on the

hematite mineral surfaces, the presence of biofilm is not apparent both before and after CO₂ exposure (Figure 3-10g and 3-10h).

To investigate the effects of biofilm formation on cell survival, select cultures amended with albite and QS were sonicated prior to CO₂ exposure to shake off attached biofilms. Sonicated cultures experience a 2 log reduction after 2 hours of CO₂ exposure and a near-complete removal of viable cells after 4 hours of incubation (Figure 3-11). In comparison, untreated cultures experience less than a 1 log reduction after 2 hours of incubation and only a 2 log reduction after 4 hours of CO₂ incubation.

In all cultures sampled, dissolved metals are released from the minerals, and concentrations increase after CO₂ exposure (Table 3-3). For the carbonates there is an expected increase in Ca and Mg as these minerals rapidly dissolved in high *PCO₂* environments. Dissolved aluminum increases in cultures containing silicates, and arsenic is found in cultures containing illite. SO grown with QS in media amended with dissolved Al or As has fewer viable cells after 2 hours compared to the unamended media (Figure 3-12). Both cultures with Al or As showed greater than a 3 log reduction in viable cell counts after CO₂ exposure in comparison to cultures without metals suggesting that metals have an effect on cell survival under CO₂ stress.

DISCUSSION

The rapid escape of CO₂ from solutions during depressurization is occasionally discussed as a reason CO₂ sterilizes cultures. CO₂ bubbles could expand inside cells causing lysis (Nakamura, Enomoto et al. 1994, Ballestra, Dasilva et al. 1996, Dillow, Dehghani et al. 1999, Hong and Pyun 1999, Spilimbergo and Bertuccio 2003). Evidence

supporting this hypothesis comes primarily from SEM observations on yeast cells (Nakamura, Enomoto et al. 1994). However, when cultures of *E. coli* and *L. plantarum* were treated to flash depressurization, SEM evidence of burst or lysed cells was not found (Hong and Pyun 1999).

Further, our depressurization experiments suggest that the rapid removal of gas from cultures does not play a major role in sterilization (Figure 3-3). While our experiments involve N_2 , a gas that is far less soluble than CO_2 , the ability for this nonpolar gas to transit cell membranes still allows for its rapid entrance and exit from cells, an effect that would be seen by CO_2 . To correct for the difference in solubility, 50 bar of N_2 was used to create the least optimal conditions for cell survival. No effect is seen on cell survival with the depressurization experiments, and SEM examination of mineral surface biofilms after exposure to CO_2 show no evidence of cell lysis. Also, the large increase in cell survival with pH buffering (which would not change the activity of dissolved CO_2 under constant pressure) argues against a simple cell lysis explanation for the loss in viability.

Our data on the three model organisms suggests that cell survival at elevated PCO_2 may be dose-dependent: cell death occurs once a toxic dosage of CO_2 has been reached. As CO_2 pressure increases, the survival time of SO decreases. At 25 bar there is some survival after 1 hour, while at 50 bar there is no survival at 1 hour showing that as pressure increases, cells die faster. However, a key component to cell sterilization is the presence of water for CO_2 dissolution to occur. Dry cultures exposed to gaseous CO_2 do not experience the same sterilization effects as cultures suspended in solutions (Dillow,

Dehghani et al. 1999). Therefore, CO₂ toxicity happens due to the dissolved CO₂ in solution and not just the pressure of CO₂ on the organisms.

The relationship between survival time and CO₂ pressure is complicated by the time required to dissolve CO₂ into the media. Because CO₂ fugacity decreases with increasing *P*CO₂, there will not be a linear relationship between CO₂ pressure and the total dissolved CO₂ and therefore the dissolution rate e.g., (Liss and Slater 1974, Duan, Sun et al. 2005). While CO₂ dissolution rates vary with pressure, the survival time observed is probably the time it takes to reach a toxic aqueous CO₂ concentration, which we estimate to be approximately 0.28 M (Duan, Sun et al. 2005).

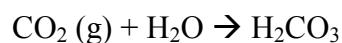
Microbial tolerances to high CO₂ pressures vary from organism to organism due to environmental, biochemical and structural characteristics (Dillow, Dehghani et al. 1999, Hong and Pyun 1999, Erkmén 2000, Spilimbergo and Bertucco 2003, Watanabe, Furukawa et al. 2003). Our study of three organisms supports the earlier reports that G⁻ organisms are the most susceptible to CO₂ toxicity while G⁺ organisms survive the longest, possibly due to slower penetration of CO₂ through their thick cell walls (Oule, Dickman et al. 2010). However, it is unclear how much of the enhanced survival is due to sporulation by the G⁺ organisms. Bacterial spores are extremely resistant to the antimicrobial effects of CO₂ compared to vegetative cells, although this also varies with species (Ballestra, Dasilva et al. 1996, Watanabe, Furukawa et al. 2003), and is dependent on temperature.

Archaea also have a high tolerance to CO₂, possibly due to their rigid cell membrane structures which allow them to withstand extreme environmental conditions

(Chong 2010). While the cell membrane is not as thick as the G⁺ organism, the structure may slow the diffusion of CO₂ across that barrier. Further, methanogens utilize CO₂ as an electron acceptor and are often found in close association with fermenting organisms that locally produce high concentrations of dissolved CO₂ (Whitman, Bowen et al. 2006).

The mechanism of cell toxicity from CO₂ exposure is both direct compound toxicity, and acidification of the medium. The growth media used for CO₂ sterilization in food science experiments is complex but highlights the importance of pH as a factor in killing microbial cells (Erkmen 2000). *L. monocytogenes* showed better survival in growth media containing a pH buffer in comparison to cultures grown in unbuffered media (Erkmen 2000). When applied to a carbon sequestration setting, this indicates that different reservoirs may have different abilities to buffer pH due to variable water composition and mineral matrix suggesting microbial activity may have different survival potential in different reservoirs.

While acidity in the medium certainly contributes to cell viability and growth, our experiments indicate that at pH values equivalent to 25 bar CO₂, SO is relatively unaffected (Figure 3-4). SO is clearly able to adapt to the acidity of the surrounding medium. In contrast, CO₂ is permeable in cell membranes and affects cells internally in addition to acidifying the surrounding medium. The dissolution of CO₂ in water creates carbonic acid, which lowers pH through the addition of a proton in the following equation:



e.g., (Appelo and Postma 2005). Geochemical modeling suggests that at equilibrium with 25 bar of CO₂, the pH of the growth medium should be ~4.3, while with a carbonate mineral buffer such as dolomite, pH should be ~5.3 (Figure 3-13) (Bethke 1996). SO has been previously shown to survive at these pH ranges by expressing genes for acid stress survival (Leaphart, Thompson et al. 2006, Biffinger, Pietron et al. 2008, Wu, Shao et al. 2010).

Our experiments show that pH buffering only provides a limited protection against CO₂. While cultures grown with any sort of buffer, mineral or otherwise, are capable of surviving longer under CO₂ stress (Figure 3-5), in all buffered cultures, no viable cells are found after 6 hours. Despite the pH buffering by minerals, cells show relatively rapid loss of viability compared to cultures grown with QS, an entirely unbuffered substrate, suggesting that the major factor affecting cell viability is the CO₂ in the solution and not just the acidity of the medium.

The survival of SO when minerals are present is apparently enhanced by biofilm formation on the mineral surfaces (Figure 3-10). SO formed biofilms on several different minerals, yet survives longest on QS, which is at first counterintuitive since quartz is not a buffering mineral. The QS however contains no toxic metals and is composed of SiO₂ suggesting that the mineral's benefit to the bacterium is purely its physical presence. The structure of the rock also is important; other quartz substrata studied provided very little protection despite a similar mineral composition (Figure 3-6). SEM imaging of QS grains show the mineral surface is quite rough, providing more surface area for biofilm formation. A higher surface area may allow for more organisms to colonize on the

mineral surface and thus more biofilm protection from CO₂. The presence of crevices on the substratum surface may also provide SO with microenvironments that protect cells from CO₂ toxicity.

As further evidence of the importance of biofilms in CO₂ survival, biofilm was physically shaken off QS and albite cultures. When the biofilm is physically removed from these mineral surfaces, cell death happens much more rapidly (Figure 3-11). By making cells in these cultures planktonic, CO₂ is able to penetrate cell cultures faster because cells on the mineral are no longer protected by a reactive barrier of EPS.

Microbial growth in a porous medium can be significant in that their physical presence in pore spaces can affect permeability. EPS secreted by microbes provides organisms with a firm attachment to a surface as well as a matrix for physical and chemical support e.g., (Mitchell, Phillips et al. 2008). EPS acts to retain water, accumulate and hang on to nutrients, and protect microbes from grazing by predators. It also decreases the permeability of a porous medium by altering fluid flow. Biofilms within pore spaces can clog pore throats altering the movement of fluids through the porous medium (Figure 3-2) (Rittmann 1993). In the context of CO₂ sequestration, biofilms have the potential to affect the movement of both scCO₂ as well as CO₂ dissolved in brines. It appears that the thick EPS present in the QS and albite may also act as a reactive barrier that slows down the penetration of CO₂ into the cell, increasing cell survival time against CO₂ toxicity (Mitchell, Phillips et al. 2008). While the data shows that SO cells will eventually die despite the presence of biofilm, biofilm structures

will continue to exist after cell death has occurred, indicating that even when cells are dead, biofilm presence will still be an important consideration during CO₂ sequestration.

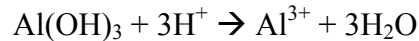
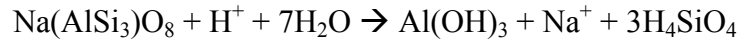
The presence of aluminum in the framework silicates helps explain why biofilm growth on aluminosilicate minerals does not provide the same degree of protection as biofilms grown on the QS (Figure 3-12). The large ranges of survival on the other aluminosilicate minerals tested may be attributed to varying aluminum concentrations in the growth media as well as the reactivity of each of the minerals. In addition, the silica sand tested contains Al, which also helps explain why it does not confer as much protection as QS. While biofilm formation on the mineral surface provides a large degree of protection against CO₂, toxic metals in the growth media appear to counter this protection.

SEM images of albite show colonization on the mineral surface similar to that of QS (Figure 3-10a to 3-10d). However, this mineral is more reactive than quartz and the increase in metal concentrations such as Al may enhance the toxic effect of CO₂ (Table 3-3). While minerals provide subsurface microbes with attachment surfaces, TEAs, and trace nutrients, minerals are also potentially harmful due to the mobilization of toxic metals such as Al (Farrah and Pickering 1978, Walther 1996). Feldspars and clays for example contain Al which is toxic to microbes (Grim 1968, Garciduenas-Pina and Cervantes 1996). Clays and feldspars also potentially contain trace amounts of toxic heavy metals, such as As, Mn, Zn, Mo, and Pb, which can be mobilized in acidic high PCO₂ water (Lu, Fu et al. 2011). Our findings indicate a release of metals due to CO₂ enhanced mineral dissolution contribute to the loss of viability in biofilm cultures under

CO₂ stress. Similar metal release was seen when Navajo sandstone was exposed to high PCO₂ (Lu, Fu et al. 2011).

Microbes have a limited tolerance to metal toxicity, and they will eventually succumb at some concentration and after some time period (Gadd 2010). To determine whether metal release contributes to cell death, biofilm cultures of SO grown on QS were amended with Al or As and exposed to CO₂. Faster loss of cell viability is observed with both elements even for resistant biofilms, suggesting that groundwater chemistry and rock water interactions are important aspects of microbial survival during CO₂ exposure (Figure 3-12).

Aluminum is a ubiquitous element in sandstone reservoirs, present in both clays and primary aluminosilicates. There is currently no known biological use for Al, and it has been shown to interact with carboxylate and phosphate groups to inhibit membrane function and transport activity (Garciduenas-Pina and Cervantes 1996). The decreased pH after CO₂ injection increases the equilibrium concentration of mobile Al species, e.g.:



(Appelo and Postma 2005). During CO₂ stress, cells are spending considerable energy attempting to maintain pH homeostasis to counter the effects of intracellular CO₂ acidity (Hong and Pyun 1999). The increase in toxic metals hastens the death of cells that are no longer able to keep up with the energy requirements to detoxify against both stresses.

We had initially hypothesized that iron oxides would enhance survival of SO, a DIRB, due to biofilm formation on a mineral surface that could act as a TEA. While

colonization is observed on the hematite, (Figure 3-10g and 3-10h), the mineral confers relatively little protection compared to the QS (Figure 3-9). This may be due to the lack of a continuous biofilm and absence of EPS on the mineral surface to act as a reactive barrier to CO₂. Furthermore, ferric iron in high concentrations catalyzes the formation of superoxides which damages cell membranes, proteins, and DNA (Andrews, Robinson et al. 2003). The acidity generated by increasing CO₂ will increase the solubility of hematite which we noted in a 5-fold increase in Fe concentrations in the growth media after exposure to CO₂ for two hours.

Our data shows that survival is enhanced in cultures amended with hematite, but only up to 6 hours, and no protection is found with magnetite-amended cultures. Magnetite contains a combination of both ferric and ferrous iron which means the mineral does not have much utility for cells as hematite as a terminal electron acceptor. Previous work has also shown that magnetite catalyzes superoxide formation, more so than other iron minerals like hematite (Fubini, Mollo et al. 1995). The magnetite used for this experiment, which consisted of very fine particles, many of which was suspended in the solution, may have put cells under oxidative stress. The high surface area of the mineral present in the solution increases the amount of superoxide in the medium in comparison to other iron minerals like hematite and pyrite. The addition of CO₂ to the solution resulted in faster cell death.

Interestingly, the SO biofilm on dolomite differs in its appearance from the SO biofilm on QS and albite. Extensive biofilm developed on dolomite (Figure 3-10a to 3-10f), but like the media containing hematite, cultures are unable to survive beyond 6

hours of CO₂ exposure (Figure 3-9). While cells appear to utilize the dolomite surface for colonization, the morphology of the EPS on the surface suggests that dolomite has a different metabolic effect on cultures than silicate and iron oxide surfaces. The cotton-like appearance of the biofilm on dolomite may not provide the same protection as the thick, smooth biofilms found on QS and albite possibly because the pores in the biofilm allow for a faster diffusion of CO₂ into the biofilm.

Clays are an important consideration for CO₂ sequestration as many sites targeted for sequestration contain clay cements (Kharaka, Cole et al. 2006, Hovorka, Choi et al. 2009) or are capped by a shale layer composed of clays (Xu, Apps et al. 2005). Organisms, including DIRB, are capable of growth on clays due to their ability to utilize adsorbed metals as TEAs (Kim, Dong et al. 2004, Perdrial, Warr et al. 2009). In soil environments, clays are also capable of maintaining pH levels for bacteria to survive by retaining water and releasing cations to buffer the medium (Marshall 1975).

Cultures grown with illite, while showing less than a 1 log reduction in viable cell counts after 2 hours of CO₂ exposure, show no survival beyond 4 hours (Figure 3-9). When we examine the water chemistry data taken from these samples at different periods of incubation, we also document the release of Al, Mn, As, and Zn during culturing and after CO₂ exposure (Table 3-3).

Aqueous suspensions of clays form envelopes around bacterial cells due to the electrostatic interactions between charged groups on the clay and bacterial surfaces (Marshall 1975). Our cultures with illite and montmorillonite form flocs, composed of clumps of cells, clays, and organic matter. This clumping of cells and clay may explain

why cultures grown with both illite and montmorillonite have only ~1 log reduction in viable cell counts after 2 hours of CO₂ exposure at 25 bar. The enveloping of clays around the bacterial cells provides a reactive barrier, allowing for less net diffusion of CO₂ into the cell. These clays may further provide cultures with a short-term pH buffer before they succumbed to the effects of CO₂ stress.

Despite the possible benefits clays provide, our experiments show that clay minerals do not provide long term protection and may actually contribute to cell death under CO₂ stress. Acidification of the media causes clays to desorb attached ions such as the As found in the growth medium (Table 3-3). Additionally, mineral dissolution of clays results in the mobilization of Al (Farrah and Pickering 1978). Mn and Zn concentrations also increase in our experiments, and both bind to proteins or nucleic acids and alter their native conformations resulting in losses in function (Hughes and Poole 1989).

Unlike all the mineral and rock samples studied, cultures grown with kaolinite show no survival after 2 hours of CO₂ exposure. This may be because cells grown with the kaolinite are exposed to high aqueous Al concentrations from the start of culturing and already are under aluminum stress when exposed to CO₂ (Table 3-3). Kaolinite also has less ability to adsorb cations and organic molecules which means this mineral did not attach around cell membranes to form a reactive barrier against the CO₂ (Grim 1968).

Interestingly, survival in media containing gibbsite (Al(OH)₃) is much longer than with kaolinite, and Al release from the gibbsite is less than that of both kaolinite and albite, in contrast to predictions from geochemical modeling. This may be because the

gibbsite used for this experiment was synthetic, perhaps showing differences in crystalline ordering compared to that of the other clays studied. This also may explain the variable survival of cells grown with gibbsite after 2 hours of CO₂ exposure.

Our results show that clays overall offer little protection for microbes against CO₂ stress. This also suggests that in deep saline aquifers, CO₂ saturated brines interacting with shale caprocks or clays in the aquifer may have mixed protective abilities. While biofilms may form on shale caprocks as seen with the other aluminosilicates studies, clays present on these substrates may increase the amounts of metals released that enhance cell death. While our study encompasses only a few hours of CO₂ exposure, the short incubation times with CO₂ and clays does show a steady increase in heavy metal concentrations in the medium. Longer interaction of CO₂ charged water with clays will presumably result in even more metal release, further enhancing microbial death.

IMPLICATIONS

Because microbes in the subsurface utilize the mineral surface for multiple reasons, including TEAs and trace nutrients, the mineral surface itself comprises the microbe's habitat. However, mineralogy can become an important factor in selecting against microbial populations particularly because of the release of toxic metals such as Al and As. While organisms in the subsurface will be selected for based on their CO₂ tolerance, the addition of toxic metals to the environment will add an additional selective pressure. Organisms most capable of handling both CO₂ and metal toxicity will ultimately be selected for and in turn, be the major influences the biogeochemistry of the subsurface after carbon sequestration.

Organisms capable of forming mineral surface biofilms may also have an advantage over other organisms present during CO₂ stress, especially biofilms that form on minerals that contain little toxic metal content. If CO₂ exposure results in flocculation and biofilm formation, then there will be a heterogeneous distribution of biofilms at both micro and macro scales as those on QS for example will be selected for against those in aluminosilicate rich zone. This is significant considering how biofilms in porous media may affect the permeability of the subsurface and the resultant transport of CO₂-charged water (Figure 3-2). There will be a heterogeneous effect on fluid flow that is related to the mineralogy and not to the initial permeability.

The ability minerals have to contribute to the selection of microbes has important consequences to the survival of different microbial populations in the subsurface. Given the right set of conditions, perhaps mineralogy may even provide long-term survival for DIRB at high *PCO*₂.

Mineral/Rock	Approximate Composition
Microcline	KAlSi_3O_8
Quartz Sand	SiO_2
Silica Sand	mostly SiO_2 (also Al and other metals)
Albite	$\text{NaAlSi}_3\text{O}_8$
K-feldspar	KAlSi_3O_8
Biotite	$\text{K}(\text{Mg}, \text{Fe}^{2+})_3(\text{Al}, \text{Fe}^{3+})\text{Si}_3\text{O}_{10}(\text{OH}, \text{F})_2$
Arkose Sandstone	composed of feldspars, cemented by calcite
Quartz Sandstone	contains quartz, cemented by quartz
Illite	$(\text{K}, \text{H}_3\text{O})(\text{Al}, \text{Mg}, \text{Fe})_2(\text{Si}, \text{Al})_4\text{O}_{10}[(\text{OH})_2, (\text{H}_2\text{O})]$
Na-Montmorillonite	$(\text{Na}, \text{Ca})_{0.33}(\text{Al}, \text{Mg})_2(\text{Si}_4\text{O}_{10})(\text{OH})_2 \cdot n\text{H}_2\text{O}$
Kaolinite	$\text{Al}_2\text{Si}_2\text{O}_5(\text{OH})_4$
Gibbsite	$\text{Al}(\text{OH})_3$
Shale	composed of clays
Apatite	$\text{Ca}_5(\text{PO}_4)_3(\text{F}, \text{Cl}, \text{OH})$
Calcite	CaCO_3
Dolomite	$\text{CaMg}(\text{CO}_3)_2$
Siderite	FeCO_3
Magnetite	Fe_3O_4
Hematite	Fe_2O_3
Pyrite	FeS_2
Basalt	Fe, Mg, Ca, Si, O
No Mineral	--
No Mineral, HEPES Buffered	--

Table 3-1 Minerals and their approximate chemical compositions used for this study.

	2 atm			10 atm			25 atm			50 atm		
	SO (G-)	GS (G+)	MT	SO (G-)	GS (G+)	MT	SO (G-)	GS (G+)	MT	SO (G-)	GS (G+)	MT
1 hour	+	+	+	+	+	+	+	+	+	-	+	+
2 hours	+	+	+	-	+	+	-	+	+	-	+	+
8 hours	+	+	+	-	+	+	-	+	-	-	+	-
24 hours	+	+	+	-	+	-	-	+	-	-	+	-

Table 3-2 CO₂ survival for SO, GS, and MT in unbuffered media with no mineral amendments.

	B	Mg	Al	Si	Ca	Mn	Fe	Ni	Cu	Zn	As	Rb	Sr	Zr (uM)	Mo (uM)	Ag (uM)	Cd (uM)	Sb (uM)	Cs (uM)	Ba (uM)	Pb (uM)	U (uM)
Kaolinite Initial	8.21	1048.53	21.30	71.25	203.57	2.73	842.79	4.56	0.34	0.31	0.15	0.31	0.29	60.08	35.27	1.64	1.21	5.79	36.23	145.81	88.21	6.36
Kaolinite Final (2h)	24.2	1320.88	135.32	162.27	300.16	3.35	651.34	6.05	0.71	0.82	0.64	0.39	0.41	186.01	166.43	4.42	4.45	8.07	55.39	921.67	133.43	37.60
Gibbsite Initial	4.45	1213.29	1.57	78.92	104.76	2.89	1075.64	5.20	0.19	0.35	0.12	0.28	0.08	65.71	30.12	3.37	0.49	4.94	2.08	102.85	6.85	0.20
Gibbsite Final (2h)	7.69	1225.41	36.87	93.95	273.58	7.31	809.56	25.01	45.50	4.69	0.12	0.28	1.18	110.48	241.84	2.11	12.02	22.04	1.62	340.21	319.58	1.76
Illite Initial	25.9	2257.95	10.56	131.66	3458.44	9.40	1006.85	6.27	0.22	0.67	1.19	1.00	5.39	107.53	125.55	1.99	8.22	6.69	56.21	280.25	72.35	1.92
Illite Final (4h)	54.7	2871.80	35.03	379.05	5059.59	16.08	535.72	14.34	0.33	2.04	9.19	1.32	5.65	844.77	314.90	2.60	8.05	23.78	49.88	196.91	83.30	5.58
Albite Initial	4.65	1282.54	4.74	80.54	348.08	3.81	1100.49	5.21	0.93	0.73	0.14	0.30	0.55	75.81	24.87	1.11	1.65	5.93	4.95	316.32	151.54	0.61
Albite Final (6h)	7.26	1274.82	478.98	771.65	1315.79	10.60	1057.61	5.40	0.22	2.25	0.33	0.32	2.18	99.72	60.56	1.15	4.46	11.62	40.04	72.16	529.12	2.07
Hematite Initial	7.93	1446.25	0.47	80.54	767.62	1.08	22.23	5.38	0.16	0.72	0.43	0.36	5.28	12.92	9.98	0.80	2.81	4.71	12.92	74.80	1.28	1.56
Hematite Final (6h)	25.3	1650.61	2.33	457.69	1478.55	6.59	113.23	5.37	0.16	1.73	4.63	0.47	12.04	4.21	39.89	0.45	7.45	6.85	33.95	62.12	0.07	0.13
Dolomite Initial	3.66	1412.39	1.62	78.58	371.73	3.55	1070.86	5.18	0.13	0.21	0.08	0.27	0.37	0.08	0.03	0.00	0.00	0.00	0.01	bdl	0.59	0.01
Dolomite Final (6h)	5.55	2367.14	17.64	135.97	1982.14	5.77	1092.11	7.42	11.94	4.22	0.28	0.29	2.02	0.23	0.14	bdl	0.01	0.01	0.02	bdl	0.75	0.18

Table 3-3 Select cation data for batch cultures containing various minerals at the start of cell culturing and after CO₂ incubation. All concentrations are in mM unless stated otherwise.

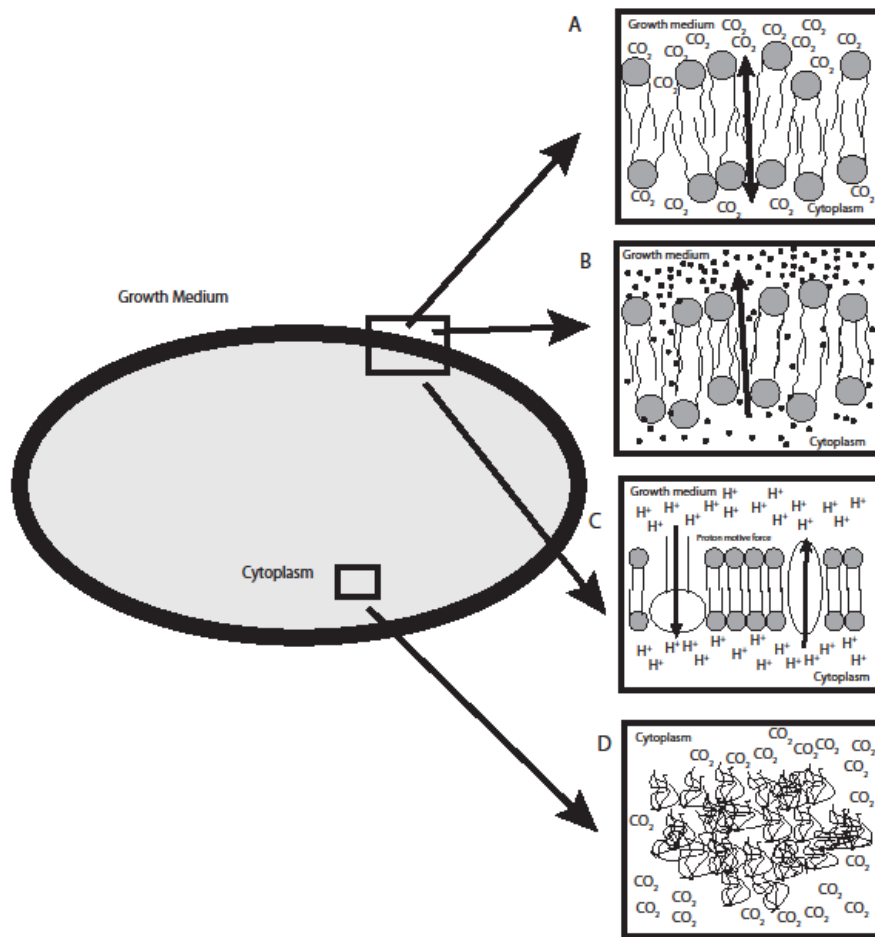


Figure 3-1 Schematic representation of how CO₂ affects a bacterial cell. High PCO₂ present in the medium (a) alters membrane fluidity, (b) changes intracellular salt concentrations due to altered membrane fluidity, (c) increases acidity in the medium interfering with the proton motive force, and (d) acidifies the cell's cytoplasm resulting in denaturation and deactivation of intracellular proteins.

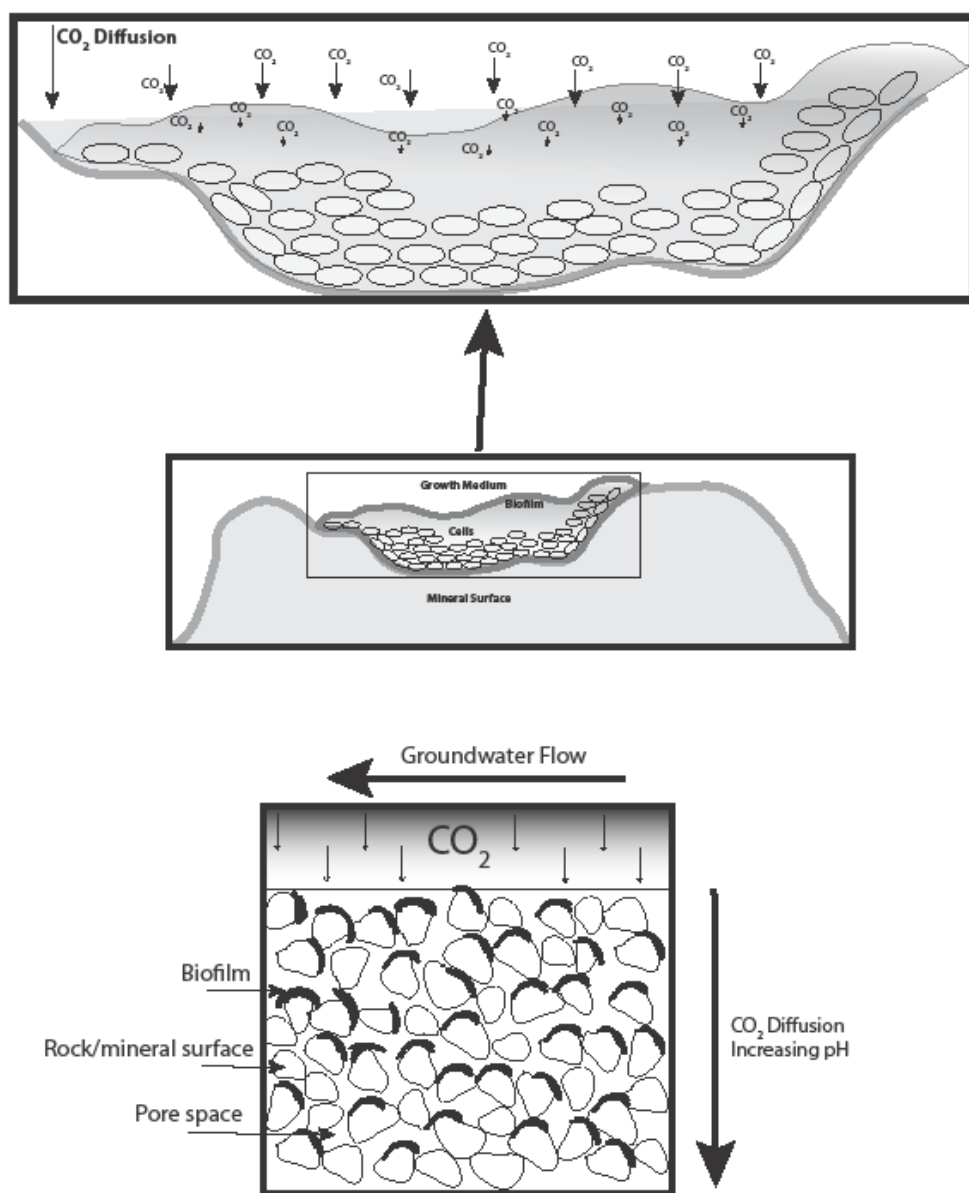


Figure 3-2 Schematic representation of biofilm colonization on the mineral surface. Cells colonize the mineral surface covered by a layer of EPS. This EPS acts as a barrier to slow the diffusion of CO_2 into the cell

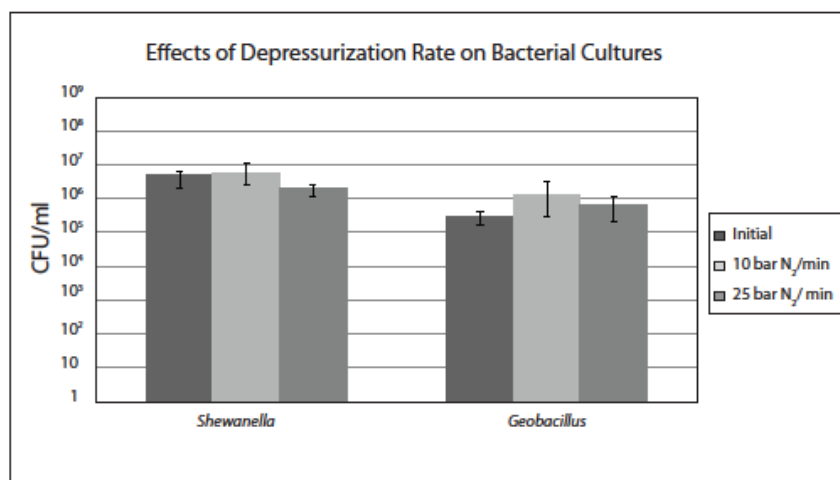


Figure 3-3 The effects of different depressurization rates on cell viability for SO and GS using rates of $10 \text{ bar } N_2 \text{ min}^{-1}$ and $25 \text{ bar } N_2 \text{ min}^{-1}$.

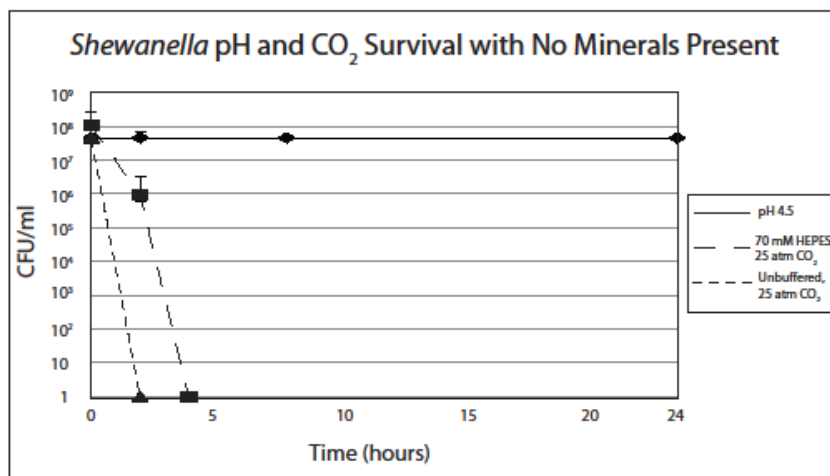


Figure 3-4 SO survival at 25 bar CO₂ in buffered and unbuffered media and in HCl acidified media simulating the pH drop at those pressures.

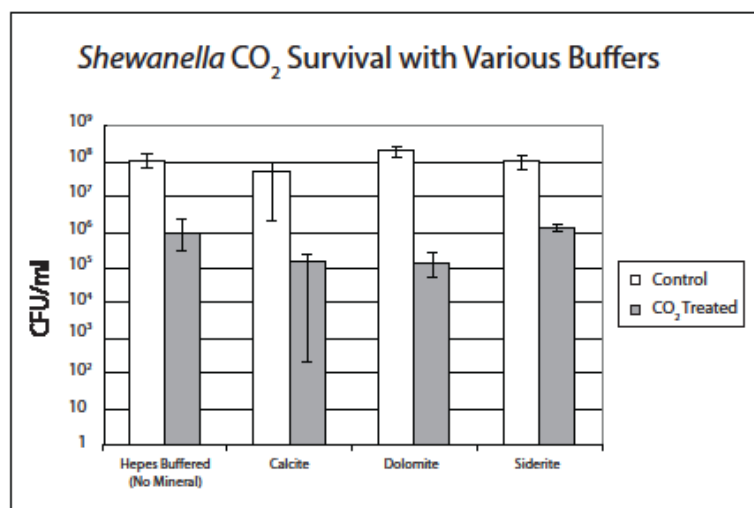


Figure 3-5 SO CO₂ survival with pH buffering minerals.

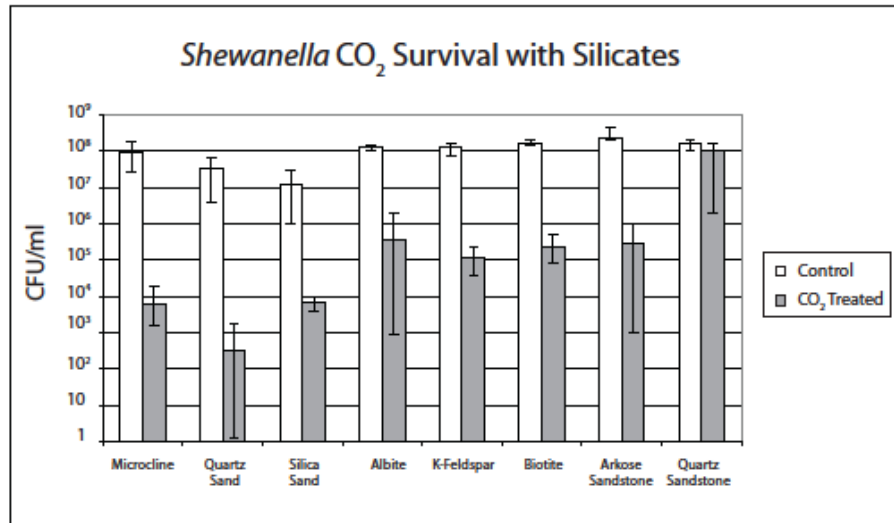


Figure 3-6 SO CO₂ survival with silicate rocks and minerals.

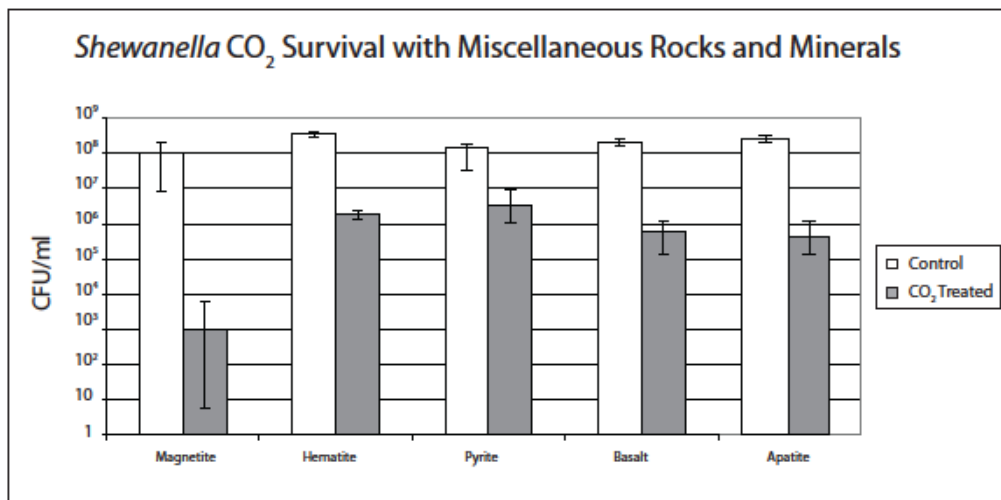


Figure 3-7 SO CO₂ survival with miscellaneous rocks and minerals.

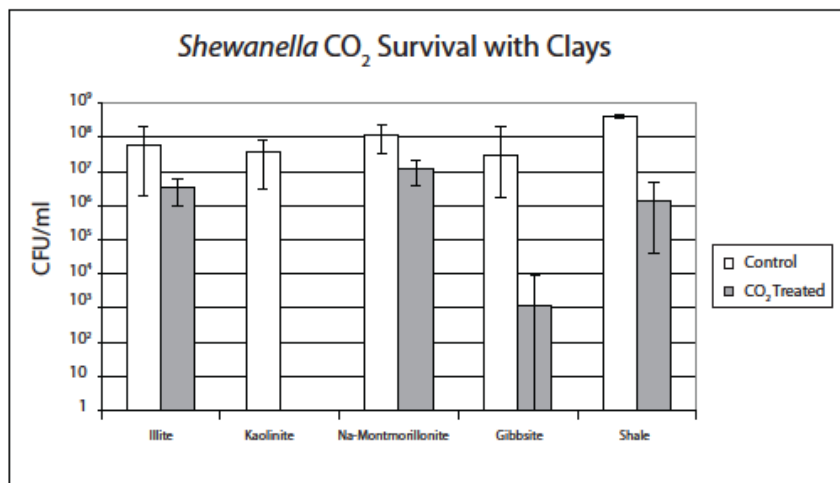


Figure 3-8 SO CO₂ survival with clays.

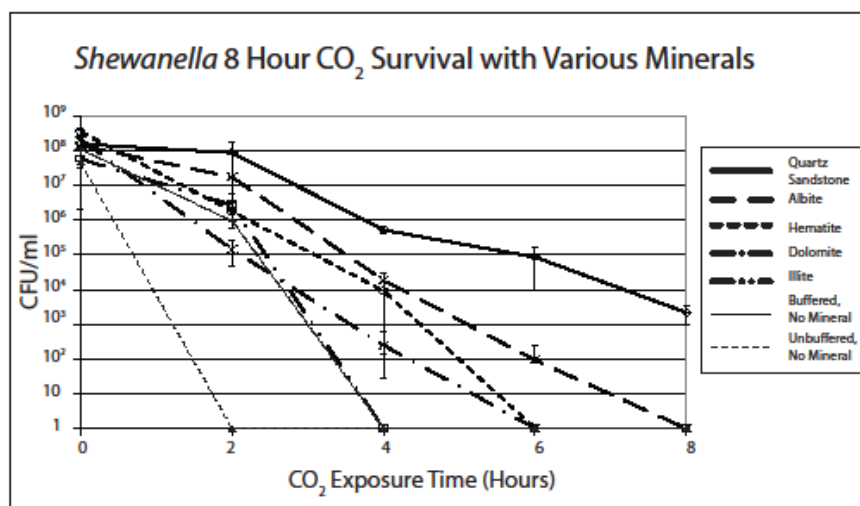


Figure 3-9 SO 8 hour CO₂ survival with various minerals.

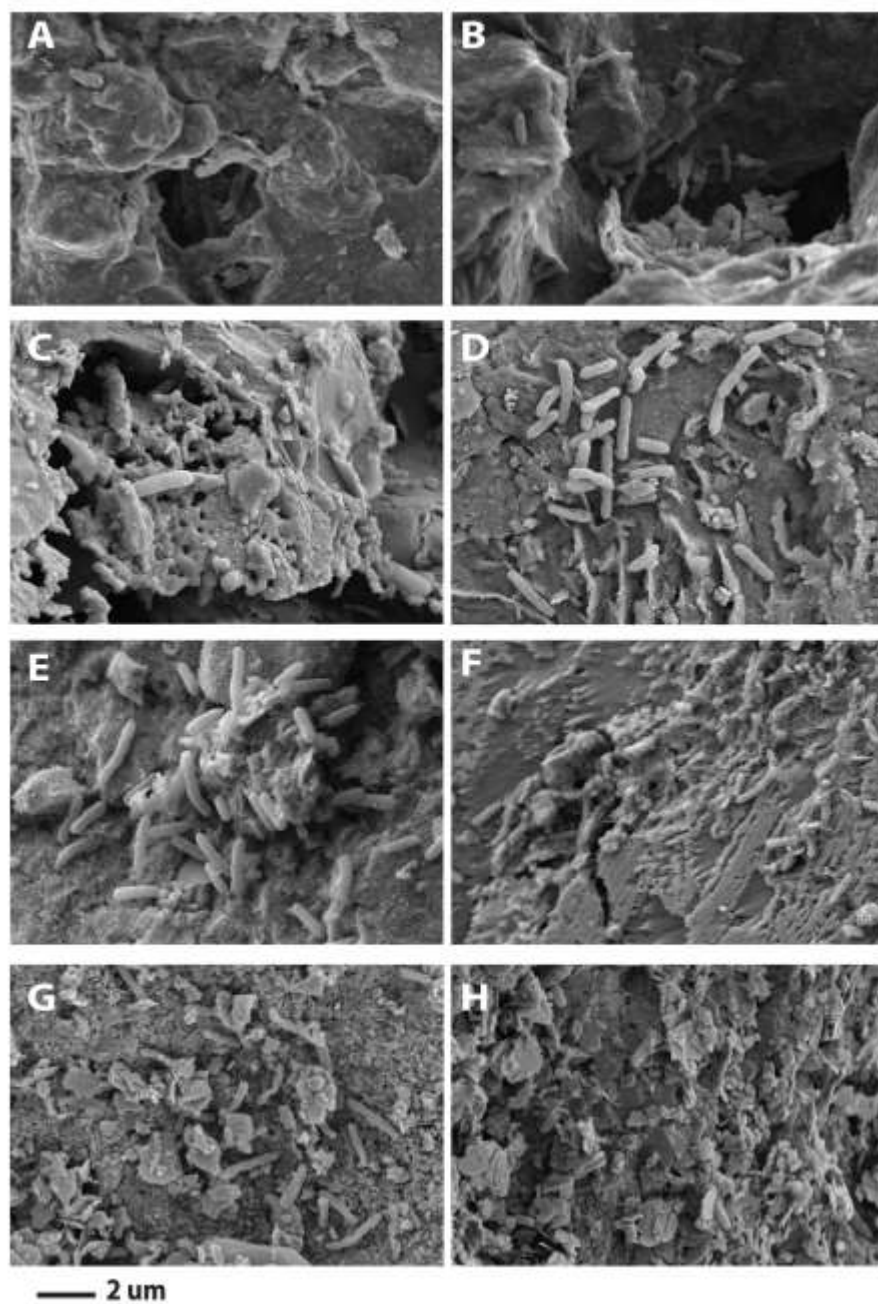


Figure 3-10 SEM images of SO on various minerals before and after 25 bar CO₂ exposure: (a) quartz sandstone, (b) quartz sandstone after 8 hours, (c) albite, (d) albite after 8 hours, (e) dolomite, (f) dolomite after 6 hours, (g) hematite, (h) hematite after 8 hours.

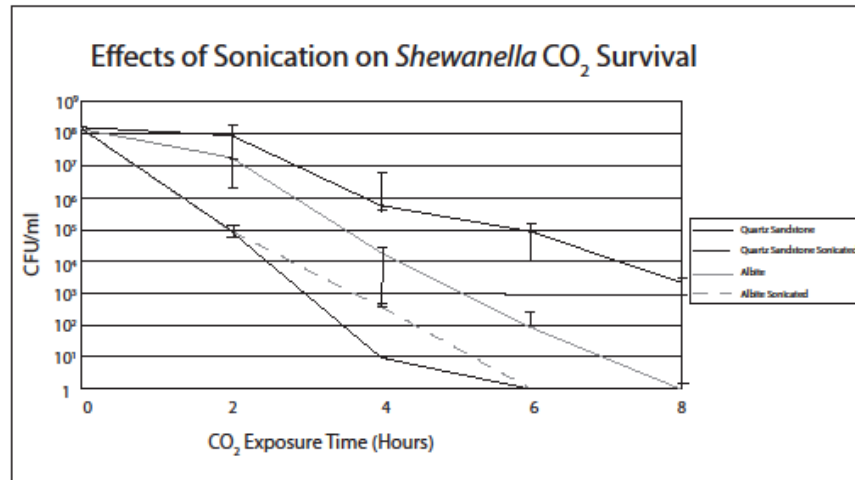


Figure 3-11 Effects of sonication on SO CO₂ survival.

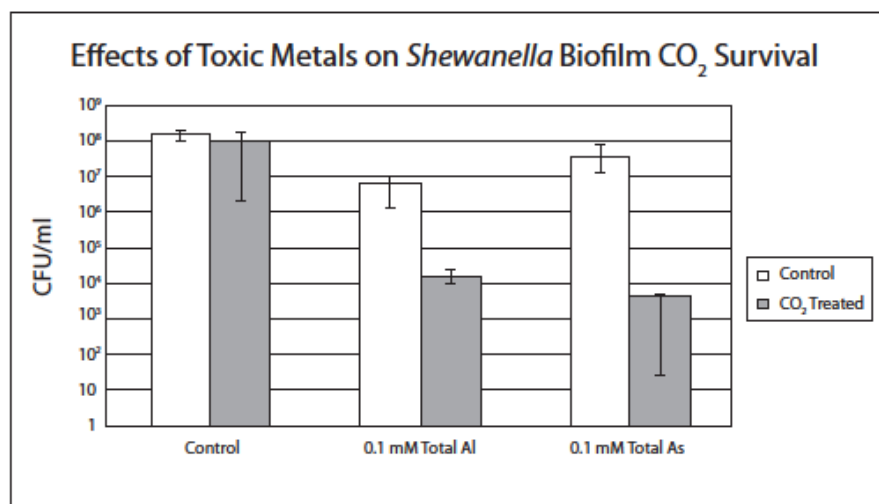


Figure 3-12 Effects of toxic metals on SO biofilm CO₂ survival.

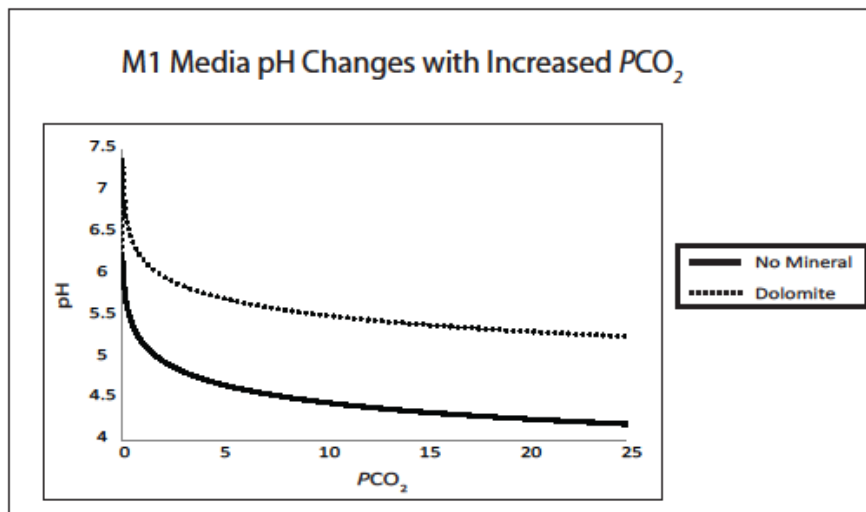


Figure 3-13 M1 media pH changes due to increased PCO_2 with and without dolomite. Geochemical modeling was performed using Geochemist's Workbench (Bethke 1996).

Chapter 4: Microbial Communities in Terrestrial CO₂ Springs

ABSTRACT

When CO₂ is sequestered in the deep subsurface, native microbial communities will be introduced to a stress which will undoubtedly change community composition. To determine the long-term influence of CO₂ on communities, terrestrial CO₂ springs can be utilized as analogues. In this study, four CO₂ springs and two non-CO₂ springs within the western United States were sampled for their geochemistry and 16S rRNA gene sequences: the Little Grand Wash Fault (LGW), UT; Arches Headquarters (AH), UT; Moab Ranch Springs (MS), UT; Bravo Dome (BD), NM; Klickitat Mineral Spring (KMS), WA. Microbial diversity decreased in sites exposed to CO₂ relative to non-exposed sites suggesting stressed communities. Communities in the sedimentary formations of LGW and BD were characterized by low diversity relative to that of the basalt formation, KMS. Of the sites sampled, Archaea were only detected in the highest diversity sites (MS and KMS), and the Archaeal community changes from unclassified sedimentary archaeal communities in MS to methanogens in KMS suggesting methane cycle may occur in CO₂ rich environments. While CO₂ tends to decrease diversity, other environmental factors may also contribute to community composition including sample depth, ionic strength, and nutrient concentrations. Results confirm the presence of microbial communities at high *PCO₂* and suggest that CO₂ present in the environment is an environmental stress that can lower diversity but that other factors beyond CO₂ also affect diversity.

INTRODUCTION

On an ecosystem scale, “stress” is defined as a chronic challenge that will impose a physiological cost (Schimel, Balser et al. 2007). When CO₂ is sequestered in the deep subsurface, native microbial communities will be introduced to a stress that will undoubtedly produce a response. Responses may include the reallocation of energy to combat CO₂ toxicity such as through the cessation of cell division to increase metabolism, a decrease in cell size, or dormancy. In many cases, there will be no response and cell death will occur. Microbes most capable of surviving the CO₂ stress will become the dominant members of the subsurface community, resulting in a community shift (Øvreås and Torsvik 1998, MacNaughton, Stephen et al. 1999). Changes in microbial communities within the subsurface will be important as this will alter the subsurface ecosystem’s function such as the biogeochemical cycling and the dominant geochemical transformations.

Previously surveyed deep subsurface microbial communities have varied by community composition but nonetheless share similarities such as a lack in diversity due to extreme stresses placed on the community including temperature, pressure, pH, salinity, and energy and nutrient availability (Hines, Lyons et al. 1992, Pedersen 1993, Colwell, Onstott et al. 1997, Fredrickson, McKinley et al. 1997, Onstott, Phelps et al. 1998, Krumholz 2000, Onstott 2003, Sahl, Schmidt et al. 2008, Griebler and Lueders 2009, Reith 2011). Many organisms found in the deep subsurface have resided in these environments due to burial or infiltration from meteoric water. While many taxa present

represent known lineages, such as Proteobacteria and Firmicutes, long residence times and isolation from the surface has also resulted in large divergence from known sequences, resulting in novel lineages (Gihring, Moser et al. 2006, Sahl, Schmidt et al. 2008, Mason, Di Meo-Savoie et al. 2009).

Deep saline aquifers, composed of sandstones capped by a shale or mudstone caprock, are potential basins to be utilized for sequestration. These locations are ideal for storage in continental locations as they are tectonically stable, have a large storage capacity, and are permeable (McGrail, Schaef et al. 2006). Flood basalts are another prospect for carbon sequestration due to their high porosity and their reactivity (McGrail, Schaef et al. 2006). Basalt is quick to weather, allowing for the dissolution of CO₂ to happen much faster (Matter, Takahashi et al. 2007). Microbes living in these deep subsurface environments utilize the surrounding rocks to survive. Various electron acceptors may be used including Fe, SO₄²⁻, and CO₂ resulting in the dissolution of host rock, precipitation of biogenic minerals, and the alteration of subsurface gas chemistry (Lovley 1993, Gihring, Moser et al. 2006, Lavalleur and Colwell 2013). Microbial communities also enhance the weathering of the host rock (Pedersen 1993, Bennett, Hiebert et al. 1996, Bennett, Rogers et al. 2001).

In this study, we examine four CO₂ springs from three different locations in the Western United States (Figure 4-1) as well as two springs from southeastern Utah for comparison. The CO₂ springs act as analogues to the long term effects of carbon

sequestration on subsurface communities providing insights into whether ecosystems exposed to CO₂ are capable of supporting life that could potentially affect subsurface biogeochemistry. These springs make ideal sampling sites as they are accessible, and discharge water from deep within the subsurface. Few studies have been performed on the diversity of bacterial and archaeal communities at high *PCO*₂ environments. Previous studies of CO₂ springs at Yellowstone, for example, have shown microbial communities present at approximately 1.88 mM to 24.5 mM of dissolved CO₂ (Spear, Walker et al. 2005, Clingenpeel, Macur et al. 2011). However, these studies focus on organisms outwashing from the spring and living at the temperature limits of life rather than communities living within the aquifer. The springs examined in these studies have calculated dissolved CO₂ concentrations at a minimum of 12 mM CO₂, though these concentrations likely increase at depth. Temperatures at these four springs were also much lower than Yellowstone (Table 4-1). Springs were sampled and measured for their geochemistry as well as their composition based on 454 sequencing at depth with the initial hypothesis that diversity in these springs would be low due to the stress created by CO₂ in the environment. However, results show that controls to diversity in the sampled springs are more complicated than simply toxicity from CO₂.

SITE DESCRIPTIONS

Little Grand Wash Fault

Two sample sites (Figure 4-4 and 4-5) are located along the Little Grand Wash Fault (LGW) near Green River, UT. The fault is on the Colorado Plateau in the northern end of the Paradox Basin where oil, methane, and CO₂ fields are actively producing. LGW cuts through several formations including the Paradox formation, several Jurassic sandstones including the Entrada, Navajo, Kayenta, and Wingate sandstones, as well as some cretaceous shales (Dockrill and Shipton 2010). CO₂ coming from these springs is thought to originate from carbonate-clay diagenesis, >800 m below the subsurface. The dissolution of carbonate-rich minerals results in an excess of subsurface CO₂, causing periodic eruptions in Crystal Geyser and the leakage of CO₂-charged water through other springs (Shipton 2004). Waters from these springs are thought to be meteoric in origin though Na and Cl concentrations suggests the possibility of mixing from a deeper brine (Heath, Lachmar et al. 2009). Fractures are present throughout LGW which eventually seal up as outgassing CO₂ charged water precipitates calcite and seals fractures. This then causes new fractures to emerge.

Crystal Geyser (CG) lies near the banks of the Green River (Shipton et al 2004). It is a cold spring (19°C) that periodically erupts with CO₂ charged water. It was formed due to the drilling of an 801 m deep oil well in 1935 (Baer and Rigby 1978). Geyser eruptions are triggered by the buildup of CO₂ in the groundwater until pressures are high enough to trigger an eruption. Carbonate and Fe rich water outflow from the well and

precipitate into iron-oxide rich travertine mounds. CO₂ discharge is not limited to the CG but to areas surrounding the geyser with CO₂ bubbling springs periodically appearing at the road near the well or with small bubbles of CO₂ escaping into Green River (Shipton 2004). The geyser also has a strong sulfur smell and small seeps of oil are found nearby.

Airport Spring (AS) is located next to the Green River Municipal Airport, approximately 10 km west of CG. The spring is located on a travertine mound approximately 10 ft high. From this spring, 26°C CO₂ charged water bubbles constantly into the travertine mound, precipitating more travertine. Discharge from the spring is less explosive than CG and much more constant. The spring is rich in ferrous iron as stream waters flowing down the mound are colored orange, presumably from the oxidation of the iron. The spring is located on the top of the travertine mound, in a hole approximately 2 m deep. There is little information on this specific spring as this has never been sampled before.

Moab Springs Ranch

Located in Moab, UT, Moab Springs Ranch (MS) contains a spring that discharges from the Glen Canyon Aquifer Group (Figure 4-2). The spring water flows through similar units as those in the Little Grand Wash Fault, including the Wingate, Kayenta, and Navajo Sandstones. The water is thought be recharged at the La Sal Mountains approximately 65 km southeast of the spring at an elevation of 2825 m. Water discharges from a cliff wall at an elevation of 1250 m (Masbruch 2014). The water, while

coming from a different hydrogeologic unit than those of the Little Grand Wash Fault, is unaffected by CO₂ and flows through similar geologic units as the LGW sites, making this a good site to compare microbial communities unaffected by CO₂ to those affected by CO₂.

Arches Headquarters

Arches Headquarters (AH) is located approximately 6 km northwest of Moab Springs Ranch at the entrance of Arches National Park. As with MS, the water originates from the Glen Canyon Aquifer Group, with the well being completed through the Navajo sandstone. Part of the water is thought to be sourced from a higher elevation, though it is likely that a significant portion of this water may be from more local flowpaths at lower elevations (Masbruch 2014). Water is pumped at an elevation of 1245 m. The well is also unaffected by CO₂ and is 52 m deep, screened between 35-52 m (Figure 4-3).

Bravo Dome

The Bravo Dome (BD, Figure 4-6) Carbon Dioxide Gas Field is located in northeastern New Mexico, which is approximately 24 km southwest of Clayton, NM. The field is operated by Oxy, with the CO₂ mined for enhanced oil recovery. The field is located on an anticline with the CO₂ bearing Tubb sandstone, approximately 760 m below the surface. The CO₂ is capped by the Cimarron anhydrite, which lies directly above the Tubb sandstone (Broadhead 1990). This has apparently proven to be an extremely effective caprock as there have been no observed surface CO₂ leakage sites in

the entire field. Helium ratios have shown that the CO₂ at BD is volcanogenic in origin, likely migrating from the McElmo Dome field within the Colorado Plateau (Gilfillan, Ballentine et al. 2008). To our knowledge, the water from this site has never been sampled and characterized for its microbiology.

Klickitat

Klickitat Mineral Spring (KMS, Figure 4-7) is located in southern Washington, approximately 45 km north of The Dalles, OR. The well was drilled into the Tertiary Wanapum Basalt which overlays the Ohanapecosh Formation, both part of the Columbia River Basalt Group (CRBG). The well lies next to an abandoned dry ice facility. CO₂ charged water flows from a well that is between 90 to 120 m below the surface (Korosec 1983). There is a constant base flow of water out of the well with transient bursts of high flow. The water is iron and carbonate rich as it flows out into orange colored travertine that then trickles into the Klickitat River. While faint, there is also a slight sulfur smell. The source of CO₂ from this spring is likely volcanogenic (Barnes 1984).

METHODS

Field Sampling

Filters, tubing, and containers used for biological field sampling were autoclaved whenever possible prior to sampling at 122°C and 15 psi for 30 minutes. When no autoclave was available, field sterilization was performed by treating materials with a 10% sodium hypochlorite solution for approximately 30 minutes followed by a sterile

10% sodium thiosulfate solution to remove excess chlorine. Materials were then rinsed with approximately 10 liters of the spring water being sampled prior to collection.

Biomass collection was performed using a peristaltic pump (Geotech, Denver, CO) with silicone tubing (Masterflex, Vernon Hills, IL). Water at CG was collected at approximately 9.7 m depth while at AS, 1.1 m depth was sampled. Sample collection at KMS, occurred at approximately 9.4 m depth. Tubing was placed at the mouth of the spring for MS and was collected through a peristaltic pump. Waters were pumped at a rate of 200 ml/min into a sterile collection container in order to allow CO₂ to exsolve except for MS, where water was filtered directly. For AH, water was collected from a hose bib upstream of a chlorinator and was filtered directly. BD was sampled from a central container, which collects condensed water from the gas from multiple wells. As a result, sampled water is an amalgamation of waters from multiple wells. All samples were filtered using a 90 mm, 0.1 µm sterile polycarbonate filter (Millipore, Billerica, MA). 50 L of water was filtered for CG and AS, 39 L from BD, and 10 L from KMS. Approximately 30 L was collected from both MS and AH. Filters were then placed aseptically into sterile Whirl-Pak bags (Nasco, Fort Atkinson, WI). Samples for DNA were preserved in a liquid nitrogen dewar until processing (Taylor-Wharton, Theodore, AL).

Water analysis was performed on samples of the filtrate. Measurements of unstable parameters taken in the field included pH, temperature, and conductivity using

an ultrameter (Carlsbad, CA). Field measurements for dissolved O₂ (DO), Fe, PO₄²⁻, NO₃⁻, and NH₄⁺ were performed photometrically using test kits and a V-2000 multi-analyte photometer from Chemetrics, Inc (Midland, VA) when possible. Samples were taken for laboratory analysis of cations, anions, and alkalinity, total nitrogen, and dissolved inorganic and organic carbon. Water for cation analysis was field-acidified using 500 µl trace metal grade nitric acid.

Geochemical Analysis

Alkalinity was determined by titration to pH 4.5 in the lab. Anions and acid-preserved metals were measured using ion chromatography or inductively coupled plasma mass spectrometry, respectively, except for MS and AH where chloride and sulfate were measured photometrically using previously stated methods. Dissolved inorganic carbon (DIC) and dissolved organic carbon (DOC) were measured with a carbon analyzer. Calculations for saturation index and *PCO*₂ were performed using Geochemist's Workbench (Bethke 1996) after balancing the water for charge using bicarbonate for CO₂ exposed sites and chloride for non-CO₂ sites.

Sequence Analysis

DNA extraction for samples from the Little Grand Wash Fault was performed using a modified phenol-chloroform extraction (Tsai and Olson 1991). For BD and KMS, DNA was extracted using the Mo Bio Power Biofilm DNA extraction kit (Mo Bio Laboratories, Inc, Carlsbad, CA). All samples were sent to Molecular Research LP

(Shallowater, TX) for 454 sequencing using 27F or 349F primers for bacterial or archaeal 16S rRNA gene sequences.

Sequence data was processed using QIIME (Caporaso, Kuczynski et al. 2010). Sequences were demultiplexed followed by denovo chimera removal through Uchime. Operational taxonomic units were defined at 97% similarity and were classified using BLASTn against a curated GreenGenes database. Calculations for alpha and beta diversity were performed at the genus level. Multivariate analysis to correlate community structure with environmental variables was performed on Vegan (Dixon 2003).

Alpha diversity metrics used were the Shannon and Simpsons indices as well as observed taxa present in sequences. The Shannon index (H) is a diversity calculation that provides more weight on rare OTUs present in a community while the Simpson's index (D) provides more weight on dominant OTUs. Values for D were expressed as the reciprocal, i.e. $1/D$ (Lande 1996).

Beta diversity calculations were assessed through both UniFrac calculations and constrained correspondence analysis (CCA). UniFrac, is a beta diversity metric that compares the shared taxa between different communities by their phylogenetic relatedness, and assigns a distance measurement between 0 and 1. Values closer to 0 indicate more community relatedness while values closer to 1 mean community dissimilarity (Lozupone and Knight 2005). The CCA plot is utilized to determine community composition of the different sample sites with each other as well as with

environmental parameters. The distribution of the different data points in the resultant plot represents the relatedness of the various sample sites, with samples most closely related plotting nearest each other. Environmental variables are represented by different vectors, with vector lengths representing the degree of change that occurs with each parameter. Data points are most correlated to those parameters when they are closest to the vectors (Dixon 2003, Oksanen February 8, 2013). Correlations between community composition and environmental parameters are also assigned an r^2 value.

RESULTS

Water Chemistry

Table 4-1 and Figure 4-8 describe spring or well compositions. Water temperature varied between 4.4 to 26.8 °C. However, due to the geothermal gradient, temperatures are likely higher, especially for CG and BD, where water temperatures reflect temperatures at the surface during time of collection. Sample pH ranges for CO₂ affected sites were between 5.83 to 7.71 although the pH is expected to be lower at depth for the CO₂-exposed sites before surface outgassing of CO₂. BD was the most saline of the waters while MS was the least. CG, AS, and KMS were rich in reduced Fe (0.1 to 0.25 mM) and abundant Fe oxides in the travertine suggests total Fe may be even higher and that Fe is being oxidized as water reaches the surface. Sulfate was present in high concentrations in CG, AS, and BD (19.03 to 23.98 mM). All CO₂ waters were high in alkalinity (17.96 to 94.40 mM). Phosphate concentrations varied between the sites, with KMS having the

highest concentration at 8.32 uM while CG, MS, and AS had concentrations below detection limits. Nitrate concentrations were low, ranging between 0.004 to 1.24 uM, with BD having the highest concentration. When measured, ammonia concentration was highest at KMS at 360.31 uM while BD contained 9.76 uM. PCO_2 appears to be highest in BD though the measured values probably underestimate the concentration in the formation. DOC was variable, with CG and BD having the highest of the concentrations. The piper diagram shows the variability in water composition but indicates the waters from the sedimentary locations cluster closer together in water composition while KMS is the most distinct of the 6 samples.

Diversity

A phylum-level summary of the bacteria present at all the sample sites is presented in Figure 4-9. Over 50% of the phyla present at MS belong to the Proteobacteria. Other bacteria present at this site belong to the phyla Planctomycetes, Acidobacteria, Nitrospirae, Bacteroidetes, Chloroflexi, Firmicutes, Actinobacteria, Fibrobacteres, Verumicrobia, Elusimicrobia, Armatimonadetes, and Cyanobacteria. In addition, the candidate phyla OP3, OD1, and NC10 are also present. Over 673 novel OTUs are observed (Table 4-2), and the distribution of these OTUs shows no one taxon dominates the sequences.

Fewer phyla are represented at AH than at MS. Of the sequences at AH, 66% belonged to the Proteobacteria, 15% belonged to the Firmicutes, 9% to Actinobacteria,

9% to Cyanobacteria, 0.8% Bacteroidetes, and 0.1% to Chloroflexi. In addition, the number of unique OTUs present was 66, with the genera *Bradyrhizobium* and *Pseudomonas* comprising 28% and 26% of the sequences, respectively. No Archaea were detected during the sampling of AH.

Both springs at the LGW share very similar sequence compositions. CG differed with AS by the presence of the NK candidate phylum and the VC candidate class as well as the absence of Bacteroidetes. Greater than 97% of the sequences in both sites belong to the Proteobacteria with Actinobacteria, Bacteroidetes, and Firmicutes composing the rest. Within the Proteobacteria, the genus *Acinetobacter* was the most prevalent of the sequences. No Archaeal sequences were amplified through pyrosequencing.

Sequences at BD are composed mainly of Proteobacteria (88.1%) with Bacteroidetes, Firmicutes, and Actinobacteria composing the rest of the sequences. Within the Betaproteobacteria, the genus *Burkholderia* the most prevalent. Pyrosequencing did not detect any Archaea.

There were far more phyla represented at KMS than at the other CO₂ sites, many of which group together with unclassified and uncultured bacteria. The phylum Actinobacteria, specifically the candidate class OPB41, comprises over 25% of the sequences. Proteobacteria comprise 15.1% of the community. Additionally, Elusimicrobia, specifically the candidate class OP2 make up 13% of sequences. Nitrospirae and Firmicutes comprise 9.8% and 12.1% of sequences, respectively.

Chloroflexi, Chlorobi, Bacteroidetes are also represented as well as the candidate phyla OP3, OD1, AC1, and OP11.

Figure 4-10 shows Archaea at the sample sites. The majority of Archaea at MS at this site are composed of Euryarchaeota (90%) as well as Crenarchaeota (10%). Of the Euryarchaeota, the majority of the sequences belong to unclassified Archaeal classes including Parvarchaea and Thermoplasmata. Of the Crenarchaeota, sequences belong mainly to the unclassified Thaumarchaeota. Archaea at KMS contain a similar composition with differing genus-level distributions. Sequences are largely (74.6%) represented by the phylum Euryarchaeota. Crenarchaeota and unclassified archaea make up the rest of sequences. Unlike MS, the Euryarchaeota are dominated by Methanomicrobia, Thermoplasmata, and the candidate classes Micrarchaea and DSEG.

Table 4-4 lists values for several bacterial alpha diversity metrics including unique OTUs present, Shannon index, and the reciprocal Simpson's index. MS and AH display higher numbers of unique OTUs present as well as higher Shannon and Simpson's indices relative to the LGW sites which display low richness and evenness. BD displays moderate OTU richness and evenness, with numbers slightly lower than those found at AH. KMS displays both high richness and evenness in bacterial diversity, comparable to MS. Rarefaction curves for bacteria are displayed in Figure 4-11. At the subsampling set used, AH, AS, CG and BD curves have leveled off, indicating a good

sampling depth while MS and KMS continue to increase, indicating there are still more OTUs present that were not sequenced.

Table 4-3 compares bacterial unweighted Unifrac distance matrix values between the bacterial communities of the different sites. The values between CG and AS is 0.54, indicating similarity between community compositions. Both CG sites have values of 0.82 between BD indicating less similarity, while CG, AS, and BD all have values greater than 0.97 with KMS indicating highly dissimilar sites.

Figure 4-12 shows the results of a constrained correspondence analysis describing the relationship of the various sites to each other as well as to select environmental variables. There is a strong ($r^2=0.9$) correlation of the sites to increasing sulfate concentrations. KMS and MS are most similar to each other with phosphate and ferrous iron correlating to their community structures. AH community is most correlated to nitrate concentrations. BD relates most to nitrate and ionic strength. Both CG and AS are the most similar of the sites, grouping closely together on the plot and furthest away from all the other sites. DOC, pH, and temperature are factors that may explain the structure of the LGW communities though other factors likely contribute to their variation.

DISCUSSION

Based on the findings from Santillan et al. (2013), we had initially hypothesized that microbial communities in CO₂-exposed sites would represent stressed communities, resulting in low Shannon and Simpson's indices. Our findings show that while

communities in CO₂ springs show lower diversity relative to non-CO₂ springs, other environmental interactions complicate and alter the diversity in these subsurface environments.

Furthermore, based on previous findings by Chapelle et al. (2002) and Lavalleur and Colwell (2002), we also hypothesized that microbial communities in CO₂ springs from basalt sites would show higher diversity relative to those in sedimentary and sandstone environments due to the buffering capabilities of basalt as well as the nutrient contents available. Diversity in the basalt environment is higher relative to the sedimentary formations, though much lower than previously sampled sites from the same formation (Lavalleur and Colwell 2013). Based on this comparison, it does appear that basalt sites affected by CO₂ can support more diversity than sandstone sites, but that these sites are also stressed in comparison to unaffected sites.

The springs all varied greatly in their community compositions, having very few shared phylotypes between sites, with the exception of CG and AS which had 39 phylotypes in common of the 50 unique OTUs present. This dissimilarity in community composition is likely a result of geographic separation as the sites sampled are sourced from distinct aquifers, with the exception of CG and AS.

MS shows the highest diversity of all the sites, with 673 unique OTUs detected, resulting in a Shannon index of 8.7 and a Simpson's index of 216.3 showing the highest OTU richness of the sites sampled. The sampling depth was low suggesting not all the

diversity was captured during sequencing and that more unique OTUs are present (Figure 4-11). Agricultural soils have been reported to have Shannon indices ranging between 6-7.2 and Simpsons indices ranging between 36 to 349 (Ma, Ibekwe et al. 2013). Grassland soils have reported Shannon indices between 2 and 3 while pristine aquifers have indices reported between 0.5 and 4 (Drissner, Blum et al. 2007, Zhou, Kellermann et al. 2012). The diversity and evenness at MS appears consistent with that of soil environments, suggesting much of the water discharging from this spring may come from a shallow source that has been influenced by a soil zone. The presence of soil organisms belonging to the orders such as Rhizobiales, Pseudomonadales, Bacilliales, Actinomycetales, all corroborate the hypothesis that much of this water's composition reflects that of a soil environment. Additionally, water recharged from this site may come from the La Sal Mountains, 65 km away, suggesting the sequences at this site may also be reflecting a more regional microbial ecology than just the ecology of the specific spring.

In contrast, the AH well, which is likely sourced from more localized part of Moab, shows significantly less diversity than MS, with 66 unique OTUs, Shannon index of 3.6, and a Simpson's index of 6.3. Its lower diversity relative to MS suggests the Navajo Sandstone may contain low microbial diversity. Unlike MS, AH shows unevenness in OTU distribution, with the orders Rhizobiales, Pseudomonadales, and Bacilliales representing the majority of the sequences. The decrease in diversity and

evenness suggests a more stressful environment than that of MS (MacNaughton, Stephen et al. 1999, Bordenave, Goni-Urriza et al. 2007, Schimel, Balser et al. 2007).

Both LGW sites display similar community composition (Unifrac value of 0.35) with slight differences in the presence or absence of taxa. The most striking feature of both sites is the overwhelming dominance of the Gamaproteobacteria, specifically from the genus *Acinetobacter*. *Acinetobacter* is a common, gram-negative, nonmotile bacterium generally classified as aerobic (Vos, Garrity et al. 2011). It has also been found in other subsurface environments where water is still oxygenated and may constitute up to 0.001% of the total aerobic population of soil and water (Pedersen, Arlinger et al. 1996, Pedersen, Arlinger et al. 1996). If this organism is similar to previous findings, *Acinetobacter* at LGW likely comes from oxic water closer to the surface and is one of the few organisms able to survive in the CO₂ rich water. Both BS and AH, presumably from shallower waters but from the same sedimentary formations as LGW, show the presence of *Acinetobacter*, though the abundance of these sequences is below 1% in both samples. The source of water at CG is still inconclusive. However, it is probably a mixture of brine upwelling from the Paradox Basin mixing with meteoric water from the San Rafael Swell (Heath, Lachmar et al. 2009). If *Acinetobacter* comes from shallower water, this would explain similarities in community composition between the LGW sites despite the large discrepancy in salinity. The dominance of *Acinetobacter* over other sequences suggests extremely low diversity at depth pointing to a highly stressful

environment that essentially selects for a single organism resilient enough to adapt to the environmental conditions.

As with CG and AS, the BD community is heavily dominated by a specific taxon. In this case, 65% of sequences are comprised of organisms from the genus *Burkholderia*, a Gram-negative, aerobic organism common to soil environments (Vos, Garrity et al. 2011). Based on the Shannon and Simpson's indices, which account for the distribution of these OTUs, BD shows lower diversity, also showing evidence of a stressful environment like the LGW sites.

KMS exhibited far more diversity and evenness than the sedimentary sites affected by CO₂. KMS sequences were represented both by soil bacteria as well as novel lineages often found in locations such as Yellowstone such as the novel class OPB41 (Figure 4-9). The composition of bacteria at KMS differ markedly from previously sampled microbes in the same geologic formation. The CRBG has been shown to host a variety of unique taxa, capable of utilizing the surrounding environment to perform various metabolisms such as Fe and SO₄²⁻ reduction (Stevens, McKinley et al. 1993, Lavalleur and Colwell 2013). Lavalleur and Colwell (2013) also found that organisms in the CRBG consist mainly (77%) of Beta- and Gammaproteobacteria prior to CO₂ injection. In contrast, only 15% of KMS taxa are from the Proteobacteria, with Betaproteobacteria seen at 9% and Gammaproteobacteria being less than 1% of the sequences. This major difference in diversity suggests community composition will shift

as a result of CO₂ to favor organisms such as from the OP divisions that may be capable of tolerating high CO₂ concentrations.

Of the sites sampled, both MS and KMS contained the most diversity, and were the only sites to test positive for Archaea suggesting the subsurface sedimentary environments are not conducive to Archaea possibly because of a lack of nutrients available or because the stressful conditions of these environments make it so that bacteria outcompete archaea. Many of the Archaea present at MS represent unclassified lineages that have been identified mainly in marine sediment with very few methanogens (Tatsuhiko 2013).

In contrast, Archaeal sequences in KMS are dominated by the genus *Methanoplanus*. The presence of this taxon in KMS suggests the possibility of methanogenesis and a methane cycle. While a detailed gas analysis was not performed, previous studies on KMS indicate that there is some methane present in the gases, comprising approximately 0.11% of the overall water's gas composition (Barnes 1984). Previous studies have shown that microbially mediated methanogenesis does happen in the CRBG possibly through the utilization of H₂ generated from basalt, though the weathering of ultramafic rocks may also result in the release of some abiogenic CH₄. The abundance of CO₂, which methanogens reduce to make methane, makes this location ideal for methanogenesis as CO₂ will not be limiting for them. The presence of these taxa

also suggests that methanogens can live in CO₂ sequestration conditions and transform the sequestered CO₂ into CH₄.

In comparison to Lavalleur and Colwell (2013), Archaeal phyla will shift from a Crenarchaeota-dominated community to a Euryarchaeota dominated community, likely a result of selection for methanogens. The high diversity of the Wanapum basalt might be attributed to H₂ generation during the weathering of ultramafic minerals present in this environment (Chapelle, O'Neill et al. 2002, Spear, Walker et al. 2005, Morrill, Kuenen et al. 2013) providing fuel for microbial communities and an increase in diversity. However, the addition of CO₂ results in an increase in stress, causing a significant reduction in microbial richness and evenness.

Of the sedimentary sites sampled, diversity and evenness tended to be lower in CO₂-exposed sites in comparison to the non-CO₂ sites suggesting CO₂ will be an added stress to subsurface environments during CO₂ sequestration. Using DIC as a proxy for the amount of CO₂ present at each site, there appears to be some correlation between a decrease in diversity and an increased DIC among the sites in Utah ($r^2=0.28$). When KMS and BD are added to the comparison, the correlation decreases indicating that while CO₂ is a factor in decreasing diversity, not all CO₂ springs will be alike in their composition and that these differences in composition may be attributed to other environmental factors. This also suggests that during CO₂ sequestration, changes to microbial communities will differ depending on the location where CO₂ is sequestered.

The constrained correspondence analysis of Figure 4-12 provides a means to visualize commonalities among sites as well as potential correlations of environmental factors to variations in community composition. One aspect the low diversity sites (AH, BD, CG, AS) all share is high sulfate concentrations ($r^2=0.9$) though the taxa present at these sites do not represent lineages traditionally associated with sulfate reducers or sulfate metabolisms. The high correlation to sulfate may be a proxy variable for depth, such as the location of the communities within the stratigraphic column. In the Utah sites, the Jurassic sandstones that compose the Glen Canyon Group for CG, AS, MS, and AH overlie the Chinle Formation, a fluvial site with gypsiferous shales. Waters for CG and AS may be located lower in the stratigraphic column and are influenced by this formation, bringing saturation indices close to equilibrium with gypsum. AH may also have some contact with this, though SI is still undersaturated with respect to gypsum suggesting this water is located in a shallower part of the formation. The depth of the samples may have implications for diversity as shallower sites will have more access to TEAs and nutrients such as oxygen which decrease with depth. BD groups with these samples as well as the caprock for BD is the Cimarron anhydrite (Johnson 1983, Broadhead 1990, Gilfillan, Ballentine et al. 2008).

One factor that relates the high diversity sites together may be the amount of limiting nutrients available. KMS and MS appear to be less correlated to DIC, temperature, and ionic strength, and more closely correlated to changes with PO_4^{3-}

concentrations which increases from >0.003 mM to 0.6 mM between MS and KMS, though concentrations do vary among all the 6 sites. This makes sense for KMS as previous work has shown that basalt can be an important substratum for microbial colonization due to rich nutrient contents (Jones in press). KMS contains the highest amounts of limiting nutrients relative to the other sites with both high phosphate and ammonia concentrations. Due to the similarity in community structure to KMS, MS also groups together closely with phosphate, though it is possible other factors also explain the high diversity of MS. Furthermore, KMS is also correlated to an increase in Fe^{2+} concentration which offers the possibility that metabolisms at the site involve iron, such as Fe reduction or Fe oxidation.

AH and BD are most closely correlated to changes in nitrate concentration as well as ionic strength, though BD is more closely correlated to ionic strength than AH. This suggests one factor that can explain the decrease in diversity in these two sites in comparison to the two high diversity sites may be stresses related to salinity, which causes microbes to expend energy to maintain their osmolarity (White 2007). Furthermore, their correlation to nitrate suggests community composition is also controlled by nitrogen cycling. Of the sites surveyed, BD had the highest nitrate concentrations (1.24 μM) and was dominated by *Burkholderia*, a genus of bacteria known to perform nitrate reduction (Vos, Garrity et al. 2011). Furthermore, 27% of the

OTUs at AH are composed of the genus *Bradyrhizobium*, a group of organisms that are known nitrogen fixers (Vos, Garrity et al. 2011).

Both sites from LGW, while closely related to each other, were the most distinct from the other 4 sites. Composition among these sites is partially explained by pH, temperature, and DOC, though other variables may also affect community composition. The pH values used to perform the multivariate analysis may not be entirely representative of the pH values at depth at the LGW due to the increase in PCO_2 . The relatively low diversity in these sites may partially be resultant from acidic conditions downhole. At 25 bar, the pH at these sites may drop to 4.3 and will decrease further with increasing PCO_2 . Additionally, the LGW cuts up to 800 m below the subsurface, where waters for both CG and AS may originate. At these depths, water temperatures may be closer to 40°C, which adds heat stress to communities in addition to stresses related to acidity and PCO_2 resulting in low diversity. Furthermore, diversity in these two sites is also related to the amount of organic substrates available for organisms to consume, which are high relative to the other sites, with BD as the exception. This makes sense as oil seeps are observed along the LGW, suggesting a great deal of organic carbon may be dissolved in the groundwater that can contribute as substrates for microbes present for consumption and the resultant community composition.

Previous work has shown that CO_2 has a toxic effect on microbes. During CO_2 sequestration, a new stress will be added to already stressed microbial communities. Here

we show that despite this perturbation, bacteria and archaea are present in CO₂ rich environments indicating organisms are capable of surviving CO₂ sequestration. These communities, which have been residing in these springs for thousands of years, will likely represent what will be present after CO₂ is sequestered and allowed to interact with the subsurface environment. While the microbial communities that will eventually survive CO₂ sequestration will differ from environment to environment, communities present appear to show low species richness and evenness in sedimentary formations and high richness and evenness relative to sites that are unaffected. The presence of microbial communities at CO₂ springs will also affect the geochemistry of the systems. Both LGW sites as well as KMS are abundant in reduced Fe, suggesting communities in these environments are capable of reducing Fe. Additionally, the presence of potential methanogenic archaea, suggests methanogens may survive high CO₂ pressures and could convert CO₂ in the environment into methane, the presence of organisms related to nitrogen and sulfur bacteria suggests other microbial metabolisms that may continue to survive and metabolize even after CO₂ has been sequestered.

	T (°C)	Cond (mS)	DO (ppm)	DOC (ppm)	pH	Na	K	Ca	Mg	Si	Cl	HCO ₃	SO ₄	Fe	PO ₄ (uM)	NO ₃ (uM)	NH ₄ (uM)	PCO ₂ (bar)
Moab Springs	16.5	0.30	-	3.38	7.71	0.56	0.04	0.76	0.50	0.15	0.59	2.15	0.33	0.0003	bdl	0.004	-	0.002
Arches Headquarters	15.3	1.553	-	2.43	7.28	7.28	0.24	2.39	1.52	0.2	5.91	3.79	2.79	0.0002	bdl	0.07	-	0.009
Crystal Geyser	19.6	19.91	0.32	134.52	6.57	174.28	8.98	24.58	9.24	0.07	133.23	91.16	23.58	0.20	bdl	0.23	180.10	0.768
Airport Spring	26.8	0.50	0.17	6.73	6.32	20.92	2.45	19.85	8.14	1.05	4.39	35.59	19.03	0.10	2.22	0.44	98.78	0.501
Klickitat	25.4	0.15	0.08	1.38	5.83	2.89	0.27	3.32	4.56	2.64	0.58	17.96	0.02	0.26	8.32	0.60	360.31	0.393
Bravo Dome	4.4	44.02	-	20.88	5.85	393.91	8.23	46.63	38.05	0.58	445.27	94.40	23.96	0.05	3.90	1.24	9.76	1.416

Table 4-1 Composition of sites sampled. Values in mM unless stated otherwise.

	Subsampled	Observed Taxa	Shannon Index	Reciprocal Simpson's Index
Moab Springs	1720	672.7	8.7	216.4
Arches Headquarters	1720	66.4	3.6	6.3
Crystal Geyser	1720	49.7	1.5	1.5
Airport Spring	1720	50.2	1.4	1.4
Bravo Dome	1720	80.0	3.1	3.2
Klickitat	1720	525.8	6.6	14.5

Table 4-2 Bacterial alpha diversity values for sites sampled.

	BD	KMS	CG	AS
BD	0	0.97	0.83	0.82
KMS	0.97	0	0.98	0.98
CG	0.83	0.98	0	0.54
AS	0.82	0.98	0.54	0

Table 4-3 Unweighted unifrac values for sites sampled.



Figure 4-1 Sample locations within the United States.



Figure 4-2 Moab Springs Ranch sample site.



Figure 4-3 Arches Headquarters sampling site.



Figure 4-4 Crystal Geyser, located on the Little Grand Wash Fault. The spring periodically erupts with CO₂ charged water.



Figure 4-5 Airport Spring, located approximately 10 km northwest of Crystal Geyser. CO₂ charged water bubbles out of a spring at the top of the travertine mound and flows downhill to precipitate more carbonate.



Figure 4-6 Bravo Dome. Water vapor from CO₂ condenses and is emptied into a centralized collection container.



Figure 4-7 Klickitat Mineral Spring.

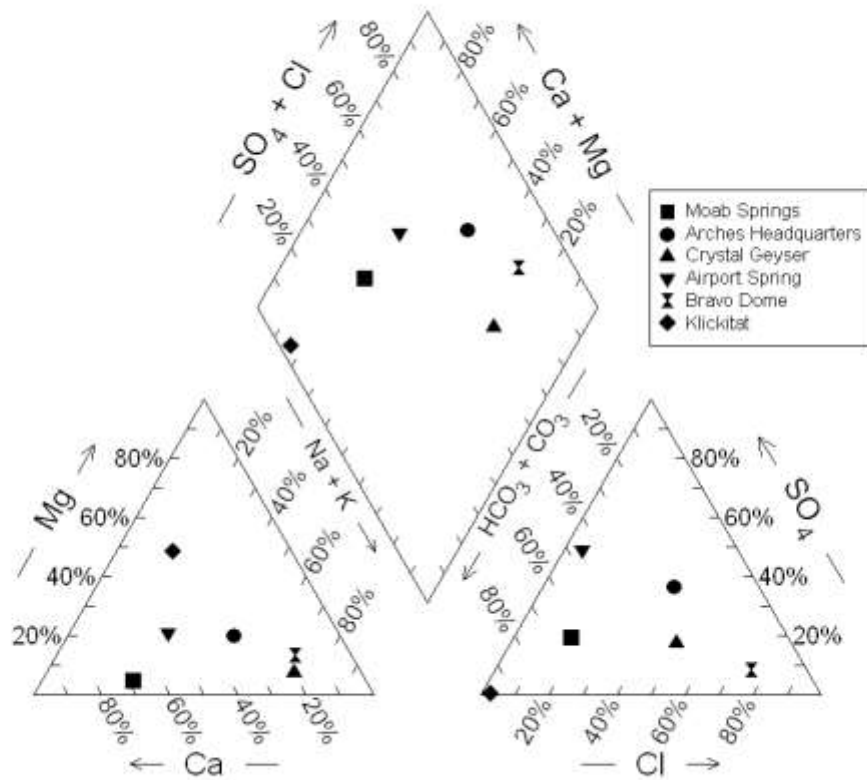


Figure 4-8 Piper diagram representing the water chemistry of the springs sampled.

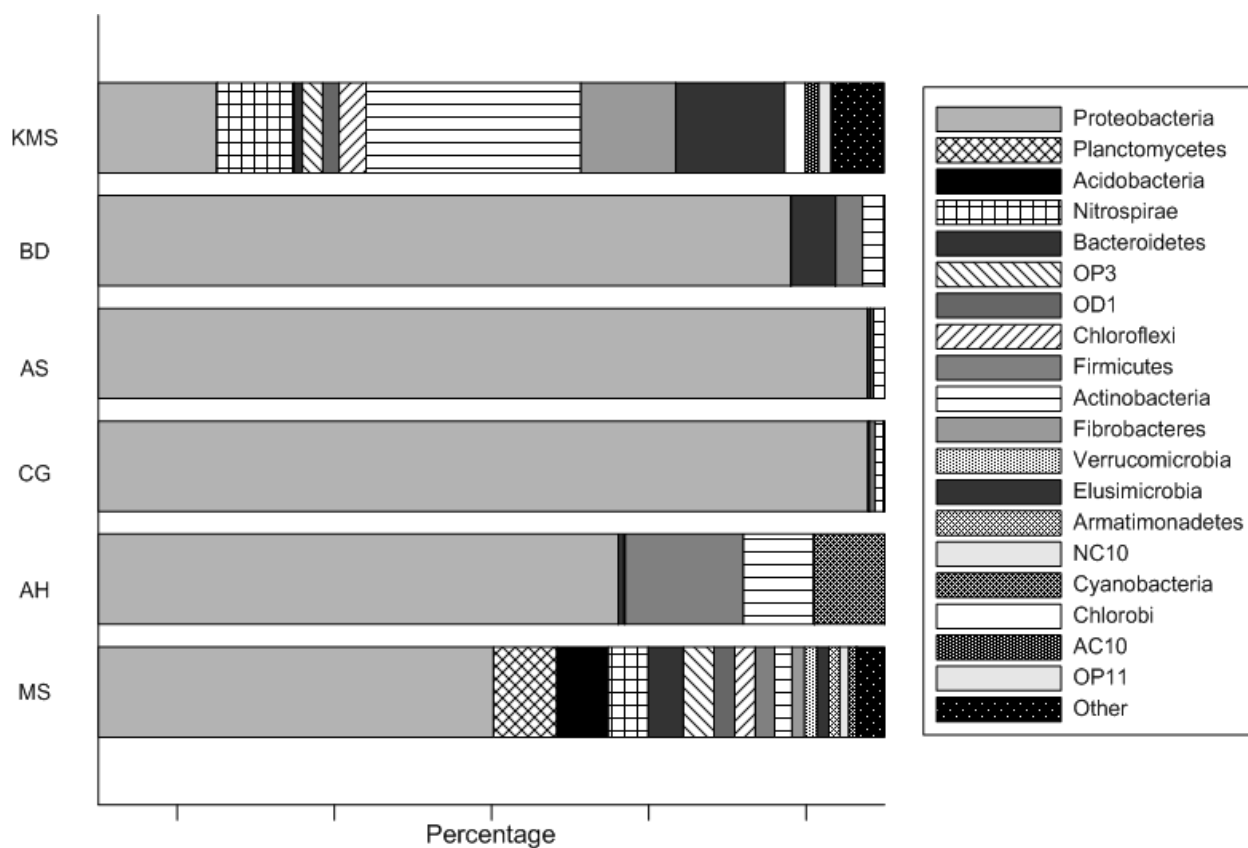


Figure 4-9 Bacterial community composition of the springs sampled.

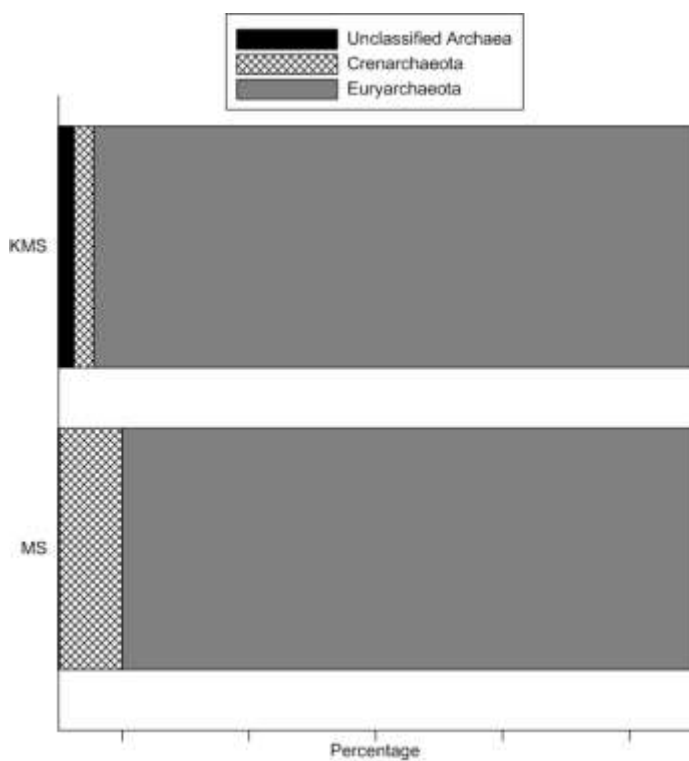


Figure 4-10 Archaeal community composition of the springs sampled.

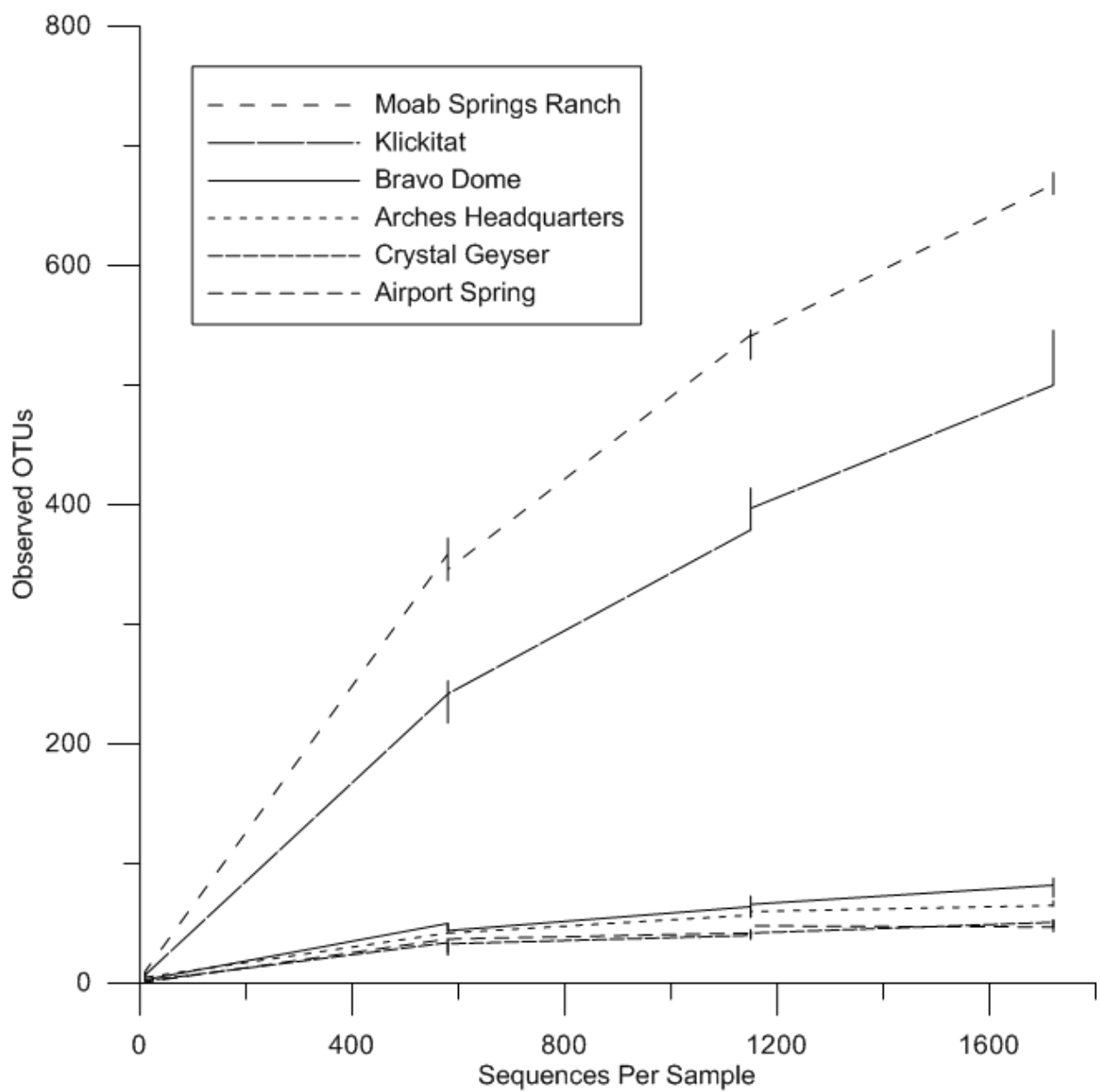


Figure 4-11 Bacterial rarefaction curves.

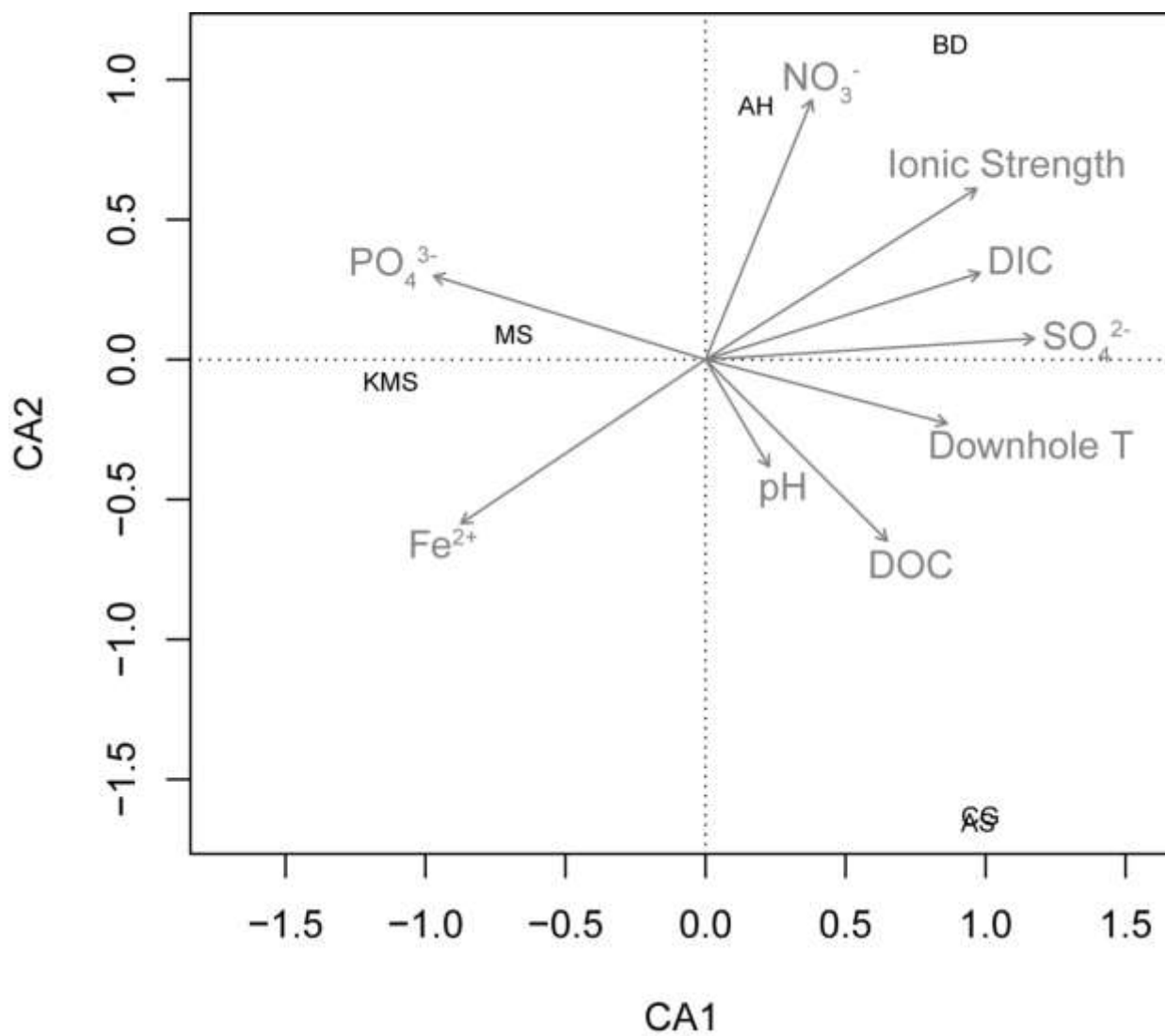


Figure 4-12 Constrained correspondence analysis of the sites sampled.

Chapter 5: Isolation and Characterization of a Novel CO₂-Tolerant Lactobacillus Strain from Crystal Geyser, Utah, U.S.A.

ABSTRACT

The long-term biogeochemical impacts of geologic CO₂ sequestration into saline aquifers remain unknown, however it is hypothesized that capnophiles, microorganisms that grow in CO₂-rich environments, will dominate under these new conditions. To understand the effects of CO₂ on capnophiles, an isolate from Crystal Geyser, Utah, U.S.A., a CO₂- rich spring considered a carbon sequestration analogue, was characterized. The isolate was cultured under varying CO₂, pH, salinity, and temperature, as well as different carbon substrates and terminal electron acceptors (TEAs) to elucidate growth conditions and metabolic activity. Designated CG-1, the isolate is related (98.5%) to *Lactobacillus casei*, growing at *PCO*₂ between 0 to 10 bar. Growth is inhibited at 25 bar, but stationary phase cultures exposed to this pressure survive beyond 5 days. At 50 bar, survival is at least 24 hours. It grows in neutral pH, 0.25 M NaCl, and between 25° to 45°C. It consumes glucose, sucrose, or crude oil, likely performing lactic acid fermentation. Fatty acid expression between 1 bar to 10 bar suggests decreases in cell size and increases in membrane rigidity. Transmission electron microscopy reveals rod shaped bacteria at 1 bar. At 10 bar, cells are smaller, amorphous, and produce abundant capsular material. Results suggest that bacteria such as CG-1 can survive under CO₂ sequestration, with the potential to change the geochemistry of saline aquifers and the fate of stored CO₂. Its tolerance to CO₂ pressures higher than other known capnophiles

suggests this microorganism should be classified as a new kind of extremophile, a hypercapnophile.

INTRODUCTION

Capnophiles are microbes that grow in CO₂ rich environments with optimal growth between 0.04 to 0.25 bar CO₂ in the gas phase. They are phylogenetically diverse, perform a variety of metabolic activities, and share very little evolutionary relationship to each other (Song, Lee et al. 2007, Bringel, Hammann et al. 2008, Arioli, Roncada et al. 2009). Capnophiles have been isolated from a variety of habitats including plants, mammalian cavities, wastewater, and animal rumens (Ballestra, Dasilva et al. 1996, Bringel, Hammann et al. 2008, Ueda, Tagami et al. 2008, Arioli, Roncada et al. 2009). Many capnophiles are pathogenic, such as *Streptococcus pneumonia* and *Haemophilus influenza* (Bringel, Hammann et al. 2008). Other capnophilic microorganisms such as *Lactobacillus plantarum* and *Mannheimia succiniciproducens* carry biotechnological significance, being utilized in fermentation processes to create cheese and other dairy products as well as succinate for biofuels (Bringel, Hammann et al. 2008). While a large degree of attention has been given to these bacteria for food and disease studies, little has been given to their presence and environmental significance in the deep subsurface.

Although capnophiles exhibit a variety of metabolic pathways, many of them appear to be fermentative and most characterized capnophiles have not been associated with gas production such as CO₂ and H₂ (Scanlan 1992, Song, Lee et al. 2007, Bringel,

Hammann et al. 2008, Arioli, Roncada et al. 2009, Mavrommatis, Gronow et al. 2009, Hertzberger, Pridmore et al. 2013). During fermentation, a complex carbon source goes through a series of rearrangements and internal electron transfers in the absence of a terminal electron acceptor (TEA). Rearrangements of the carbon compound produce nicotinamide adenine dinucleotide phosphate (NADP), which can then be used to make adenosine triphosphate (ATP). Lactic acid bacteria, for example, take a molecule of glucose and rearrange it in a series of steps to phosphoglyceraldehyde, then pyruvate, and eventually lactate. The oxidation of phosphoglyceraldehyde and pyruvate yields 2 ATP and results in lactate as a byproduct (White 2007).

Capnophiles may also use CO₂ for metabolic processes. *Clostridium*, for example, uses CO₂ decarboxylated from pyruvate to add as the carbonyl group in acetyl-CoA (Wynne and Foster 1948). Other organisms, such as *Mannheimia succiniciproducens*, use CO₂ to carboxylate phosphoenolpyruvate into oxaloacetate and eventually succinate, an important component in the tricarboxylic acid cycle (Song, Lee et al. 2007). In addition, many different enzymes can be used to incorporate CO₂ into microbial biomass. Carbonic anhydrase, for example, catalyzes the hydration of CO₂ to H₂CO₃ for easier incorporation into amino acids. Other suggested enzymes include phosphoenolpyruvate carboxylase and carbamoyl-phosphate synthase (Maren 1967, Smith and Ferry 2000, Arioli, Roncada et al. 2009, Hertzberger, Pridmore et al. 2013).

Fermenters in the deep subsurface have substantial environmental relevance, as many of these organisms live syntrophically with other microbial metabolic guilds, breaking down complex organic pollutants while contributing to microbial community viability. For example, fermenters typically generate H_2 , which is an important component for interspecies hydrogen transfer (Konhauser 2006). They are found associated with methanogens that consume excess H_2 thereby maintaining favorable thermodynamic conditions for continuing both fermentation and methanogenesis (Kosaka, Uchiyama et al. 2006). The mere breakdown and rearrangement of organic byproducts during fermentation results in other carbon sources useful for microbial communities, such as lactate or succinate (Konhauser 2006).

The sequestering of anthropogenic CO_2 via pumping into the formation waters of deep saline aquifers will create new environmental subsurface conditions (Kharaka, Cole et al. 2006, Kaszuba, P. et al. 2009, Little and Jackson 2010). CO_2 will reside in the reservoir as a plume of supercritical fluid and will gradually dissolve into the water. Given that high aqueous CO_2 concentrations are generally toxic to most microorganisms as the molecule interferes with intracellular functions (Hong and Pyun 1999, Spilimbergo and Bertuccio 2003, Watanabe, Furukawa et al. 2003, Damar and Balaban 2006, Mitchell, Phillips et al. 2008, Santillan, Kirk et al. 2013), this change will initially stress the native microbial population. However, over longer time scales, these new conditions may create

a niche for CO₂-tolerant bacteria that will select for a new community of microorganisms capable of resisting CO₂ toxicity.

While it is currently difficult to assess the impact of CO₂ sequestration on the subsurface biosphere *in situ*, terrestrial CO₂ springs, are accessible analogues to determine the long-term impacts of CO₂ on subsurface organisms as they can be readily sampled for microbial community composition, biomass, and viability. One such example is Crystal Geyser (CG), Utah (Figure 5-1), an open well bore that periodically erupts with anaerobic, cool (19°C), CO₂ charged water. It originated as an unsuccessful exploratory oil well spudded in 1935 and small seeps of oil are found nearby (Baer and Rigby 1978). Carbonate and Fe rich water flow from the well and precipitate out iron-oxide rich travertine mounds. Using Crystal Geyser as a window into the subsurface, the goal of this work was to isolate and characterize viable microbes in a CO₂-rich environment to better understand how microbes in the deep biosphere will be affected by high CO₂ conditions resulting from carbon sequestration, as well as their subsequent long-term impact on the geochemistry and possible structural geology of subsurface environments.

MATERIALS AND METHODS

Field sampling

Filters, tubing, and containers used for sampling were autoclaved at 122°C and 15 psi for 30 minutes prior to field work. For field sterilization of large equipment, a 10%

sodium hypochlorite solution was applied to surfaces for approximately 30 minutes followed by treatment with a 10% sodium thiosulfate solution to remove excess chlorine. Materials were then rinsed with approximately 10 liters of discharging spring water prior to any sampling .

Biomass sampling was performed using a peristaltic pump (Geotech, Denver, CO). Approximately 9.7 m of silicone tubing (Masterflex, Vernon Hills, IL) was lowered into the Crystal Geyser outlet and water pumped at a rate of 200 ml/min into a sterile container to allow for excess CO₂ to exsolve. This water was then filtered through a 90 mm, 0.1 µm sterile polycarbonate filter (Millipore, Billerica, MA) in a sterile stainless steel filter apparatus with 50 L of water was allowed to flow through each filter to collect sufficient biomass.

Filters and their collected biomass were designated for phospholipid fatty acid (PLFA) analysis and culturing. Samples for PLFA analysis were preserved at -79°C in a dry dewar (Taylor-Wharton, Theodore, AL) until processing.

Filters used for culturing were placed into Luria-Bertani broth (LB) immediately after filtering. This media was prepared aerobically and was amended with 15 g/l NaCl to maintain the approximate salinity found at Crystal Geyser (Heath, Lachmar et al. 2009). The inoculated media was immediately placed in a 4 L pressure vessel (Alloy Products Corp, Waukesha, WI) and made anaerobic through the use of a GasPakTM EZ Anaerobe

Container System Sachet (BD, Franklin Lakes, NJ). The samples were then pressurized to 10 bar in the field with ultrapure CO₂.

Culture Experiments

Cultures were allowed to incubate at room temperature under 10 bar of CO₂ for approximately 1 month before reculture. Tryptic soy broth (TSB) with 15 g/L NaCl was used for further enrichments and subsequent culture experiments as cultures appeared to show the best growth in this broth (data not shown). After 3 successive transfers over the course of 3 months, TSB cultures were then diluted to extinction by performing a 9-fold serial dilution to obtain an isolate. After 1 month of incubation at 10 bar and room temperature, cultures taken from the 8-fold dilution were transferred to fresh TSB broth and recultured. Cultures were then transferred into fresh broth at 1 bar PCO₂ periodically to maintain a stock.

The isolate, designated CG-1, was assessed for growth under various conditions that focused on CO₂, temperature, salinity, pH, carbon substrates, electron acceptors, and fermentation capability. In all cases, growth was evaluated by taking 200 µl of stock cultures into 10 ml of fresh TSB media and observing growth for one week by measuring optical density (OD₇₀₀) using a LaMotte Smart Spectro spectrophotometer (Chestertown, MD).

CO₂: Growth and survival was tested under CO₂ pressures of 0, 1, 2, 4, 10, 25, and 50 bar. Cultures grown at 0-4 bar were grown in hungate tubes with butyl stoppers.

For cultures grown at 10, 25, and 50 bar, samples were incubated in culture tubes inside modified stainless steel Parr reactors (Parr Instruments, Moline, IL). Samples grown at 1 bar and at 10 bar were also harvested for lipid analysis.

Temperature, salinity, pH, carbon source: CG-1 growth at various temperatures was evaluated by incubation at 5, 10, 25, 30, 45, and 60°C containing 1 bar CO₂. Cultures tested for salinity were grown in similar conditions but kept at room temperature with media amended with 0, 0.1, 0.25, 0.5, 0.75, and 1 M NaCl. For pH experiments, 1 N HCl or NaOH was used to change media pH to values between 3-10. Growth experiments for pH contained no CO₂ in the headspace. Carbon sources tested include acetate, pyruvate, formate, lactate, sucrose, glucose, no carbon source, and Teapot Dome crude oil. A set of cultures grown with no CO₂ and at 1 bar CO₂ were also amended with approximately 1 mM of the carbonic anhydrase inhibitor acetazolamide to determine whether CO₂ growth and survival was influenced by the enzyme. These growth experiments are summarized in Table 5-1.

Electron acceptor: To determine the isolate's metabolic capabilities, pre-reduced anaerobically sterilized (PRAS) TSB was amended with various electron acceptors including 2 mM NO₃⁻, SO₄²⁻, Fe-citrate, or with no electron acceptors present (Gosden and Ware 1977). 200 µL of stock culture was then transferred into the different media and grown at 4 bar.

Fermentation: To determine the isolate's fermentative capabilities, cultures were grown in agar slants of triple sugar iron agar (TSI) e.g., (Engel 2004). Triple sugar iron agar contains 3 sugars, a pH indicator, and sodium thiosulfate and ferrous sulfate to determine fermentative sulfide production. Stab cultures into the agar slants were performed and incubated anaerobically under 0 and 1 bar until growth was seen.

Lipid Analysis

Filters collected from the field were frozen immediately and freeze-dried upon return to the lab. For bacterial cultures grown in the lab, prior to lipid extraction, cultures were centrifuged and then freeze-dried. Lyophilized samples were weighed out and then microwave extracted (CEM MARS 100°C, 10 minutes) using 20 mL of a 9:1 methylene chloride:methanol mixture to provide a total lipid extract. The lipid extract was evaporated under N₂ and saponified at 70°C for 1 hour using a 0.5 M NaOH solution. The solution was cooled, acidified, and extracted 3 times using methyl tert-butyl ether. Samples were then evaporated and resuspended in methylene chloride for column purification.

Solid phase extraction of fatty acids was performed using an amino-propyl stationary phase (0.5 g of Supelclean-NH₂⁺, Supelco, Bellefonte, PA). Fatty acids were eluted with 50:1 DCM/formic acid. The fraction was then evaporated under N₂ and resuspended in hexane.

Fatty acids were converted to fatty acid methyl esters (FAMES) using previously described methods (Rodriguez-Ruiz, Belarbi et al. 1998). Samples were methylated using a 20:1 methylation mixture of methanol/acetyl chloride. Samples were then heated at 100°C for 10 minutes and cooled to room temperature. After cooling, distilled water was added to create two phases. The upper hexane phase was extracted, and concentrated prior to analysis.

Samples were characterized and quantitated by gas-chromatography mass-spectrometry. One microliter of the sample in hexane was injected into an Agilent 7890A GC with a split/splitless injector operated in splitless mode at 300°C, a DB-5 column (0.25mm.i.d., 0.25 μ m film thickness, 30m length), 2.0 cm³ min⁻¹ He flow and programmed heating of the oven from 40 to 170°C at 4°C/min then to 240°C at 30°C/min. An Agilent 5973 quadrupole mass spectrometer was used for detection. Compounds were identified by elution time and comparison with published mass-spectra.

Cloning, Sanger Sequencing

Cloning was performed on the CG isolate. DNA from the isolate was extracted using the Mo Bio Power Biofilm DNA extraction kit (Mo Bio Laboratories, Inc., Carlsbad, CA). Extracted DNA from stationary phase cultures were polymerase chain reaction (PCR) amplified for the 16S rRNA gene using 8F and 1492R primers under the following conditions: denaturation at 94°C for 5 minutes, primer annealing 50°C for 30

seconds, and chain extension at 72°C for 1.5 minutes for 45 cycles. Cloning was completed using the TOPO TA Cloning Kit (Life Technologies, Grand Island, NY). PCR product was ligated onto pCRII-TOPO vector and heat shocked into chemically competent *Escherichia coli*. DNA from 40 ampicillin-resistant clones was then extracted and sent to the University of Austin ICMB Core Facility for Sanger Sequencing (Austin, TX). Sequences were then subjected to a Basic Local Alignment Search Tool search (BLASTn) search (<http://blast.ncbi.nlm.nih.gov/>) to determine the organism's taxonomic identity. A phylogenetic tree relating the isolate to related sequences was made using CLUSTALX (Chenna, Sugawara et al. 2003).

Transmission Electron Microscopy

Samples were prepared for transmission electron microscopy (TEM) following methods outlined by (Romanovicz 2011). Pelleted samples were first fixed overnight in a 2.5% glutaraldehyde solution. After 2 washes and centrifugations with a 0.1 N Na-cacodylic buffer, cultures were stained using a 1 mL mixture of 1% OsO₄ solution and 2% K-ferrocyanide for 1 hour. Stained pellets were washed with cacodylic buffer and suspended in thin (approximately 0.5 cm) 3% agarose strings. Agarose-suspended samples were incubated in 50% ethanol for 15 minutes and transferred to a solution containing 2% uranyl acetate in 70% ethanol for 2 hours. After incubation in uranyl acetate, samples were sequentially dehydrated in ethanol solutions starting with 90% to

100% for 15 minutes each. Samples were twice rinsed in LR White resin and embedded in the same resin.

Embedded samples were sliced into 70 nm thin sections with a diamond knife (DiATOME, Hatfield, PA) using a Leica Ultracut UTC Ultramicrotome at the University of Texas ICMB Core Facility (Austin, TX). Sections were viewed using a FEI Tecnai Transmission Electron Microscope at the same facility using an accelerating voltage of 80kV.

RESULTS

The total amount of PLFA extracted at CG was 1.0 ng/ml. Using a conversion factor of 2×10^4 cells/ng of PLFA, CG had approximately 2×10^4 cells/ml (Stroes-Gascoyne, Schippers et al. 2007). The dominant fatty acids present at this site were even-numbered, saturated fatty acids, specifically C12 (9.8%), C14 (27.1%), C16 (34.3%), and C18 (25.0%) with some unsaturated C18 present (1.3%). Other fatty acids were present, but only made a combination of 2.7% of the total fatty acid content, including the cyclopropyl C19 lipid characteristic of *Lactobacillus* which made less than 0.1% of the fatty acid content (Figure 5-2).

Sanger sequence data for CG-1 indicates that of the 40 clones selected, 39 clones were related to *Lactobacillus casei* with one clone showing an errant sequence due to an error in the sequencing, an incomplete transformation into *E. coli*, or a chimeric sequence. Figure 5-3 shows the organism in relation to related *Lactobacillus* species. The

isolate is approximately 98.5% related to *Lactobacillus casei*, suggesting we have isolated a new strain of *Lactobacillus*.

Growth was similar between atmospheric CO₂ pressures to 4 bar of CO₂ at room temperature with stationary phase reached after approximately 30 hours at these pressures. At 10 bar of CO₂ exposure, OD₇₀₀ was only half the OD₇₀₀ of cultures at lower PCO₂, with cultures reaching stationary phase in approximately 48 hours. At 25 bar, a doubling was observed after approximately 24 hours of exposure followed by a flattening out of the growth curve (Figure 5-4A). Cultures grown at 1 bar and amended with the carbonic anhydrase inhibitor acetazolamide appeared unchanged in comparison to cultures grown without inhibitor.

During survival tests, most stationary phase cultures incubated at pressures from 2 to 50 bar survived beyond the 24 hour limit tested. Cultures at 10 bar have since been recultured and remain viable after 3 weeks of incubation. We also observed cultures exposed to 25 bar to survive at least 5 days of exposure. At 50 bar, only one of the two cultures tested showed viability after 24 hours of exposure.

Cultures grew optimally at temperatures between 25 to 45°C with fastest growth and highest cell density occurring at 25°C. Between 30 to 45°C, growth curves followed similar shapes. No growth was observed at 5, 10, and 60°C (Figure 5-4B), however, when these cultures were taken out of the incubators and left at room temperature, cultures kept at 5 and 10°C exhibited growth while 60°C cultures did not. Growth was

observed between pH 4 to 8 at atmospheric CO₂ with optimal growth at pH values of 5, 6, and 8, with slower growth at pH 7, and no growth at pH 3, 9, and 10 (Figure 5-4F). Lag phases for these cultures were longer due to the fact that cultures were taken from stationary phase and were not supplied with CO₂.

CG-1 grew under a wide range of salinities. Cultures grown with 0.25 M NaCl showed both the fastest growth and the highest cell density, which was similar in salinity to the waters emerging from Crystal Geyser. Lag phase increased and cell densities decreased at salinities below and above 0.25 mM NaCl, with the least growth observed with 0 M NaCl and 1.0 M NaCl (Figure 5-4C). Lag phase was longest at 1 M NaCl but did not reach stationary phase at the end of the experiment. At 0 M NaCl, stationary phase was reached in approximately 45 hours but OD₇₀₀ was lowest.

Growth was variable for different carbon sources. However, the most growth was seen with long-chained carbon molecules, with double the growth measured with glucose in comparison to the next best carbon sources, sucrose and lactose. There was also growth with Teapot Dome crude oil, but this growth was lower than that of glucose, lactose, and sucrose. Growth was poor with shorter-chained carbon sources including acetate, pyruvate, formate, and lactate. No measurable growth was found when no carbon source was supplied (Figure 5-4E).

Growth curves look similar for all the electron acceptors tested, though there was an approximate 17%- increase in growth with Fe-citrate. Culture growth was high with

no electron acceptors present in the TSB (Figure 5-4D). Color change occurred in TSI slants, indicating pH in the slant cultures indicative of acid release during fermentation. Growth on slants also shows consumption of glucose, lactose, and sucrose during fermentation. Furthermore, there was no black precipitate present, indicating no sulfide was produced.

Table 5-1 lists fatty acids expressed at 1 bar and 10 bar PCO_2 . While there are more cells per ml of solution present at low PCO_2 , the amount of fatty acids per mg of biomass is lower than at high PCO_2 (Table 5-1). At low PCO_2 , cells express a higher relative abundance of monounsaturated fatty acids (MUFA). At high PCO_2 , this relative abundance decreases and an increase in cyclopropyl (CFA) and saturated fatty acids (SFA) is seen (Figure 5-5) with cyclopropyl C19 (cycC19) fatty acids showing the largest increase in abundance.

Gram staining on the isolate reveals that the organism is Gram-positive. At 1 bar CO_2 , cells are rod-shaped and elongated, averaging 2 μm long and 400 nm wide with cytoplasm evenly distributed throughout the cells (Figure 5-6). The cell wall structure suggests that they are Gram-positive, which was verified with a Gram stain. In contrast, TEM micrographs of cultures grown at 10 bar reveal amorphous cell structures that are rod shaped but trending towards cocci. These cells appear surrounded by extensive capsular material. Additionally, cells contain visible invaginations, suggesting growth and division occurs even under the high PCO_2 conditions (Figure 5-6).

DISCUSSION

The characteristic cycC19 lipid produced by *Lactobacilli* was detected at CG, though this amount constituted less than 0.1% of the total lipids present. While selection of this organism in the lab indicates a culture bias, enrichment of CG-1 at high CO₂ pressures suggests this organism may come from deeper within the well, surviving where CO₂ pressures are much higher than at 10 m, the depth at which samples were collected. Its ability to grow at a wide range of temperatures, but especially between 25° to 45° C shows it may survive throughout the depth of the well as the geothermal gradient increases. The estimated geothermal gradient for Crystal Geyser is 29°C/km, based on geothermal data from 8 wells within a 30 km radius of the site (Blackett 2004) suggesting a bottom hole temperature of up to 45° C for this 800 m deep well. The proposed source of water for CG and the springs in the area is a mixture of brine seeping up from the underlying Paradox Basin mixing with a shallow aquifer of meteoric water recharged from the San Rafael Swell (Shipton 2004, Heath, Lachmar et al. 2009). The ability for CG-1 to grow in 1 M salt solutions also suggests it can survive where groundwater may be more saline, likely deeper in the well. Higher growth in media supplemented with Fe-citrate (Figure 5-4D) indicates that Fe may also be important to its growth consistent with the Fe-rich environment of CG.

A comparison of CG-1 to its closest cultured relative shows it is approximately 98.5% similar to *Lactobacillus casei* strain ATCC 334, indicating this capnophilic isolate represents a new strain of *Lactobacillus casei* (Figure 5-3). CG-1's relation to

Lactobacillus casei makes sense in that this organism has demonstrated remarkable adaptability to diverse habitats including raw and fermented dairy products, plant products, intestinal tracts, and reproductive systems, though to our knowledge, its presence has not been previously reported in a geologic setting (Cai, Rodriguez et al. 2007). While this microorganism has been found in a broad range of ecological niches, CG-1 is the first reported strain coming from an underground, CO₂-rich environment. Its ability to adapt to various environments comes from extensive gene loss and acquisition through bacteriophage or conjugation mediated horizontal gene transfer (Cai, Rodriguez et al. 2007). The isolate is also closely related to *Lactobacillus zae*, and most distantly related to *Lactobacillus plantarum* and *Lactobacillus suebicus*, among the *Lactobacillus* species.

Many Lactobacilli are defined as capnophilic and fermentative, growing syntrophically with CO₂ and acid-producing organisms (Bringel, Hammann et al. 2008). CO₂ enriched environments for cultured Lactobacilli are between 4 to 25% CO₂ or 0.04 to 0.25 bar CO₂ (Song, Lee et al. 2007, Bringel, Hammann et al. 2008, Arioli, Roncada et al. 2009). In contrast, CG-1 can grow at 10 bar, or 40 times the CO₂ utilized by *L. plantarum*. Stationary phase cultures can also survive at pressures 200 times known capnophilic culture conditions (Figure 5-4A).

Our isolate grows equally well under CO₂ pressures ranging from 0 to 4 bar, shows approximately half that growth at 10 bar, and demonstrates at least one doubling at

25 bar. The organism appears unaffected by CO₂ toxicity at relatively low pressures and shows less growth at higher pressures. Moreover, when 3 week-old cultures, which are at long term stationary phase, are recultured, there is a much longer lag phase for samples grown with no CO₂ present in contrast to cultures grown with 1 to 4 bar CO₂. This suggests that cultures are not just CO₂ tolerant, they may also require CO₂ for their metabolic requirements. CG-1 may be auxotrophic for some amino acids and the addition of CO₂ in the atmosphere aids in its ability to synthesize specific essential amino acids. *Streptococcus thermophilus*, for example, is auxotrophic to uracil and arginine, requiring CO₂ in the atmosphere to produce these amino acids (Arioli, Roncada et al. 2009).

The organism demonstrates a remarkable resilience to CO₂ pressures. CO₂ is widely used in the food science industry for sterilization, with most microorganisms inactivated at CO₂ pressures of 25 bar or greater for even short exposures (Santillan, Kirk et al. 2013). While growth and cell division appears to slow at 10 bar, the organism can still survive at 25 and 50 bar for some time, further suggesting its ability to survive deep in Crystal Geyser. It also demonstrates that while CO₂ will initially have a bactericidal effect on native microbial populations under sequestration conditions, some will survive or may even thrive. Survival at 50 bar is poor, however, indicating that this microorganism has limited ability to detoxify at such high *PCO₂*, possibly due to intracellular cell changes or a saturation of active sites in enzymes responsible for detoxifying CO₂. Native populations very close to the phase-separated supercritical CO₂

will be unlikely to continue to metabolize, although spores may still survive (Santillan, Kirk et al. 2013).

One possibility for the organism's ability to survive CO₂ is through the use of the enzyme carbonic anhydrase, which catalyzes the hydration of CO₂ to H₂CO₃ and then eventually to HCO₃⁻ (Maren 1967). The enzyme is widespread in nature, found in all domains of life, and is used for multiple reasons. Cyanobacteria utilize it for carbon fixation while organisms like *Neisseria* and *E. coli* use it as the first step in amino acid synthesis (Smith and Ferry 2000). Carbonic anhydrases are also inhibited by sulfonamides such as acetazolamide (Smith and Ferry 2000). However, when grown under high PCO₂ and supplemented with 1 mM of acetazolamide, CG-1 showed no change in growth, suggesting either this organism's form of carbonic anhydrase is resistant to acetazolamide or that this organism contains another method for CO₂ utilization not yet previously described. Some other possible enzymes that may aid in CO₂ survival are phosphoenolpyruvate carboxylase and carbamoyl-phosphate synthetase, both enzymes previously described for metabolite synthesis in bacteria (Arioli, Roncada et al. 2009, Banks, Taylor et al. 2010).

Geochemical modeling of Crystal Geyser's water in equilibrium with 25 bar CO₂, the pressures CG-1 continues to survive in, indicates that the pH of the spring could be as low as 5.2 (Bethke 1996). The pH of growth media used to culture CG-1 in equilibrium with 25 bar CO₂ can reach pH 4.3 indicating the growth media is less buffered than the

natural water. CG-1 showed optimal growth between pH values of 5 to 8, though growth is still observed at pH values of 4 (Figure 5-4F). At CO₂ pressures between 1 to 10, pH ranges between 4.7 to 5.6. Its ability to grow optimally within circumneutral pH ranges indicates that its decreased viability at higher PCO₂ is likely a combination of acid stress on cells in addition to CO₂.

At extreme pH values, CG-1 is sensitive, both to highly acidic and highly alkaline conditions, conditions that are not seen naturally in Crystal Geyser. As with other *Lactobacilli*, growth is slowed in acidic and basic conditions possibly due to the inhibition of pH sensitive enzymes such as lactate dehydrogenase, an essential enzyme to lactate fermentation (Garvie 1980). This pH inhibition but eventual recovery suggests this organism has mechanisms to adapt to pH stress (Figure 5-4F).

Many *Lactobacilli* are fermentative, and CG-1 shows evidence of this. The fact that the CG isolate grew nonselectively in PRAS media containing Fe³⁺, SO₄²⁻, and NO₃⁻ as electron acceptors as well as with no TEAs suggests the organism can either utilize all three TEAs, or more likely, can grow fermentatively. Its inability to grow in media without a carbon source indicates it is not performing peptone catabolism. The isolate's ability to grow with no TEA present as well as its close relation to other *Lactobacilli* suggests that this organism is likely performing lactic acid fermentation. Evidence from TSI slants corroborate this as its growth suggests glucose, lactose and sucrose

fermentation. Furthermore, the color change from red to yellow throughout the slants suggests it produces acid during fermentation, possibly lactic acid.

Growth is poor when supplied with short-chained carbon sources for electron donors and little or no growth was observed with acetate, formate, and lactate (Figure 5-4E). These are likely poor carbon sources for CG-1 because it does not have the ability to ferment these fermentation byproducts. Growth was also poor when supplied with pyruvate. While this is an intermediate during fermentation, it appears that CG-1 does not have the mechanisms to assimilate this molecule during growth. Additionally, during lactic acid fermentation, the rearrangement of glucose to pyruvate produces ATP while the breakdown of pyruvate to lactate produces NADP. There is considerably less energy to receive from the breakdown of pyruvate which would result in sluggish growth.

Growth was best on glucose, sucrose, lactose, and Teapot Dome crude oil, all complex carbon molecules (Figure 5-4E). Its ability to grow on complex carbon sources is consistent with other *Lactobacilli*, which ferment molecules like carbohydrates, sugars and starches (de Vries, Vaughan et al. 2006, Cai, Rodriguez et al. 2007). Its ability to grow well with crude oil also further indicates its environmental relevance to CG as many oil seeps are present in the surrounding environment that may provide a carbon source to the subsurface microbial populations. Many fermentative organisms have been found and isolated from oil fields degrading hydrocarbons and contributing to the indigenous

microbial communities they are part of (Onstott, Phelps et al. 1998, Winderl, Anneser et al. 2008, Duncan, Gieg et al. 2009).

Unstressed CG-1 cells have an appearance similar to other *Lactobacilli*. CG-1 is rod-shaped and contains a distinct cell wall (Figure 5-6). It is Gram-positive and produces no endospores based on TEM observations. Cells grown at 1 bar PCO_2 appear elongated and turgid. At 10 bar PCO_2 , they are slightly amorphous in appearance. The images at 10 bar capture cells in multiple life stages, with some cells appearing like they are degrading while many other cells are attached together and contain invaginations. These invaginations are indicative of binary fission, evidence that cultures are capable of growth and survival at what are commonly bactericidal CO_2 pressures.

Cells grown at 10 bar are surrounded by a capsule material, likely composed of extracellular polymeric substances (EPS). This could have multiple purposes. Many cells responding to environmental stresses, such as acidity, produce EPS to create a physical barrier to slow the diffusion of the toxic substance into the cell, which in this case would be CO_2 (Cotter and Hill 2003, Kidd 2011). The presence of EPS could also be a means for cells to maintain cell integrity and structure in the presence of a toxic substance.

CG-1 exhibited variable lipid compositions at 1 and 10 bar of CO_2 , demonstrating a physiological response to CO_2 pressures (Figure 5-5, Table 5-2). Interestingly, while cell density at 10 bar was lower than at 1 bar CO_2 , there was a higher lipid to biomass ratio for cells at 10 bar (Table 5-1). This ratio could either mean cells are creating thicker

cell membranes or that cell sizes are decreasing. Observations by TEM would be more consistent with a cell size decrease. Bacteria demonstrate cell size decrease during starvation (Chien, Hill et al. 2012) and smaller cell sizes for CO₂ stressed CG-1 may indicate a state similar to starvation. While the same nutrients at 10 bar are present at 1 bar, increased CO₂ toxicity may be inhibiting nutrient uptake, resulting in smaller cells.

Cells grown at 1 and 10 bar shared similar lipid compositions, with the highest variability coming from C14, C16, and C18 fatty acids in both treatments, possibly owing to the variability of fatty acid compositions present for cells in stationary phase.

However, the relative abundance of different fatty acids change with increased *PCO*₂. At low *PCO*₂, lipid composition favors MUFA. At high *PCO*₂, this relative abundance decreases and an increase in SFA and CFA occurs. The difference in lipid composition at different CO₂ pressures may reflect structural changes cells must make to maintain cell shape or fluidity under stress. SFAs, for example, pack together much more tightly than MUFAs, which would be consistent with a decrease in cell size under high *PCO*₂. Such responses have been documented for temperature, pH, and osmotic stresses but not for CO₂ (To and Etzel 1997, de Vries, Vaughan et al. 2006, Bringel, Hammann et al. 2008).

Cyclopropyl C19 fatty acids, or lactobacillic acid, is characteristic of *Lactobacillus* species (Veerkamp 1971). Previous work with different *Lactobacilli* has shown that under stress, *Lactobacillus* converts unsaturated fatty acids into CFA (Guerzoni, Lanciotti et al. 2001). With CG-1 at 10 bar, there is a decrease in the relative

abundance of unsaturated fatty acids along with an increase in the relative abundance of CFA. CFAs are energetically costly for cells to produce and are often found during the transition from growth to stationary phase, as a response to starvation, and as a response to acidic conditions (Brown, Ross et al. 1997, Chang and Cronan 1999). Here, we document another stress response that generates an increase in CFA.

CFAs increase rigidity in cell membranes (Veerkamp 1971, Brown, Ross et al. 1997, Chang and Cronan 1999, Guerzoni, Lanciotti et al. 2001). TEM micrographs show that cultures at high PCO_2 appear smaller, more amorphous, and less turgid than cultures exposed to lower PCO_2 . The presence of molecules such as CFA in the cell membrane may be a way to maintain some form of rigidity for cell shape. In high PCO_2 cultures, this relative increase suggests cells are actively responding to CO_2 despite the energy costs possibly by increasing the efficiency of maintaining cell structure at the expense of other energetically costly activities such as cell division (Santillan, Kirk et al. 2013).

This work demonstrates that microorganisms can survive in CO_2 rich environments suggesting microbial communities under CO_2 stress can eventually adapt and potentially influence the geochemistry of CO_2 sequestration. Organic acids produced by fermenters like CG-1, for example, may present a biological link to the geochemistry of the site. Acids produced by bacteria, such as lactic acid, though weak, may present a feedback to mineral dissolution in CG in addition to CO_2 (Zafar and Ashraf 2007) which

in turn could help in the enhancement or production of pathways that make up fractures near and around Crystal Geyser.

ORGANISM DESCRIPTION

Lactobacillus casei strain CG-1 is a Gram-positive, non-sporulating, facultative anaerobic bacterium isolated from Crystal Geyser, Utah. The organism is fermentative, putatively converting glucose, sucrose, or long-chained hydrocarbons into lactate and producing no CO₂, acid, or sulfide, during this process. The bacterium grows optimally at 25°C in 100% CO₂ atmospheres, and pressures ranging from 1 to 4 bar CO₂, with less growth at 10 bar, and no growth but continued survival at 25 bar. Stock cultures recultured after long-term stationary phase exhibit shorter lag phase when supplied with CO₂ indicating a metabolic need for CO₂. The organism is pH sensitive, growing optimally between pH values of 6 to 8, and exhibits a longer lag phase under acidic and basic conditions. Its optimal salinity is 0.25 M NaCl, though it shows versatility in that it can grow between 0 to 1 M NaCl. It expresses a suite of fatty acids, but most notably cycC19, especially under extreme CO₂ conditions. The organism is rod-shaped at 1 bar PCO₂ but begins to surround itself with a thick capsule structure and exhibits a somewhat amorphous morphology when cultured under 10 bar CO₂ pressures. CG-1, which was found in a CO₂ rich environment is capnophilic. However, its ability to tolerate CO₂ pressures beyond known capnophiles makes this organism a hyper-capnophile.

Characteristic	Media Amendment	Amount
CO ₂ growth/survival	CO ₂	1, 2, 4, 10, 25, 50 bar
Temperature	Incubation temperature	5, 10, 25, 30, 45, 60°C
Salinity	NaCl	0, 0.1, 0.25, 0.5, 0.75, 1 M
Carbon Source	Acetate, pyruvate, formate, lactate, sucrose, glucose, Teapot Dome crude oil, no carbon source	2 mM
pH	HCl or NaOH	pH 3 to 10
Terminal Electron Acceptor	NO ₃ ⁻ , SO ₄ ²⁻ , Fe-citrate, no electron acceptor	2 mM
CO ₂ Detoxification through Carbonic Anhydrase	Acetazolamide	~ 1 mM

Table 5-1 CG-1 physiological parameters examined.

	$\mu\text{g/ml}$ dry weight	
	1 bar	10 bar
C9	16.6 ± 0.19	n.d.
C10	20.0 ± 0.19	34.2 ± 1.55
C12	28.2 ± 7.20	64.6 ± 2.76
C14:1	9.0 ± 0.61	14.4 ± 1.69
C14:1	7.5 ± 0.14	12.4 ± 0.28
C14	51.9 ± 15.16	112.3 ± 17.46
meC15	4.4 ± 0.04	7.3 ± 0.30
C16:1	31.5 ± 11.73	29.1 ± 17.89
C16:1	30.0 ± 15.53	33.1 ± 25.15
C16	450.1 ± 250.35	616.6 ± 260.88
C16:2	0.8 ± 0.084	1.0 ± 0.82
cycC17	6.4 ± 0.15	19.2 ± 3.74
C18:2	7.6 ± 0.48	12.8 ± 0.70
C18:1	30.8 ± 1.75	52.2 ± 1.05
C18:1	105.2 ± 46.29	40.7 ± 31.77
C18	45.9 ± 7.83	89.2 ± 14.24
cycC19	46.5 ± 13.48	155.0 ± 14.93
cycC23	8.3 ± 0.01	14.0 ± 0.07
Total	900.6	1308.1

Table 5-2 CG-1 fatty acid content at 1 and 10 bar CO₂.

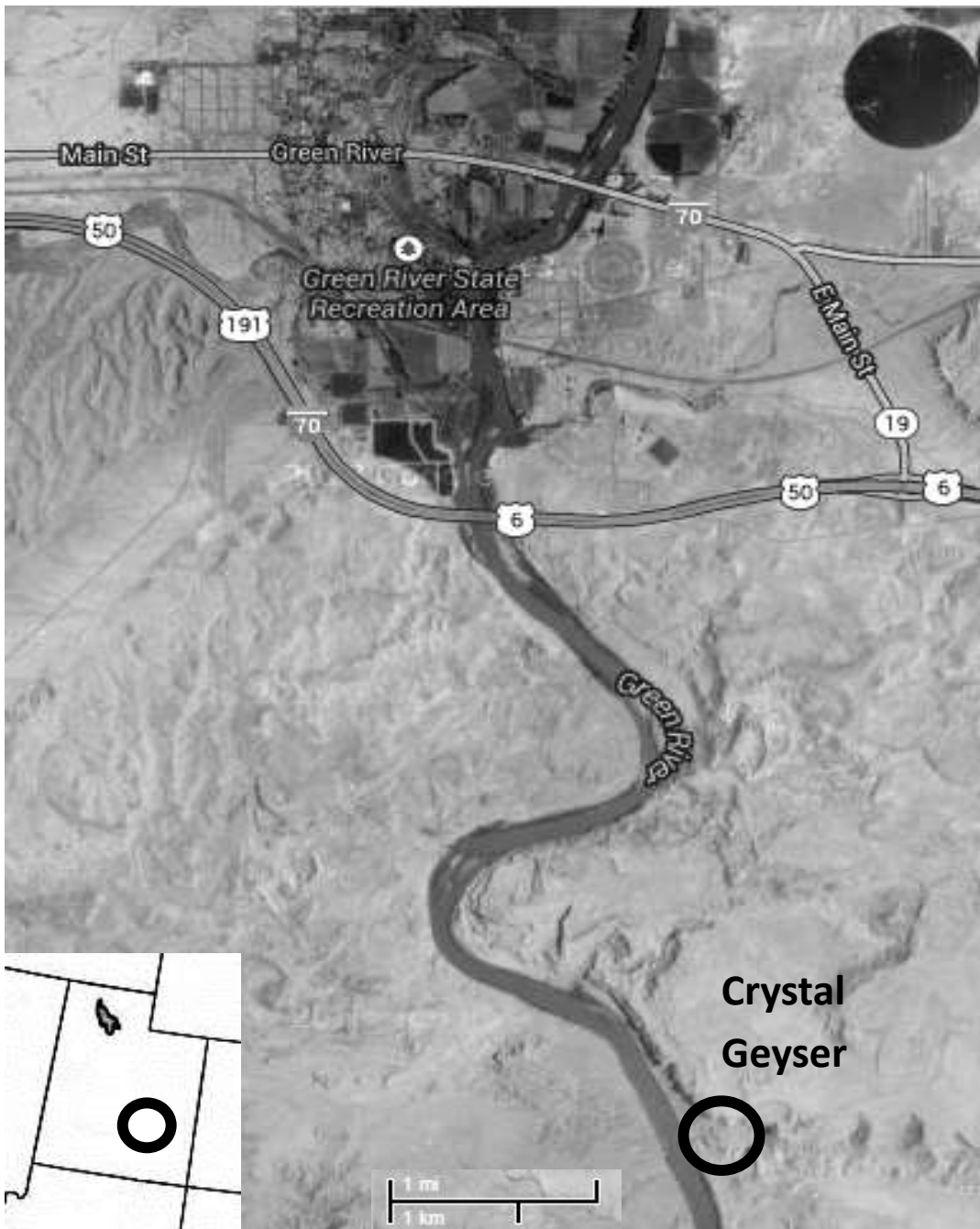


Figure 5-1 Location of Crystal Geyser, adapted from Google Maps.

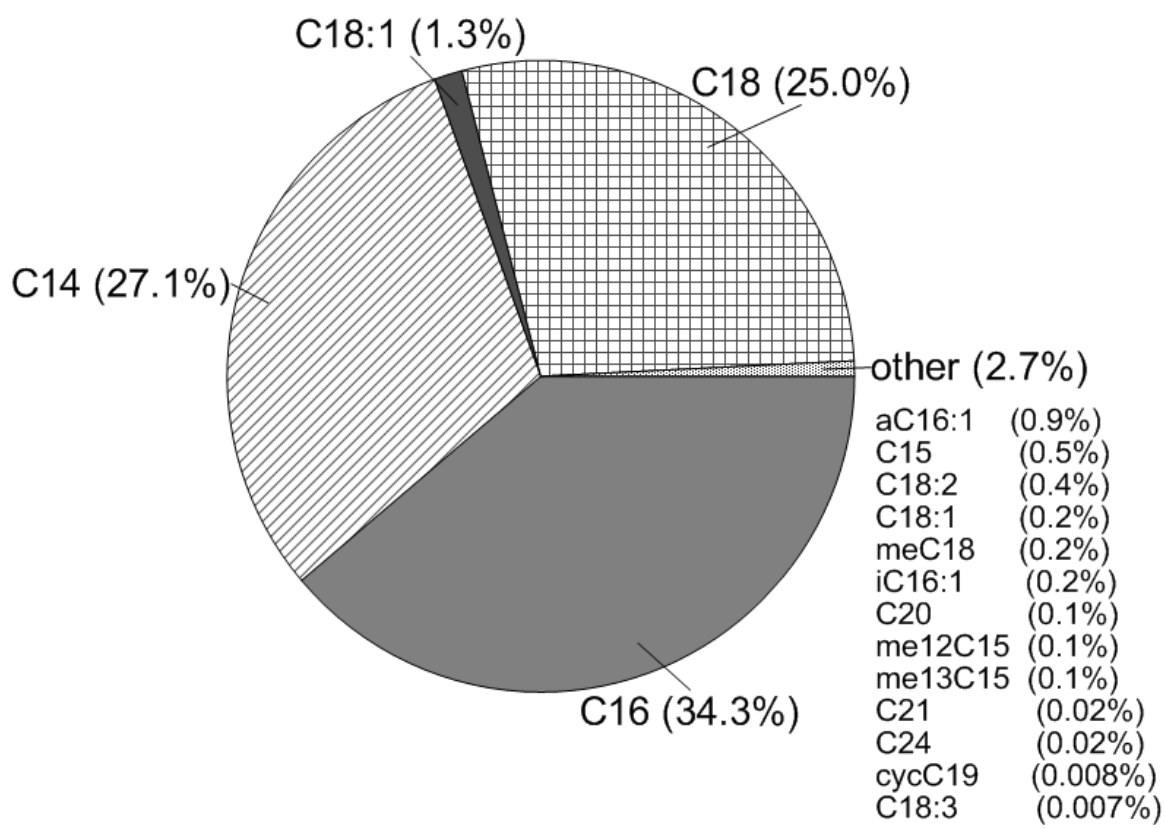


Figure 5-2 Lipid composition of the water at Crystal Geyser.

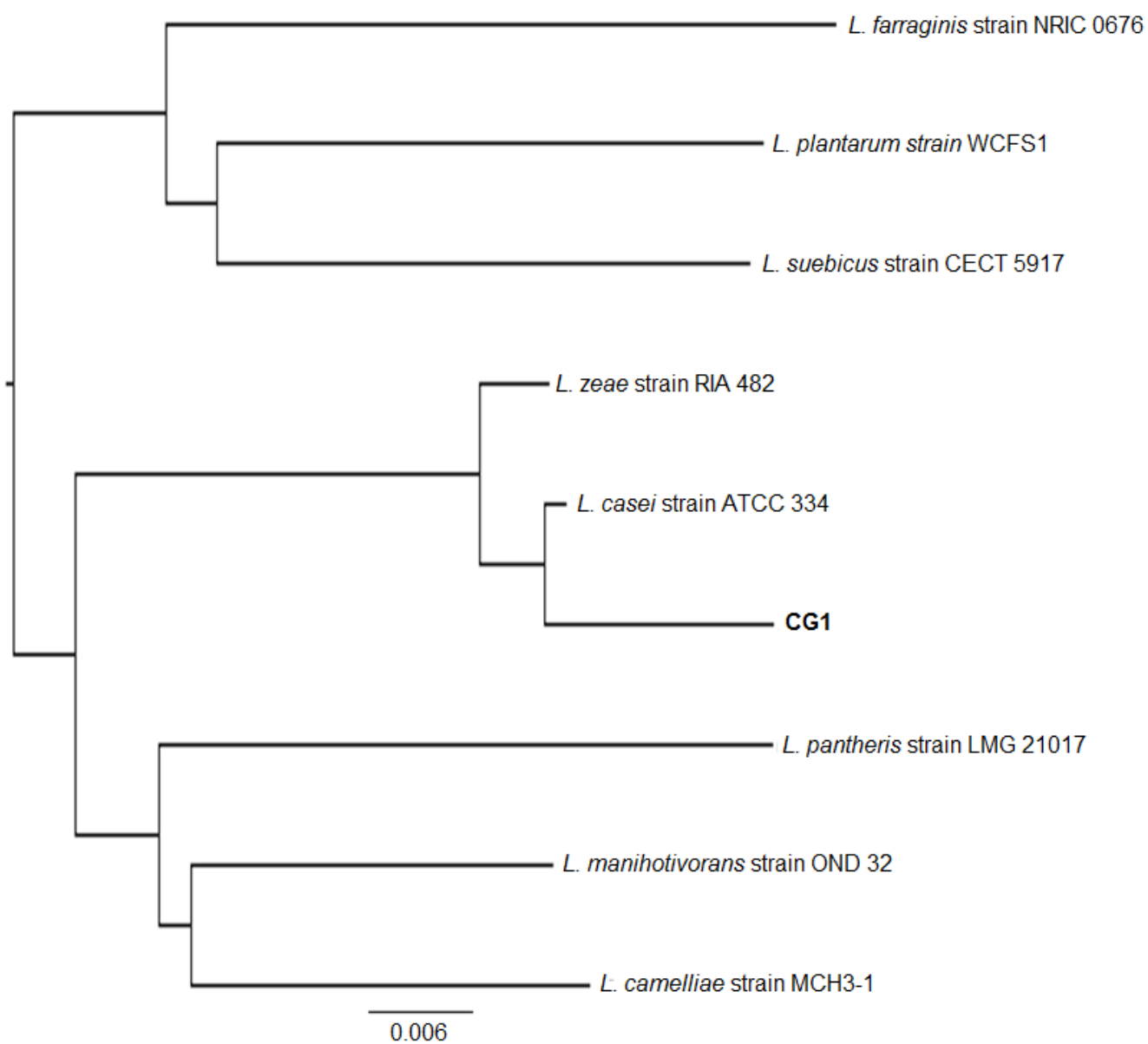


Figure 5-3 Phylogenetic tree showing CG-1 in relation to other organisms belonging to the genus *Lactobacillus*

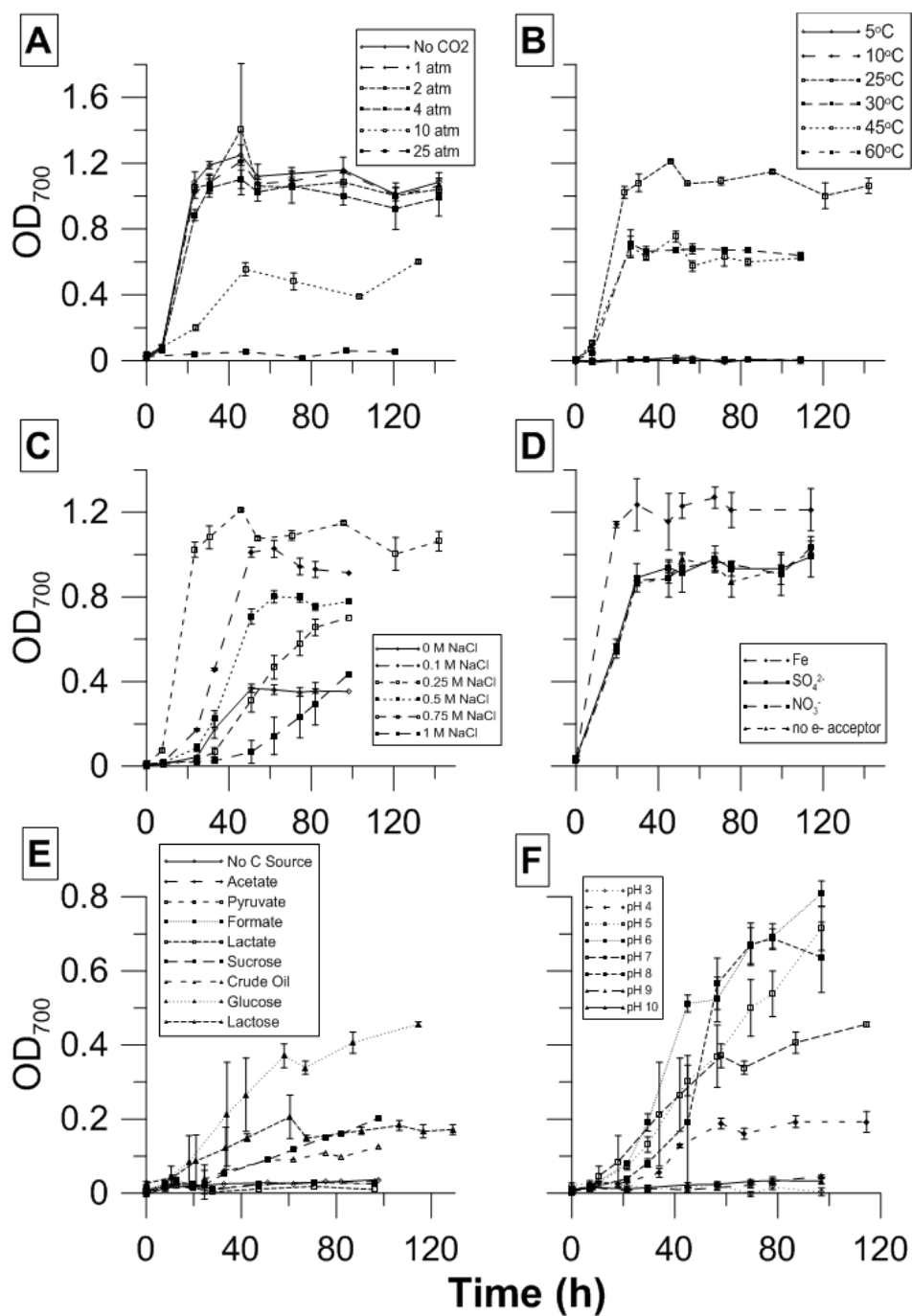


Figure 5-4 CG-1 physiological data showing growth with varying (A) PCO_2 , (B) temperature, (C) salinity, (D) electron acceptor, (E) carbon source, and (F) pH.

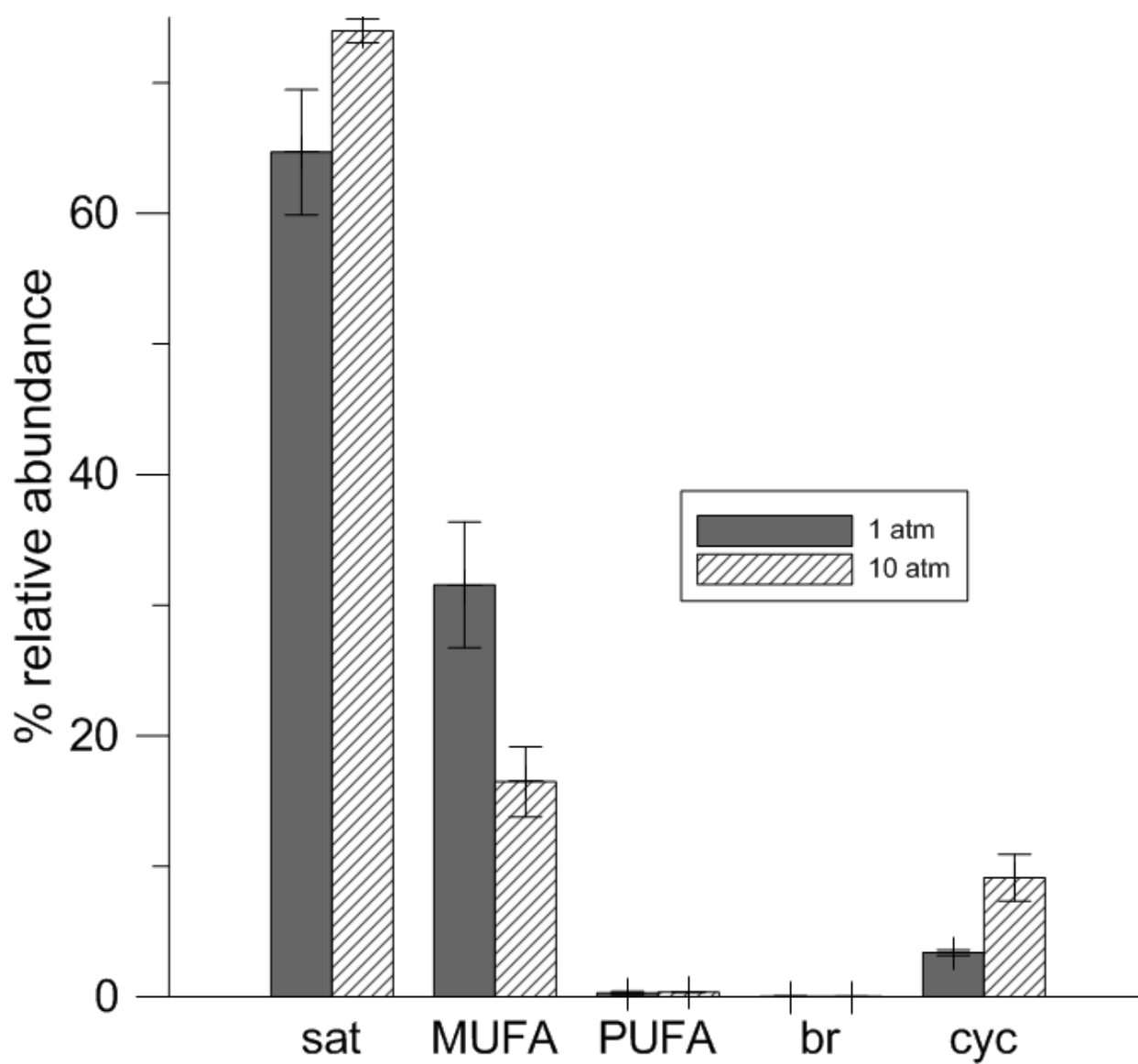


Figure 5-5 CG-1 fatty acid composition at 1 bar and 10 bar CO₂.

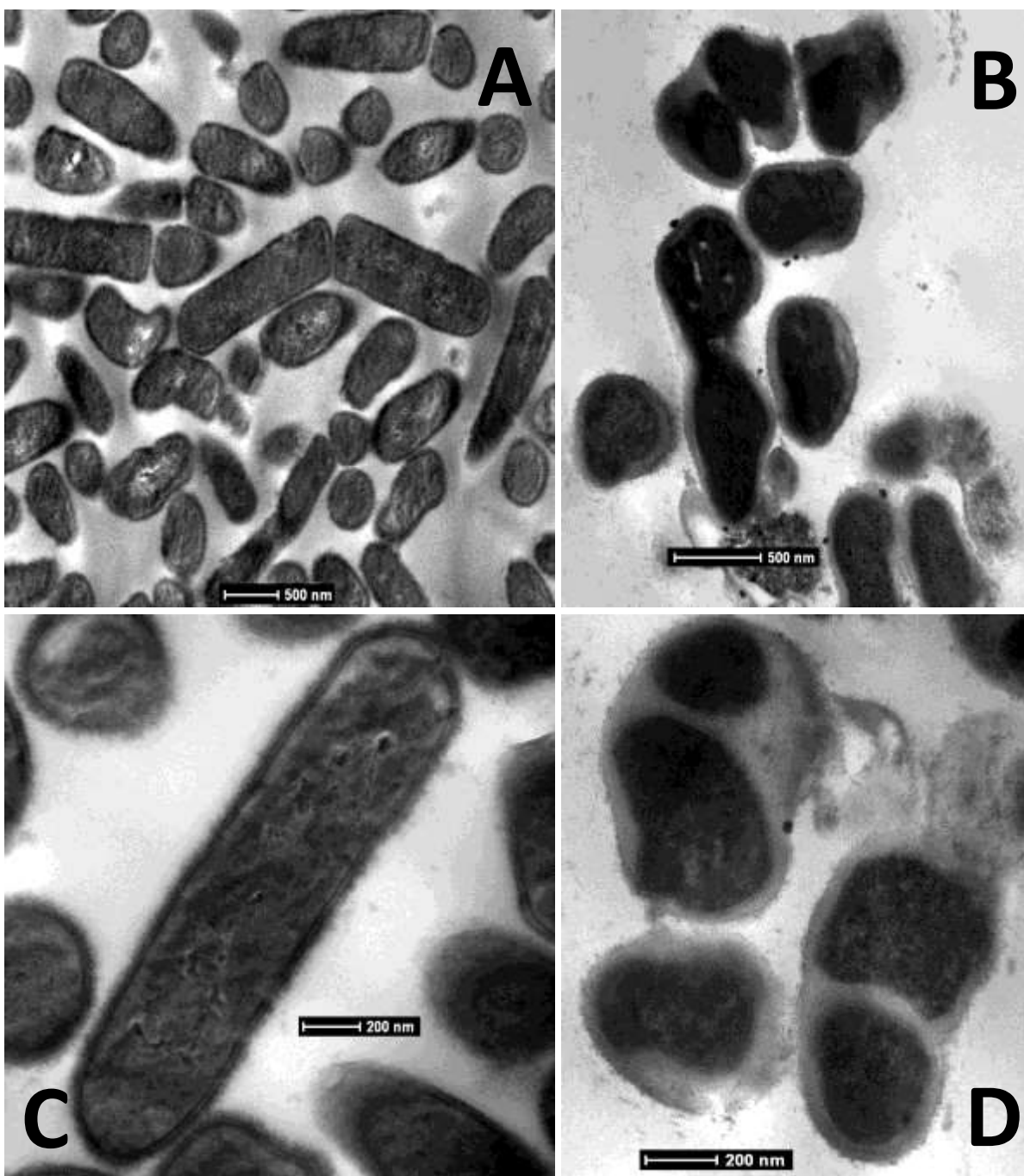


Figure 5-6 TEM images of CG-1 at 1 bar CO₂ (A,C) and 10 bar CO₂ (B,D).

Chapter 6: Conclusions

The survival of deep subsurface microbes in the presence of CO₂ highlights the persistence and adaptability of life to extreme environments. Despite the extreme perturbation CO₂ creates during sequestration, microorganisms can still survive and their presence and metabolisms will be an important factor to consider for the hydrologic and geochemical implications of CO₂ storage.

At the cellular level, CO₂ is both bacteriostatic and bactericidal. CO₂ is lethal at pressures greater than 10 bar for most of the organisms examined, and greater than 25 bar for the capnophile, CG-1. This effect is due to an intracellular disruption where the liposoluble CO₂ molecule readily enters cell membranes, acidifies the cytoplasm, and changes cell functions. This occurs regardless of cell wall thickness or membrane structure. Dead cells are important as they will clog pore spaces resulting in a change in permeability (Kirk et al., 2012). Endospores are the only cell structures that survive bactericidal CO₂ pressures beyond 25 bar. However, while endospores can survive at high *PCO*₂ and even liquid and supercritical conditions (Damar and Balaban, 2006; Dillow et al., 1999; Watanabe et al., 2003; Wynne and Foster, 1948), spores are non-viable and non-metabolizing, doing very little to affect the subsurface environment.

At lower CO₂ pressures, limited growth and metabolism begins to occur, showing microorganisms can have a limited tolerance to CO₂ despite its toxicity. This tolerance to CO₂ varies between organisms: at 10 bar, CG-1 was still capable of growth and

metabolism, *Methanothermobacter* was able to continue growth and methane production at 4 bar, and *Shewanella oneidensis* (SO) could continue growth and Fe reduction at 1.4 bar. This suggests that CO₂ sequestered in the subsurface will create zones that select for different microbial populations based on CO₂ tolerance. For example, capnophilic fermenters may be located in areas of high PCO₂, such as closest to the supercritical CO₂ plume, with methanogens located further away, and DIRB and G⁺ cells located on the outer fringes of the solubility-trapped CO₂ (Figure 6-1).

Organisms with membrane-bound respiratory processes, such as SO, which performs Fe reduction on its cell membrane, were least tolerant to CO₂ toxicity. While this tolerance to CO₂ was low, exposure to CO₂ does enhance the efficiency of respiration, possibly because cells are spending more energy in an effort to detoxify. SO, for example, demonstrates that more Fe is reduced *per cell* at 1.4 bar than unexposed cells. However, at pressures greater than 1.4 bar, cells were no longer able to metabolize, showing CO₂ eventually inactivates cells.

Fe reduction in the deep subsurface may be a significant way to enhance the dissolution of CO₂ into the saline aquifers as this process can remove a great deal of acidity from the groundwater. This process has been outlined by Kirk (2011) and shown to be a favorable reaction based on bioenergetics calculations and experimental results (Kirk et al., 2013). However, while our data does show an enhancement of Fe reduction

per cell as predicted, our results indicate that cellular tolerances to CO₂ toxicity will be a major control of changes in Fe reduction in response to high CO₂ pressures.

The organisms studied with higher CO₂ tolerance were those with internal metabolic processes, such as methanogens and fermenters. This suggests that cells best capable of surviving CO₂ will have internal rather than external responses to combat toxicity, possibly through cytoplasmic buffering or the conversion of CO₂ into nontoxic products. For example, *Methanothermobacter thermoautotrophicus* produces methane by the reduction of CO₂ intracellularly, utilizing enzymes and cofactors to capture and remove cytoplasmic CO₂. Methanogens are important organisms to consider in sequestration conditions as their metabolism can remove CO₂ from the environment by conversion to CH₄. However, because of its lower solubility than CO₂, the CH₄ produced by these organisms may migrate closer to the caprock, making it potentially more susceptible to leakage.

The method of CO₂ survival for the capnophilic CG-1 has not been elucidated, though CO₂ itself may be important for its metabolic processes, such as through the synthesis of amino acids. This is supported by growth experiments where supplementing cultures with CO₂ decreased the organism's lag phase and enhanced growth. Fermenters have potentially important environmental consequences as fermenters like CG-1 produce acid during their metabolisms, creating a feedback to the aggressive mineral dissolution of CO₂-charged brine. Fermentative processes also produce byproducts, such as organic

acids or H₂ that can feed other microbial populations, allowing for the growth of organisms such as methanogens.

While cells are important to consider for their geochemical consequences, microorganisms in the environment exist as communities composed of biofilms colonized on mineral surfaces. Biofilms are potentially important for CO₂ sequestration because they could affect the movement of both supercritical and solubility-trapped CO₂ by reducing porosity and influencing the adhesion of liquid CO₂ droplets on mineral surfaces (Chaudhary et al., 2013; Kirk et al., 2012). Over larger scales, this may also mean an influence on predicting CO₂ plume migration.

The distribution of viable biofilms in the subsurface after sequestration will likely be controlled by both CO₂ tolerance as well as subsurface mineralogy which can create favorable and unfavorable habitats for survival (Santillan et al., 2013). Most minerals provide colonization surfaces for the formation of biofilms. Unreactive minerals, such as quartz, will provide the best environment for biofilms because they are slow to dissolve and contain relatively few toxic metals to stress organisms.

On the other hand, mineral dissolution resulting from CO₂ (and possibly organic acids produced by capnophilic fermenters), will release toxic metals including Al, As, and Pb, to name a few. These toxic metals add an extra stress to biofilms already stressed by CO₂ exposure, resulting in cell death. This means the distribution of viable biofilms in

the subsurface will likely occur in places containing unreactive minerals, increasing subsurface heterogeneity.

Given the great deal of horizontal gene transfer among prokaryotes, it is possible that multiple populations of cells will eventually adapt to CO₂ and form viable communities in groundwater. Locations like the Little Grand Wash Fault (LGW), Bravo Dome (BD), and Klickitat (KMS), all provide analogues to microbial communities that have adapted to high pressures of CO₂ and give us a means to hypothesize the community functions. Furthermore, the isolation of CG-1 from the Little Grand Wash Fault confirms that communities observed in these environments are viable and will likely be influencing the geochemistry of these regions.

Despite the differences in community composition and diversity among CO₂ analogues, communities in CO₂ exposed sites all show signs of stress as evidenced by a decrease in diversity in comparison to similar, unexposed sites. They also show a lopsided distribution of phylotypes typical of environmentally stressed ecosystems. Cells may be able to eventually adapt to CO₂, but this component in the environment will remain a stress that will select for only a few organisms that are best at survival.

While sites exposed to CO₂ generally had lower diversity than sites not exposed to CO₂, the diversity among CO₂ exposed sites varied considerably. This suggests that in addition to stresses created by CO₂, other factors may also influence community composition in CO₂ exposed environment. Understanding the microbial community

contribution to the geochemistry of sequestered CO₂ will have to be assessed from location to location as no one analogue will be truly representative of all sites.

The differences in diversity between the basalt site KMS versus the sandstone and sedimentary sites of LGW and BD further highlight the importance of mineralogy and microbial survival at high *PCO*₂. LGW, for example, located in the Navajo Sandstone, has low diversity. The sandstone, largely composed of feldspars, contain Al, which has been shown to decrease cell viability under high *PCO*₂ (Lu et al., 2011; Parry et al., 2009; Santillan et al., 2013). In contrast, the basalt site, which may be nutrient rich and lower in toxic metal content, may help increase diversity.

While it is difficult to infer the overall community function based on phylogeny, several hypotheses may be made based on field observations. Abundant Fe-oxide rich travertines in LGW and KMS, for example, suggests iron cycling in the subsurface, showing DIRB may be active in affecting geochemistry at high *PCO*₂. Fermenters, such as CG-1, may be providing a biological feedback to the fault creation in the LGW through the release of organic acids, further enhancing the leakage of CO₂. The detection of methanogenic Archaea in KMS also suggests methanogens capable of living under high *PCO*₂ conditions, though basalt environments may be the best at supporting these organisms.

The geochemical and hydrological effects of microbes during CO₂ sequestration are complicated, and this study has provided important considerations to be made

regarding the microbial contribution to the storage, movement, dissolution, and ultimately the security of CO₂ sequestered. Future work can focus on scaling up these findings to core, field, and basin scale studies to find ways to incorporate the biogeochemical component to existing prediction models.

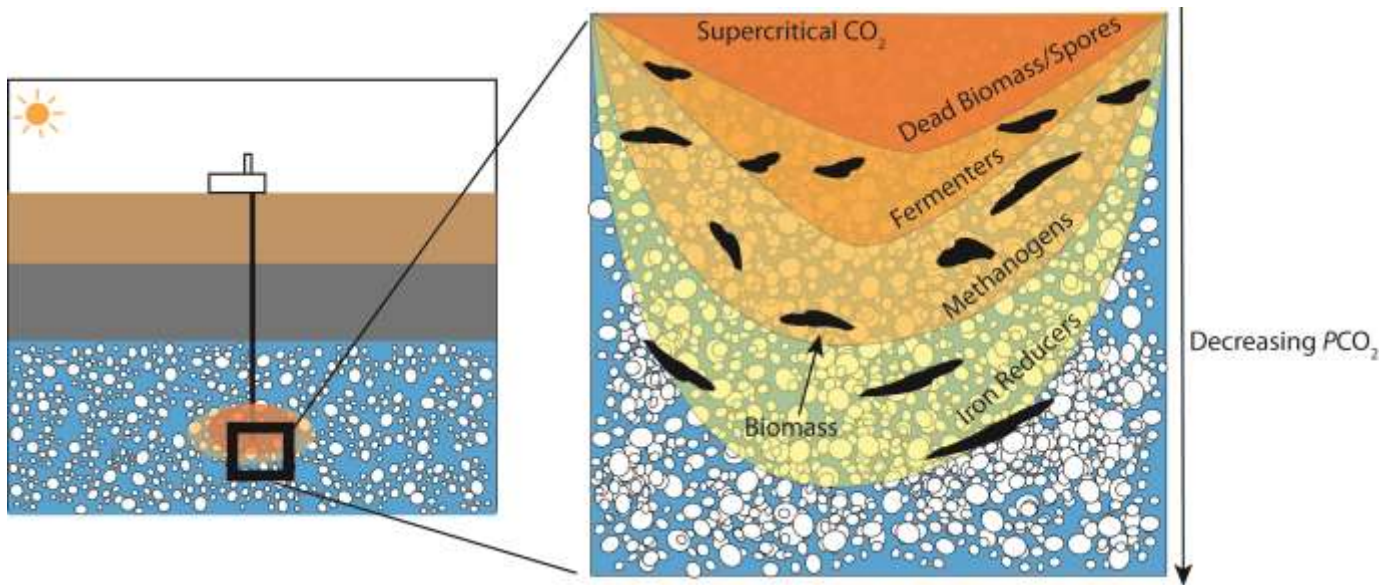


Figure 6-1 Conceptual model of microbial redistribution due to CO₂ sequestration. Microbial metabolic guilds as well as biomass will be redistributed based on both CO₂ tolerance as well as subsurface mineralogy.

Bibliography

- Andrews, S. C., A. K. Robinson and F. Rodriguez-Quinones (2003). "Bacterial iron homeostasis." FEMS Microbiology Reviews **27**(2-3): 215-237.
- Appelo, C. and D. Postma (2005). Geochemistry, groundwater, and pollution. Amsterdam, AA Balkema Publishers.
- Arakawa, K., H. Kano, T. Eguchi, Y. Nishiyama and K. Kakinuma (1999). "Significance of the 72-membered macrocyclic structure found in archaeal membrane lipids: Model studies of the macrocyclic tetraether diphospholipids by calorimetric, P-31 NMR, and electron microscopic analyses." Bulletin of the Chemical Society of Japan **72**(7): 1575-1581.
- Arioli, S., P. Roncada, A. M. Salzano, F. Deriu, S. Corona, S. Guglielmetti, L. Bonizzi, A. Scaloni and D. Mora (2009). "The relevance of carbon dioxide metabolism in *Streptococcus thermophilus*." Microbiology **155**(6): 1953-1965.
- Bachu, S. (2008). "CO₂ storage in geological media: Role, means, status and barriers to deployment." Progress in Energy and Combustion Science **34**(2): 254-273.
- Baer, J. L. and J. K. Rigby (1978). "Geology of the Crystal Geyser and environmental implications of its effluent, Grand County, Utah." Utah Geology **5**(2): 125-130.
- Baker, B. J., L. R. Comolli, G. J. Dick, L. J. Hauser, D. Hyatt, B. D. Dill, M. L. Land, N. C. VerBerkmoes, R. L. Hettich and J. F. Banfield (2010). "Enigmatic, ultrasmall, uncultivated Archaea." Proceedings of the National Academy of Sciences **107**(19): 8806-8811.
- Ballestra, P., A. A. Dasilva and J. L. Cuq (1996). "Inactivation of *Escherichia coli* by carbon dioxide under pressure." Journal of Food Science **61**(4): 829-&.
- Banks, E. D., N. M. Taylor, J. Gulley, B. R. Lubbers, J. G. Giarrizo, H. A. Bullen, T. M. Hoehler and H. A. Barton (2010). "Bacterial calcium carbonate precipitation in cave environments: A function of calcium homeostasis." Geomicrobiology Journal **27**(5): 444-454.
- Barnes, I. (1984). "Volatiles of Mount St. Helens and their origins." Journal of Volcanology and Geothermal Research **22**(1-2): 133-146.
- Bennett, P., A. Engel and J. Roberts (2007). Counting and imaging bacteria on mineral surfaces. Clay Mineral Society Workshop Proceedings.
- Bennett, P. C., F. K. Hiebert and W. J. Choi (1996). "Microbial colonization and weathering of silicates in a petroleum-contaminated groundwater." Chemical Geology **132**(1-4): 45-53.
- Bennett, P. C., J. R. Rogers and W. J. Choi (2001). "Silicates, silicate weathering, and microbial ecology." Geomicrobiology Journal **18**(1): 3-19.
- Bethke, C. (1996). Geochemical reaction modeling. New York, Oxford University Press.

Biffinger, J. C., J. Pietron, O. Bretschger, L. J. Nadeau, G. R. Johnson, C. C. Williams, K. H. Nealson and B. R. Ringeisen (2008). "The influence of acidity on microbial fuel cells containing *Shewanella oneidensis*." Biosensors & bioelectronics **24**(4): 906-911.

Blackett, R. E. (2004). Geothermal gradient data for Utah. Utah Geological Survey Open-File Report 431.

Bordenave, S., M. S. Goni-Urriza, P. Caumette and R. Duran (2007). "Effects of heavy fuel oil on the bacterial community structure of a pristine microbial mat." Applied and Environmental Microbiology **73**(19): 6089-6097.

Bringel, F., P. Hammann, V. Kugler and F. Arsène-Ploetze (2008). "*Lactobacillus plantarum* response to inorganic carbon concentrations: PyrR2-dependent and -independent transcription regulation of genes involved in arginine and nucleotide metabolism." Microbiology **154**(9): 2629-2640.

Broadhead, R. (1990). Bravo Dome Carbon Dioxide Gas Field. TR: Structural Traps I: Tectonic Fold Traps, American Association of Petroleum Geologists: 213-232.

Brown, J. L., T. Ross, T. A. McMeekin and P. D. Nichols (1997). "Acid habituation of *Escherichia coli* and the potential role of cyclopropane fatty acids in low pH tolerance." International Journal of Food Microbiology **37**(2-3): 163-173.

Cai, H., B. T. Rodriguez, W. Zhang, J. R. Broadbent and J. L. Steele (2007). "Genotypic and phenotypic characterization of *Lactobacillus casei* strains isolated from different ecological niches suggests frequent recombination and niche specificity." Microbiology-Sgm **153**: 2655-2665.

Caporaso, J. G., J. Kuczynski, J. Stombaugh, K. Bittinger, F. D. Bushman, E. K. Costello, N. Fierer, A. G. Pena, J. K. Goodrich, J. I. Gordon, G. A. Huttley, S. T. Kelley, D. Knights, J. E. Koenig, R. E. Ley, C. A. Lozupone, D. McDonald, B. D. Muegge, M. Pirrung, J. Reeder, J. R. Sevinsky, P. J. Tumbaugh, W. A. Walters, J. Widmann, T. Yatsunenko, J. Zaneveld and R. Knight (2010). "QIIME allows analysis of high-throughput community sequencing data." Nature Methods **7**(5): 335-336.

Cervantes, C., G. Y. Ji, J. L. Ramirez and S. Silver (1994). "Resistance to arsenic compounds in microorganisms." FEMS Microbiology Reviews **15**(4): 355-367.

Chang, Y. Y. and J. E. Cronan, Jr. (1999). "Membrane cyclopropane fatty acid content is a major factor in acid resistance of *Escherichia coli*." Molecular Microbiology **33**(2): 249-259.

Chapelle, F. H., K. O'Neill, P. M. Bradley, B. A. Methe, S. A. Ciufo, L. L. Knobel and D. R. Lovley (2002). "A hydrogen-based subsurface microbial community dominated by methanogens." Nature **415**(6869): 312-315.

Chaudhary, K., M. B. Cardenas, W. W. Wolfe, J. A. Maisano, R. A. Ketcham and P. C. Bennett (2013). "Pore-scale trapping of supercritical CO₂ and the role of grain wettability and shape." Geophysical Research Letters: n/a-n/a.

Chenna, R., H. Sugawara, T. Koike, R. Lopez, T. J. Gibson, D. G. Higgins and J. D. Thompson (2003). "Multiple sequence alignment with the Clustal series of programs." Nucleic Acids Research **31**(13): 3497-3500.

Chien, A.-C., Norbert S. Hill and Petra A. Levin (2012). "Cell size control in bacteria." Current biology : CB **22**(9): R340-R349.

Chong, P. L. G. (2010). "Archaeobacterial bipolar tetraether lipids: Physico-chemical and membrane properties." Chemistry and Physics of Lipids **163**(3): 253-265.

Clingenpeel, S., R. E. Macur, J. J. Kan, W. P. Inskeep, D. Lovalvo, J. Varley, E. Mathur, K. Nealson, Y. Gorby, H. C. Jiang, T. LaFracois and T. R. McDermott (2011). "Yellowstone Lake: high-energy geochemistry and rich bacterial diversity." Environmental Microbiology **13**(8): 2172-2185.

Colwell, F. S., T. C. Onstott, M. E. Delwiche, D. Chandler, J. K. Fredrickson, Q. J. Yao, J. P. McKinley, D. R. Boone, R. Griffiths, T. J. Phelps, D. Ringelberg, D. C. White, L. LaFreniere, D. Balkwill, R. M. Lehman, J. Konisky and P. E. Long (1997). "Microorganisms from deep, high temperature sandstones: Constraints on microbial colonization." FEMS Microbiology Reviews **20**(3-4): 425-435.

Cotter, P. D. and C. Hill (2003). "Surviving the acid test: Responses of gram-positive bacteria to low pH." Microbiology and Molecular Biology Reviews **67**(3): 429-+.

Damar, S. and M. O. Balaban (2006). "Review of dense phase CO₂ technology: Microbial and enzyme inactivation, and effects on food quality." Journal of Food Science **71**(1): R1-R11.

Davidson, M. M., B. J. Silver, T. C. Onstott, D. P. Moser, T. M. Gihring, L. M. Pratt, E. A. Boice, B. S. Lollar, J. Lippmann-Pipke, S. M. Pfiffner, T. L. Kieft, W. Seymore and C. Ralston (2011). "Capture of Planktonic Microbial Diversity in Fractures by Long-Term Monitoring of Flowing Boreholes, Evander Basin, South Africa." Geomicrobiology Journal **28**(4): 275-300.

de Vries, M. C., E. E. Vaughan, M. Kleerebezem and W. M. de Vos (2006). "*Lactobacillus plantarum*—survival, functional and potential probiotic properties in the human intestinal tract." International Dairy Journal **16**(9): 1018-1028.

Dillow, A. K., F. Dehghani, J. S. Hrkach, N. R. Foster and R. Langer (1999). "Bacterial inactivation by using near- and supercritical carbon dioxide." Proceedings of the National Academy of Sciences of the United States of America **96**(18): 10344-10348.

Dixon, P. (2003). "VEGAN, a package of R functions for community ecology." Journal of Vegetation Science **14**(6): 927-930.

Dockrill, B. and Z. K. Shipton (2010). "Structural controls on leakage from a natural CO₂ (sub 2) geologic storage site; central Utah, U.S.A." Journal of Structural Geology **32**(11): 1768-1782.

Drissner, D., H. Blum, D. Tscherko and E. Kandeler (2007). "Nine years of enriched CO₂ changes the function and structural diversity of soil microorganisms in a grassland." European Journal of Soil Science **58**(1): 260-269.

- Duan, Z. H., R. Sun and J. W. Hu (2005). "A model for calculating the solubility of gases (CO₂, H₂S,...)used for the sequestration of global warming gases." Geochimica Et Cosmochimica Acta **69**(10): A158-A158.
- Duncan, K. E., L. M. Gieg, V. A. Parisi, R. S. Tanner, S. G. Tringe, J. Bristow and J. M. Suflita (2009). "Biocorrosive thermophilic microbial communities in Alaskan Worth Slope Oil Facilities." Environmental Science & Technology **43**(20): 7977-7984.
- Ehrlich, G. G. (1971). "Role of biota in underground waste injection and storage." American Association of Petroleum Geologists Bulletin **55**(11): 2083-&.
- Engel, A. S. (2004). Geomicrobiology of sulfuric acid speleogenesis: Microbial diversity, nutrient cycling, and controls on cave formation. PhD, The University of Texas at Austin.
- Erkmen, O. (2000). "Effect of carbon dioxide pressure on *Listeria monocytogenes* in physiological saline and foods." Food Microbiology **17**(6): 589-596.
- Farrah, H. and W. F. Pickering (1978). "Extraction of heavy-metal ions sorbed on clays." Water Air and Soil Pollution **9**(4): 491-498.
- Ferry, J. G. (1999). "Enzymology of one-carbon metabolism in methanogenic pathways." Fems Microbiology Reviews **23**(1): 13-38.
- Finkel, S. E. (2006). "Long-term survival during stationary phase: evolution and the GASP phenotype." Nature Reviews Microbiology **4**(2): 113-120.
- Fredrickson, J. K., J. P. McKinley, B. N. Bjornstad, P. E. Long, D. B. Ringelberg, D. C. White, L. R. Krumholz, J. M. Suflita, F. S. Colwell, R. M. Lehman, T. J. Phelps and T. C. Onstott (1997). "Pore-size constraints on the activity and survival of subsurface bacteria in a late cretaceous shale-sandstone sequence, northwestern New Mexico." Geomicrobiology Journal **14**(3): 183-202.
- Fredrickson, J. K., J. M. Zachara, D. W. Kennedy, H. Dong, T. C. Onstott, N. W. Hinman and S.-m. Li (1998). "Biogenic iron mineralization accompanying the dissimilatory reduction of hydrous ferric oxide by a groundwater bacterium." Geochimica et Cosmochimica Acta **62**(19-20): 3239-3257.
- Fubini, B., L. Mollo and E. Giamello (1995). "Free-radical generation at the solid/liquid interface in iron-containing minerals." Free Radical Research **23**(6): 593-614.
- Furukawa, S., T. Watanabe, T. Tai, J. Hirata, N. Narisawa, T. Kawai, H. Ogihara and M. Yamasaki (2004). "Effect of high pressure gaseous carbon dioxide on the germination of bacterial spores." International Journal of Food Microbiology **91**(2): 209-213.
- Gadd, G. M. (2010). "Metals, minerals and microbes: geomicrobiology and bioremediation." Microbiology-Sgm **156**: 609-643.
- Gambacorta, A., A. Trincone, B. Nicolaus, L. Lama and M. Derosa (1994). "UNIQUE FEATURES OF LIPIDS OF ARCHAEA." Systematic and Applied Microbiology **16**(4): 518-527.
- Garciduenas-Pina, R. and C. Cervantes (1996). "Microbial interactions with aluminium." Biomaterials **9**(3): 311-316.
- Garvie, E. I. (1980). "Bacterial lactate dehydrogenases." Microbiol Rev **44**(1): 106-139.

Gihring, T. M., D. P. Moser, L. H. Lin, M. Davidson, T. C. Onstott, L. Morgan, M. Milleson, T. L. Kieft, E. Trimarco, D. L. Balkwill and M. E. Dollhopf (2006). "The Distribution of Microbial Taxa in the Subsurface Water of the Kalahari Shield, South Africa." Geomicrobiology Journal **23**(6): 415-430.

Gilfillan, S. M., C. J. Ballentine, G. Holland, D. Blagburn, B. S. Lollar, S. Stevens, M. Schoell and M. Cassidy (2008). "The noble gas geochemistry of natural CO₂ gas reservoirs from the Colorado Plateau and Rocky Mountain provinces, USA." Geochimica Et Cosmochimica Acta **72**(4): 1174-1198.

Gorbushina, A. A. (2007). "Life on the rocks." Environmental Microbiology **9**(7): 1613-1631.

Gosden, P. E. and G. C. Ware (1977). "Method for production of pre-reduced anaerobically sterilized culture media." Journal of Applied Bacteriology **42**(1): 77-79.

Griebler, C. and T. Lueders (2009). "Microbial biodiversity in groundwater ecosystems." Freshwater Biology **54**(4): 649-677.

Grim, R. (1968). Clay mineralogy. New York, McGraw-Hill Book Company.

Guerzoni, M. E., R. Lanciotti and P. S. Cocconcelli (2001). "Alteration in cellular fatty acid composition as a response to salt, acid, oxidative and thermal stresses in *Lactobacillus helveticus*." Microbiology **147**(8): 2255-2264.

Hazel, J. R. and E. Eugene Williams (1990). "The role of alterations in membrane lipid composition in enabling physiological adaptation of organisms to their physical environment." Progress in Lipid Research **29**(3): 167-227.

Heath, J. E., T. E. Lachmar, J. P. Evans, P. T. Kolesar and A. P. Williams (2009). "Hydrogeochemical characterization of leaking, carbon dioxide-charged fault zones in east-central Utah, with implications for geological carbon storage." Geophysical Monograph **183**: 147-158.

Heidelberg, J. F., I. T. Paulsen, K. E. Nelson, E. J. Gaidos, W. C. Nelson, T. D. Read, J. A. Eisen, R. Seshadri, N. Ward, B. Methe, R. A. Clayton, T. Meyer, A. Tsapin, J. Scott, M. Beanan, L. Brinkac, S. Daugherty, R. T. DeBoy, R. J. Dodson, A. S. Durkin, D. H. Haft, J. F. Kolonay, R. Madupu, J. D. Peterson, L. A. Umayam, O. White, A. M. Wolf, J. Vamathevan, J. Weidman, M. Impraim, K. Lee, K. Berry, C. Lee, J. Mueller, H. Khouri, J. Gill, T. R. Utterback, L. A. McDonald, T. V. Feldblyum, H. O. Smith, J. C. Venter, K. H. Nealson and C. M. Fraser (2002). "Genome sequence of the dissimilatory metal ion-reducing bacterium *Shewanella oneidensis*." Nature Biotechnology **20**(11): 1118-1123.

Hertzberger, R. Y., R. D. Pridmore, C. Gysler, M. Kleerebezem and M. J. T. de Mattos (2013). "Oxygen Relieves the CO₂ and Acetate Dependency of *Lactobacillus johnsonii* NCC 533." Plos One **8**(2).

Hines, M. E., W. B. Lyons, R. M. Lent and D. T. Long (1992). "Sedimentary biogeochemistry of an acidic, saline groundwater discharge zone in Lake Tyrrell, Victoria, Australia." Chemical Geology **96**(1-2): 53-65.

Hong, S. I. and Y. R. Pyun (1999). "Inactivation kinetics of *Lactobacillus plantarum* by high pressure carbon dioxide." Journal of Food Science **64**(4): 728-733.

Hovorka, S. D., J. W. Choi, T. A. Meckel, R. H. Trevino, H. L. Zeng, M. Kordi, F. P. Wang and J. P. Nicot (2009). Comparing carbon sequestration in an oil reservoir to sequestration in a brine formation-field study. Greenhouse Gas Control Technologies **9**. J. Gale, H. Herzog and J. Braitsch. Amsterdam, Elsevier Science Bv. **1**: 2051-2056.

Hughes, M. and R. Poole (1989). Metals and microorganisms. London, Capman and Hall.

Isenschmid, A., I. W. Marison and U. von Stockar (1995). "The influence of pressure and temperature of compressed CO₂ on the survival of yeast cells." Journal of Biotechnology **39**(3): 229-237.

Johnson, R. E. (1983). Bravo Dome Carbon Dioxide Area, Northeast New Mexico. Oil and Gas Fields of the Four Corners Area. **3**: 745-748.

Jones, A. A., Bennett, P.C. (in press). "Mineral microniches control the diversity of subsurface microbial populations." Geomicrobiology Journal.

Jones, D. M., I. M. Head, N. D. Gray, J. J. Adams, A. K. Rowan, C. M. Aitken, B. Bennett, H. Huang, A. Brown, B. F. J. Bowler, T. Oldenburg, M. Erdmann and S. R. Larter (2008). "Crude-oil biodegradation via methanogenesis in subsurface petroleum reservoirs." Nature **451**(7175): 176-U176.

Kaneda, T. (1977). "Fatty-acids of the genus *Bacillus* - Example of branched-chain preference." Bacteriological Reviews **41**(2): 391-418.

Kaneda, T. (1991). "Iso-fatty and anteiso-fatty acids in bacteria - biosynthesis, function, and taxonomic significance." Microbiological Reviews **55**(2): 288-302.

Kaszuba, J. P., Janecky and D. R. (2009). Geochemical impacts of sequestering carbon dioxide in brine formations. Washington, DC, ETATS-UNIS, American Geophysical Union.

Keweloh, H. and H. J. Heipieper (1996). "Trans unsaturated fatty acids in bacteria." Lipids **31**(2): 129-137.

Kharaka, Y., J. Thordsen, E. Kakouros, G. Ambats, W. Herkelrath, S. Beers, J. Birkholzer, J. Apps, N. Spycher, L. Zheng, R. Trautz, H. Rauch and K. Gullickson (2010). "Changes in the chemistry of shallow groundwater related to the 2008 injection of CO₂ at the ZERT field site, Bozeman, Montana." Environmental Earth Sciences **60**(2): 273-284.

Kharaka, Y. K., D. R. Cole, S. D. Hovorka, W. D. Gunter, K. G. Knauss and B. M. Freifeld (2006). "Gas-water-rock interactions in Frio Formation following CO₂ injection: Implications for the storage of greenhouse gases in sedimentary basins." Geology **34**(7): 577-580.

Kidd, S. P. (2011). Stress response in pathogenic bacteria, Cabi.

Kim, J., H. L. Dong, J. Seabaugh, S. W. Newell and D. D. Eberl (2004). "Role of microbes in the smectite-to-illite reaction." Science **303**(5659): 830-832.

- Kirk, M. F. (2011). "Variation in energy available to populations of subsurface anaerobes in response to geological carbon storage." Environmental Science & Technology **45**(15): 6676-6682.
- Kirk, M. F., E. F. U. Santillan, L. K. McGrath and S. J. Altman (2012). "Variation in hydraulic conductivity with decreasing pH in a biologically-clogged porous medium." International Journal of Greenhouse Gas Control **11**: 133-140.
- Kirk, M. F., E. F. U. Santillan, R. A. Sanford and S. J. Altman (2013). "CO₂-induced shift in microbial activity affects carbon trapping and water quality in anoxic bioreactors." Geochimica Et Cosmochimica Acta **122**: 198-208.
- Koch, A. (2007). Growth measurement. Methods for general and molecular microbiology. B. T. Reddy C, Breznak J, Marzluf G, Schmidt M, Snyder L. Washington, DC, ASM Press: 172-199.
- Konhauser, K. O. (2006). Introduction to geomicrobiology, Wiley.
- Korosec, M. A., Phillips W.M, Schuster, J.E. (1983). The 1980-1982 Geothermal Resource Assessment Program in Washington. W. S. D. o. N. R. D. o. G. a. E. Resources. Olympia, Washington.
- Kosaka, T., T. Uchiyama, S.-i. Ishii, M. Enoki, H. Imachi, Y. Kamagata, A. Ohashi, H. Harada, H. Ikenaga and K. Watanabe (2006). "Reconstruction and regulation of the central catabolic pathway in the thermophilic propionate-oxidizing syntroph *Pelotomaculum thermopropionicum*." Journal of Bacteriology **188**(1): 202-210.
- Kostka, J. and K. H. Nealson (1998). Isolation, cultivation and characterization of Iron- and Manganese-reducing bacteria. Techniques in microbial ecology. A. R. Burlage R, Stahl D, Geesey G, Sayler G. New York, Oxford University Press: 58-75.
- Kotelnikova, S. (2002). "Microbial production and oxidation of methane in deep subsurface." Earth-Science Reviews **58**(3-4): 367-395.
- Kotsyurbenko, O. R., M. W. Friedrich, M. V. Simankova, A. N. Nozhevnikova, P. N. Golyshin, K. N. Timmis and R. Conrad (2007). "Shift from acetoclastic to H₂-dependent methanogenesis in a West Siberian peat bog at low pH values and isolation of an acidophilic *Methanobacterium* strain." Applied and Environmental Microbiology **73**(7): 2344-2348.
- Krumholz, L. R. (2000). "Microbial communities in the deep subsurface." Hydrogeology Journal **8**(1): 4-10.
- Lande, R. (1996). "Statistics and partitioning of species diversity, and similarity among multiple communities." Oikos **76**(1): 5-13.
- Lavallaur, H. J. and F. S. Colwell (2013). "Microbial characterization of basalt formation waters targeted for geological carbon sequestration." FEMS Microbiology Ecology **85**(1): 62-73.
- Leaphart, A. B., D. K. Thompson, K. Huang, E. Alm, X. F. Wan, A. Arkin, S. D. Brown, L. Y. Wu, T. F. Yan, X. D. Liu, G. S. Wickham and J. Z. Zhou (2006). "Transcriptome

profiling of *Shewanella oneidensis* gene expression following exposure to acidic and alkaline pH." Journal of Bacteriology **188**(4): 1633-1642.

Lee, R. K., P. M. James, A. U. Glenn and M. S. Joseph (1997). "Confined subsurface microbial communities in Cretaceous rock." Nature **386**(6620): 64-66.

Lever, M. A. (2013). "Functional gene surveys from ocean drilling expeditions a review and perspective." FEMS Microbiology Ecology **84**(1): 1-23.

Li, J. Y., R. K. Xu, D. Tiwari and G. L. Ji (2006). "Effect of low-molecular-weight organic acids on the distribution of mobilized Al between soil solution and solid phase." Applied Geochemistry **21**(10): 1750-1759.

Lies, D. P., M. E. Hernandez, A. Kappler, R. E. Mielke, J. A. Gralnick and D. K. Newman (2005). "*Shewanella oneidensis* MR-1 uses overlapping pathways for iron reduction at a distance and by direct contact under conditions relevant for biofilms." Applied and Environmental Microbiology **71**(8): 4414-4426.

Liss, P. S. and P. G. Slater (1974). "Flux of Gases across the Air-Sea Interface." Nature **247**(5438): 181-184.

Little, M. G. and R. B. Jackson (2010). "Potential impacts of leakage from deep CO₂ geosequestration on overlying freshwater aquifers." Environmental Science & Technology **44**(23): 9225-9232.

Liu, S. V., J. Z. Zhou, C. L. Zhang, D. R. Cole, M. Gajdarziska-Josifovska and T. J. Phelps (1997). "Thermophilic Fe(III)-reducing bacteria from the deep subsurface: The evolutionary implications." Science **277**(5329): 1106-1109.

Lovley, D. R. (1993). "Dissimilatory metal reduction." Annual Review of Microbiology **47**: 263-290.

Lozupone, C. and R. Knight (2005). "UniFrac: a New Phylogenetic Method for Comparing Microbial Communities." Applied and Environmental Microbiology **71**(12): 8228-8235.

Lu, P., Q. Fu, W. E. Seyfried, A. Hereford and C. Zhu (2011). "Navajo Sandstone-brine-CO₂ interaction: implications for geological carbon sequestration." Environmental Earth Sciences **62**(1): 101-118.

Ma, J., A. M. Ibekwe, C.-H. Yang and D. E. Crowley (2013). "Influence of bacterial communities based on 454-pyrosequencing on the survival of *Escherichia coli* O157:H7 in soils." FEMS Microbiology Ecology **84**(3): 542-554.

MacNaughton, S. J., J. R. Stephen, A. D. Venosa, G. A. Davis, Y.-J. Chang and D. C. White (1999). "Microbial population changes during bioremediation of an experimental oil spill." Applied and Environmental Microbiology **65**(8): 3566-3574.

Madigan, M. T. (2012). Brock biology of microorganisms. San Francisco, Benjamin Cummings.

Maren, T. H. (1967). "Carbonic anhydrase - chemistry, physiology, and inhibition." Physiological Reviews **47**(4): 595-&.

- Marshall, K. C. (1975). "Clay mineralogy in relation to survival of soil bacteria." Annual Review of Phytopathology **13**: 357-373.
- Masbruch, M. D. (2014). Groundwater Age Dating in and Near Arches National Park, Utah.
- Mason, O. U., C. A. Di Meo-Savoie, J. D. Van Nostrand, J. Z. Zhou, M. R. Fisk and S. J. Giovannoni (2009). "Prokaryotic diversity, distribution, and insights into their role in biogeochemical cycling in marine basalts." Isme Journal **3**(2): 231-242.
- Matter, J. M., T. Takahashi and D. Goldberg (2007). "Experimental evaluation of in situ CO₂-water-rock reactions during CO₂ injection in basaltic rocks: Implications for geological CO₂ sequestration." Geochemistry Geophysics Geosystems **8**.
- Mavrommatis, K., S. Gronow, E. Saunders, M. Land, A. Lapidus, A. Copeland, T. G. Del Rio, M. Nolan, S. Lucas, F. Chen, H. Tice, J. F. Cheng, D. Bruce, L. Goodwin, S. Pitluck, A. Pati, N. Ivanova, A. Chen, K. Palaniappan, P. Chain, L. Hauser, Y. J. Chang, C. D. Jeffries, T. Brettin, J. C. Detter, C. Han, J. Bristow, M. Goker, M. Rohde, J. A. Eisen, V. Markowitz, N. C. Kyrpides, H. P. Klenk and P. Hugenholtz (2009). "Complete genome sequence of *Capnocytophaga ochracea* type strain (VPI 2845T)." Standards in Genomic Sciences **1**(2): 101-109.
- McGrail, B. P., H. T. Schaef, A. M. Ho, Y. J. Chien, J. J. Dooley and C. L. Davidson (2006). "Potential for carbon dioxide sequestration in flood basalts." Journal of Geophysical Research-Solid Earth **111**(B12).
- Mitchell, A. C., A. J. Phillips, M. A. Hamilton, R. Gerlach, W. K. Hollis, J. P. Kaszuba and A. B. Cunningham (2008). "Resilience of planktonic and biofilm cultures to supercritical CO₂." Journal of Supercritical Fluids **47**(2): 318-325.
- Mitchell, A. C., A. J. Phillips, R. Hiebert, R. Gerlach, L. H. Spangler and A. B. Cunningham (2009). "Biofilm enhanced geologic sequestration of supercritical CO₂." International Journal of Greenhouse Gas Control **3**(1): 90-99.
- Morrill, P. L., J. G. Kuenen, O. J. Johnson, S. Suzuki, A. Rietze, A. L. Sessions, M. L. Fogel and K. H. Nealson (2013). "Geochemistry and geobiology of a present-day serpentinization site in California: The Cedars." Geochimica Et Cosmochimica Acta **109**: 222-240.
- Nakamura, K., A. Enomoto, H. Fukushima, K. Nagai and M. Hakoda (1994). "Disruption of microbial-cells by the flash discharge of high-pressure carbon dioxide." Bioscience Biotechnology and Biochemistry **58**(7): 1297-1301.
- Nealson, K. H., A. Belz and B. McKee (2002). "Breathing metals as a way of life: geobiology in action." Antonie Van Leeuwenhoek International Journal of General and Molecular Microbiology **81**(1-4): 215-222.
- Nicholson, W. L., N. Munakata, G. Horneck, H. J. Melosh and P. Setlow (2000). "Resistance of *Bacillus* endospores to extreme terrestrial and extraterrestrial environments." Microbiology and Molecular Biology Reviews **64**(3): 548-+.
- Oksanen, J. (February 8, 2013). Multivariate analysis of ecological

communities in R: vegan tutorial.

- Onstott, T. (2003). Geochemical and Geological Significance of Subsurface Microbiology. Encyclopedia of Environmental Microbiology, John Wiley & Sons, Inc.
- Onstott, T. C., T. J. Phelps, F. S. Colwell, D. Ringelberg, D. C. White, D. R. Boone, J. P. McKinley, T. O. Stevens, P. E. Long, D. L. Balkwill, W. T. Griffin and T. Kieft (1998). "Observations pertaining to the origin and ecology of microorganisms recovered from the deep subsurface of Taylorsville Basin, Virginia." Geomicrobiology Journal **15**(4): 353-385.
- Oule, M., M. Dickman and J. Arul (2010). "Microbicidal effect of pressurized CO₂ and the influence of sensitizing additives." European Journal of Scientific Research **41**(4): 569-581.
- Oule, M. K., K. Tano, A. M. Bernier and J. Arul (2006). "*Escherichia coli* inactivation mechanism by pressurized CO₂." Canadian Journal of Microbiology **52**(12): 1208-1217.
- Øvreås, L. and V. Torsvik (1998). "Microbial diversity and community structure in two different agricultural soil communities." Microbial Ecology **36**(3-4): 303-315.
- Parry, W. T., M. A. Chan and B. P. Nash (2009). "Diagenetic characteristics of the Jurassic Navajo Sandstone in the Covenant oil field, central Utah thrust belt." Aapg Bulletin **93**(8): 1039-1061.
- Pedersen, K. (1993). "The deep subterranean biosphere." Earth-Science Reviews **34**(4): 243-260.
- Pedersen, K., J. Arlinger, S. Ekendahl and L. Hallbeck (1996). "16S rRNA gene diversity of attached and unattached bacteria in boreholes along the access tunnel to the Aspo hard rock laboratory, Sweden." Fems Microbiology Ecology **19**(4): 249-262.
- Pedersen, K., J. Arlinger, L. Hallbeck and C. Pettersson (1996). "Diversity and distribution of subterranean bacteria in groundwater at Oklo in Gabon, Africa, as determined by 16S rRNA gene sequencing." Molecular Ecology **5**(3): 427-436.
- Perdrial, J. N., L. N. Warr, N. Perdrial, M. C. Lett and F. Elsass (2009). "Interaction between smectite and bacteria: Implications for bentonite as backfill material in the disposal of nuclear waste." Chemical Geology **264**(1-4): 281-294.
- Reith, F. (2011). "Life in the deep subsurface." Geology **39**(3): 287-288.
- Rittmann, B. E. (1993). "The significance of biofilms in porous media." Water Resources Research **29**(7): 2195-2202.
- Rivett, M. O., S. R. Buss, P. Morgan, J. W. N. Smith and C. D. Bemment (2008). "Nitrate attenuation in groundwater: A review of biogeochemical controlling processes." Water Research **42**(16): 4215-4232.
- Roberts, J. A. (2004). "Inhibition and enhancement of microbial surface colonization: the role of silicate composition." Chemical Geology **212**(3-4): 313-327.
- Rodriguez-Ruiz, J., E. H. Belarbi, J. L. G. Sanchez and D. L. Alonso (1998). "Rapid simultaneous lipid extraction and transesterification for fatty acid analyses." Biotechnology Techniques **12**(9): 689-691.

- Romanovicz, D. (2011). TEM Methods.
- Sahl, J. W., R. H. Schmidt, E. D. Swanner, K. W. Mandernack, A. S. Templeton, T. L. Kieft, R. L. Smith, W. E. Sanford, R. L. Callaghan, J. B. Mitton and J. R. Spear (2008). "Subsurface microbial diversity in deep-granitic-fracture water in Colorado." Applied and Environmental Microbiology **74**(1): 143-152.
- Sander, R. (1999). "Modeling atmospheric chemistry: Interactions between gas-phase species and liquid cloud/aerosol particles." Surveys in Geophysics **20**(1): 1-31.
- Santillan, E. U., M. F. Kirk, S. J. Altman and P. C. Bennett (2013). "Mineral influence on microbial survival during carbon sequestration." Geomicrobiology Journal **30**(7): 578-592.
- Scanlan, C. M. (1992). "Cultural and biochemical characterization of a capnophilic Gram-negative bacterium from hamsters." Journal of Veterinary Diagnostic Investigation **4**(1): 84-85.
- Schimel, J., T. C. Balser and M. Wallenstein (2007). "Microbial stress-response physiology and its implications for ecosystem function." Ecology **88**(6): 1386-1394.
- Shimoda, M., Y. Yamamoto, J. Cocunubo-Castellanos, H. Tonoike, T. Kawano, H. Ishikawa and Y. Osajima (1998). "Antimicrobial Effects of Pressured Carbon Dioxide in a Continuous Flow System." Journal of Food Science **63**(4): 709-712.
- Shipton, Z. K., Evans, J. P., Kirchner, D., Heath, J., and Williams, A. P (2004). Analysis of CO₂ leakage through 'low-permeability' faults from natural reservoirs in the Colorado Plateau, East-Central Utah. Geological Society of London Special Publication. S. J. B. a. R. H. Worden. **233**: 43-58.
- Simek, M., L. Jisova and D. W. Hopkins (2002). "What is the so-called optimum pH for denitrification in soil?" Soil Biology & Biochemistry **34**(9): 1227-1234.
- Smith, K. S. and J. G. Ferry (2000). "Prokaryotic carbonic anhydrases." Fems Microbiology Reviews **24**(4): 335-366.
- Song, H., J. W. Lee, S. Choi, J. K. You, W. H. Hong and S. Y. Lee (2007). "Effects of dissolved CO₂ levels on the growth of *Mannheimia succiniciproducens* and succinic acid production." Biotechnol Bioeng **98**(6): 1296-1304.
- Spear, J. R., J. J. Walker, T. M. McCollom and N. R. Pace (2005). "Hydrogen and bioenergetics in the Yellowstone geothermal ecosystem." Proceedings of the National Academy of Sciences of the United States of America **102**(7): 2555-2560.
- Spilimbergo, S. and A. Bertucco (2003). "Non-thermal bacteria inactivation with dense CO₂." Biotechnology and Bioengineering **84**(6): 627-638.
- Stevens, T. O., J. P. McKinley and J. K. Fredrickson (1993). "Bacteria associated with deep, alkaline, anaerobic groundwaters in Southeast Washington." Microbial Ecology **25**(1): 35-50.
- Stroes-Gascoyne, S., A. Schippers, B. Schwyn, S. Poulain, C. Sergeant, M. Simonoff, C. Le Marrec, S. Altmann, T. Nagaoka, L. Mauclaire, J. McKenzie, S. Daumas, A. Vinsot, C. Beaucaire and J. M. Matray (2007). "Microbial community analysis of Opalinus Clay

drill core samples from the Mont Terri Underground Research Laboratory, Switzerland." Geomicrobiology Journal **24**(1): 1-17.

Suekane, T., T. Nobuso, S. Hirai and M. Kiyota (2008). "Geological storage of carbon dioxide by residual gas and solubility trapping." International Journal of Greenhouse Gas Control **2**(1): 58-64.

Takano, Y., M. Kaneko, J. Kahnt, H. Imachi, S. Shima and N. Ohkouchi (2013). "Detection of coenzyme F430 in deep sea sediments: A key molecule for biological methanogenesis." Organic Geochemistry **58**: 137-140.

Tatsuhiko, H., Fumio, I. (2013). "A comparative study of microbial diversity and community structure in marine sediments using poly(A) tailing and reverse transcription PCR" Frontiers in Microbiology **4**.

To, B. C. S. and M. R. Etzel (1997). "Spray drying, freeze drying, or freezing of three different lactic acid bacteria species." Journal of Food Science **62**(3): 576-&.

To, T. B., D. K. Nordstrom, K. M. Cunningham, J. W. Ball and R. B. McCleskey (1999). "New method for the direct determination of dissolved Fe(III) concentration in acid mine waters." Environmental Science & Technology **33**(5): 807-813.

Trampuz, A., K. E. Piper, M. J. Jacobson, A. D. Hanssen, K. K. Unni, D. R. Osmon, J. N. Mandrekar, F. R. Cockerill, J. M. Steckelberg, J. F. Greenleaf and R. Patel (2007). "Sonication of removed hip and knee prostheses for diagnosis of infection." New England Journal of Medicine **357**(7): 654-663.

Tsai, Y. L. and B. H. Olson (1991). "Rapid method for direct extraction of DNA from soil and sediments." Applied and Environmental Microbiology **57**(4): 1070-1074.

Ueda, K., Y. Tagami, Y. Kamihara, H. Shiratori, H. Takano and T. Beppu (2008). "Isolation of bacteria whose growth is dependent on high levels of CO₂ and implications of their potential diversity." Applied and Environmental Microbiology **74**(14): 4535-4538.

Veerkamp, J. H. (1971). "Fatty acid composition of Bifidobacterium and Lactobacillus strains." J Bacteriol **108**(2): 861-867.

Vos, P., G. Garrity, D. Jones, N. R. Krieg, W. Ludwig, F. A. Rainey, K.-H. Schleifer and W. B. Whitman (2011). Bergey's Manual of Systematic Bacteriology. Dordrecht, Springer.

Walther, J. V. (1996). "Relation between rates of aluminosilicate mineral dissolution, pH, temperature, and surface charge." American Journal of Science **296**(7): 693-728.

Wang, P. L., L. H. Lin, H. T. Yu, T. W. Cheng, S. R. Song, L. W. Kuo, E. C. Yeh, W. R. Lin and C. Y. Wang (2007). "Cultivation-based characterization of microbial communities associated with deep sedimentary rocks from Taiwan Chelungpu Drilling Project cores." Terrestrial Atmospheric and Oceanic Sciences **18**(2): 395-412.

Wanger, G., G. Southam and T. C. Onstott (2006). "Structural and chemical characterization of a natural fracture surface from 2.8 kilometers below land surface: Biofilms in the deep subsurface." Geomicrobiology Journal **23**(6): 443-452.

Watanabe, T., S. Furukawa, J. Hirata, T. Koyama, H. Ogihara and M. Yamasaki (2003). "Inactivation of *Geobacillus stearothermophilus* spores by high-pressure carbon dioxide treatment." Applied and Environmental Microbiology **69**(12): 7124-7129.

Welker, N. E. and L. L. Campbell (1963). "Induced biosynthesis of alpha-amylase by growing cultures of *Bacillus stearothermophilus*." Journal of Bacteriology **86**: 1196-1201.

White, A., D. Burns and T. W. Christensen (2006). "Effective terminal sterilization using supercritical carbon dioxide." Journal of Biotechnology **123**(4): 504-515.

White, D. (2007). The Physiology and biochemistry of prokaryotes. New York, Oxford University Press.

Whitman, W., T. Bowen and D. Boone (2006). The Methanogenic Bacteria

The Prokaryotes. M. Dworkin, S. Falkow, E. Rosenberg, K.-H. Schleifer and E. Stackebrandt, Springer New York: 165-207.

Winderl, C., B. Anneser, C. Griebler, R. U. Meckenstock and T. Lueders (2008). "Depth-resolved quantification of anaerobic toluene degraders and aquifer microbial community patterns in distinct redox zones of a tar oil contaminant plume." Applied and Environmental Microbiology **74**(3): 792-801.

Wu, B., H. B. Shao, Z. P. Wang, Y. D. Hu, Y. J. J. Tang and Y. S. Jun (2010). "Viability and Metal Reduction of *Shewanella oneidensis* MR-1 under CO₂ Stress: Implications for Ecological Effects of CO₂ Leakage from Geologic CO₂ Sequestration." Environmental Science & Technology **44**(23): 9213-9218.

Wynne, E. S. and J. W. Foster (1948). "Physiological studies on spore germination, with special reference to *Clostridium botulinum*: 3. Carbon dioxide and germination, with a note on carbon dioxide and aerobic spores." Journal of Bacteriology **55**(3): 331-339.

Xu, T. F., J. A. Apps and K. Pruess (2005). "Mineral sequestration of carbon dioxide in a sandstone-shale system." Chemical Geology **217**(3-4): 295-318.

Zafar, Z. I. and M. Ashraf (2007). "Selective leaching kinetics of calcareous phosphate rock in lactic acid." Chemical Engineering Journal **131**(1-3): 41-48.

Zeikus, J. G. and R. S. Wolfe (1972). "*Methanothermobacter thermoautotrophicus* sp, an anaerobic, autotrophic, extreme thermophile " Journal of Bacteriology **109**(2): 707-&.

Zhang, Y. M. and C. O. Rock (2008). "Membrane lipid homeostasis in bacteria." Nature Reviews Microbiology **6**(3): 222-233.

Zhou, Y., C. Kellermann and C. Griebler (2012). "Spatio-temporal patterns of microbial communities in a hydrologically dynamic pristine aquifer." FEMS Microbiology Ecology **81**(1): 230-242.